

UNIVERSITY OF OKLAHOMA
GRADUATE COLLEGE

CHEMICAL FLOOD UNDER HIGH TOTAL DISSOLVED SOLIDS (TDS)
CONDITIONS

A DISSERTATION
SUBMITTED TO THE GRADUATE FACULTY
in partial fulfillment of the requirements for the
Degree of
DOCTOR OF PHILOSOPHY

By
WEI WAN
Norman, Oklahoma
2014

CHEMICAL FLOOD UNDER HIGH TOTAL DISSOLVED SOLIDS (TDS)
CONDITIONS

A DISSERTATION APPROVED FOR THE
MEWBOURNE SCHOOL OF PETROLEUM AND GEOLOGICAL ENGINEERING

BY

Dr. Benjamin Shiau, Chair

Dr. Jeffrey Harwell

Dr. Chad Roller

Dr. Ahmad Jamili

Dr. Deepak Devegowda

Dr. Rouzbeh Ghanbarnezhad-Moghanlo

© Copyright by WEI WAN 2014
All Rights Reserved.

To my family for their motivation & constant support and to my advisors
for their encouragement and patience

Acknowledgements

I would like to appreciate all those who have supported me as I pursued my PhD degree at University of Oklahoma. I would like to acknowledge the Mewbourne School of Petroleum and Geological Engineering at University of Oklahoma for providing me the opportunity to undertake my graduate study and researches. I would also like to thank my advisors Dr. Benjamin Shiau and Dr. Jeffrey Harwell for their constructive guidance. They are always supportive and helpful throughout my years in graduate study and research. I would also like to thank Dr. Deepak Devegowda, Dr. Chad Roller, Dr. Ahmad Jamili and Dr. Rouzbeh Ghanbarnezhad-Moghanlo for their valuable suggestions to my study and researches.

I would also like to express my thanks to my colleagues from The Applied Surfactant Laboratory (ASL) for their kind help throughout my study and researches. I would also like to thank the Oklahoma Economic Development Generating Excellence (EDGE), Department of Energy, the Research Partnership to Secure Energy for America (RPSEA), Mid-Con Energy Inc., and Chemical Flooding Technologies (CFT), LLC for financially supporting this research.

Last but not the least; I would also like to thank my friends and family for providing consistent support to me.

Table of Contents

Acknowledgements	iv
Table of Contents	v
List of Tables	x
List of Figures	xii
Abstract	xviii
Chapter 1. Introduction	1
1.1. Potential of Enhanced Oil Recovery (EOR).....	1
1.2. Mechanisms of Chemical Flood	3
1.2.1. Reduce IFT	3
1.2.2. Mobility Control.....	6
1.3. Surfactants	7
1.3.1. Micelles and Wormlike Micelles.....	8
1.3.2. Microemulsions	10
1.3.3. Hydrophilic-Lipophilic Deviation	12
1.4. Polymers	14
1.5. Motivation	16
1.6. Hypothesis	19
1.7. Research Plan	19

1.7.1. Characterization of Crude Oil EACN for Surfactant Flooding Design.....	19
1.7.2. Formulating Low-IFT Microemulsions for High Salinity Formations Using Extended Surfactants	22
1.7.3. Surfactant/Polymer Formulation of Chemical Flood for Three High Salinity Reservoirs	24
1.7.4. Surfactant Formulation of Chemical Flood for a High Salinity and Temperature Reservoir	24
1.8. Summary.....	25
Chapter 2. Materials and Methods.....	26
2.1. Materials	26
2.2. Methods	30
2.2.1. Phase Behavior Test	30
2.2.2. Screening Criteria for Chemical Flood.....	31
2.2.3. Critical Factors Affecting Design of Slug Size of Surfactant	33
2.2.4. IFT Measurement	34
2.2.5. Determination of EACN of Crude Oil.....	35
2.2.6. Preparation of Polymer Solutions or Wormlike Micelles	36
2.2.7. Viscosity Measurement	37
2.2.8. Stability Test.....	37
2.2.9. Sand Packed Column Test.....	38
2.2.10. Core Flood Test	40
2.3. Summary.....	42

Chapter 3. Characterization of Crude Oil EACN for Surfactant Flooding Design 43

3.1. Indirect Method to Determine EACN of Crude Oils Using AOT and Isobutanol 43

3.2. Direct Method to Determine EACN of Crude Oils Using Conventional EOR Surfactant: AOT and Isobutanol System 49

3.3. Determination of EACN of Crude Oils Using Extended Surfactant Systems 50

3.4. Summary 55

Chapter 4. Formulating Low-IFT Microemulsions for High Salinity Formations Using Extended Surfactants57

4.1. Effects of Co-Solvent and Co-surfactants on the Formation of Middle Phase Microemulsion..... 57

4.2. Effect of Different Extended Surfactants on Middle Phase Microemulsion Formation at Various Temperatures 64

4.3. Comparison of Performance of Different Extended Surfactants and AOT in the Presence of Co-Solvent 66

4.4. Effect of ACN on Optimal Salinity Four Extended Surfactants with Oil in the Presence of Co-Solvent 68

4.5. Summary..... 70

Chapter 5. Surfactants/Polymer Formulation of Chemical Flood for Three High Salinity Reservoirs71

5.1.	Surfactants/Polymer Formulation of Chemical Flood for Miller 29 Site.....	71
5.1.1.	Surfactant Formulation.....	71
5.1.2.	Mixed Surfactants/Polymer Formulation	73
5.1.3.	Stability Test.....	74
5.1.4.	Sand Packed Column Test.....	75
5.1.5.	Core Flood Test	76
5.2.	Surfactant/Polymer Formulation of Chemical Flood for Primexx Site.....	77
5.2.1.	Surfactant Formulation.....	77
5.2.2.	Mixed Surfactant/Polymer Formulation.....	79
5.2.3.	Stability Test.....	80
5.2.4.	Sand Packed Column Test.....	81
5.2.5.	Core Flood Test	82
5.3.	Surfactant only Formulation of Chemical Flood for Litchfield Site	83
5.3.1.	Surfactant Formulation.....	83
5.3.2.	Wormlike Micelles Formulation for Litchfield Site.....	84
5.3.3.	Stability Test.....	86
5.3.4.	Sand Packed Column Test.....	87
5.3.5.	Core Flood Test	89
5.4.	Correlation of Sor after Chemical Flood and Capillary Number for Three Sites	90
5.5.	Summary.....	91

Chapter 6. Surfactant Formulation of Chemical Flood for a High Salinity and Temperature Reservoir	93
6.1. Challenges of Surfactant Formulation at High Temperature	93
6.2. Surfactant Formulation with Single Surfactant	94
6.3. Surfactant Formulation with Hexyl Glucoside.....	96
6.4. Surfactant Formulation with Isopropanol.....	97
6.5. Surfactant Formulation with sec-Butanol.....	99
6.6. Sand Packed Column Test.....	101
6.7. Core Flood Test	101
6.8. Summary.....	103
Chapter 7. Conclusions and Recommendations.....	104
7.1. Conclusions	104
7.2. Recommendations	106
Nomenclature	109
SI Metric Conversion Factors	111
References.....	112

List of Tables

TABLE 1.1—PROPERTIES OF THREE HIGH SALINITY RESERVOIRS	24
TABLE.2.1—MOLECULAR STRUCTURE OF SOME SURFACTANTS USED IN THIS STUDY.....	26
TABLE.2.2—PROPERTIES OF EXTENDED SURFACTANTS USED IN THIS STUDY.....	27
TABLE.2.3—MOLECULAR STRUCTURE OF SOME CO-SOLVENT USED IN THIS STUDY	28
TABLE 3.1—SUMMARY OF OPTIMAL NACL CONCENTRATION USED TO DETERMINE EACN OF CRUDE OIL	46
TABLE 3.2—SUMMARY OF EACN DETERMINED FOR THREE CRUDE OILS.....	48
TABLE 3.3—COMPARISON OF K AND CC OBTAINED IN THIS STUDY WITH THOSE REPORTED IN THE LITERATURE	54
TABLE 3.4— EACN FOR CRUDE OILS	55
TABLE 4.1—EFFECTS OF CO-SOLVENT AND CO-SURFACTANTS ON MIDDLE PHASE MICROEMULSION WINDOW AT ROOM TEMPERATURE.....	58
TABLE 4.2—EFFECTS OF CO-SOLVENT AND CO-SURFACTANTS ON MIDDLE PHASE WINDOW AT 46 °C	59

TABLE 4.3—EFFECTS OF DIFFERENT EXTENDED SURFACTANTS ON MIDDLE PHASE MICROEMULSION FORMATION AT BOTH ROOM TEMPERATURE AND 46 °C	65
TABLE 4.4—PARAMETERS FOR FOUR EXTENDED SURFACTANTS	69
TABLE 5.1—SUMMARY OF SAND PACKED COLUMN TESTS For Miller 29	75
TABLE 5.2—SUMMARY OF SAND PACKED COLUMN TESTS FOR PRIMEXX.....	81
TABLE 5.3—SUMMARY OF SAND PACKED COLUMN TESTS FOR LITCHFIELD	87

List of Figures

Fig.1.1—Three stages of oil production.....	1
Fig.1.2—Use of surfactants to reduce IFT to reduce capillary force that traps oil..	4
Fig.1.3—Schematic plot of correlation between the capillary number and residual oil saturation (Green and Willhite 1998).....	5
Fig.1.4—Mobility control for chemical flood (Green and Willhite 1998).	7
Fig.1.5—Definition of critical micelle concentration (CMC).	8
Fig.1.6—Schematic diagram of wormlike micells.	9
Fig.1.7—Types of microemulsions.	11
Fig.1.8—Partially hydrolyzed polyacrylamide.	14
Fig.1.9—The structure of a xanthan gum.	15
Fig.1.10—The trapped oil in Oklahoma (Boyd 2008).	17
Fig.1.11—Water flood infrastructure.....	17
Fig.1.12—Basic structure of extended surfactants.....	21
Fig.2.1—Effect of adding 300 ppm sodium gluconate on the stability of field brine at 36 °C.....	29
Fig.2.2—Flat-bottom glass vials with Teflon-lined screw caps used for phase behavior test at low temperature in this study.	30
Fig.2.3—Grace instrument M6500 spinning drop tensiometer.....	34
Fig.2.4—Magnetic stirrer for the preparation of polymer solution.	36
Fig.2.5—Blender for the preparation of polymer solution.	36
Fig.2.6—Brookfield dial reading viscometer.	38
Fig.2.7— Schematic diagram of sand packed column test.	38

Fig.2.8—The apparatus for sand packed column test used in this study.....	39
Fig.2.9— Schematic diagram of core flood apparatus.....	40
Fig.2.10—The apparatus for core flood test used in this study.....	41
Fig.3.1—Effect of NaCl concentration on phase behaviors for the mixture of AOT and isobutanol with Fox Creek crude oil.	43
Fig.3.2—Equilibrium IFT as a function of electrolyte concentration (salinity scan) for the systems of AOT and iso-butanol at different weight ratios of decane and Miller 29 crude oil.	44
Fig.3.3—Equilibrium IFT as a function of electrolyte concentration (salinity scan) for the systems of AOT and iso-butanol at different weight ratios of decane and Woods crude oil.....	45
Fig.3.4—Equilibrium IFT as a function of electrolyte concentration (salinity scan) for the systems of AOT and iso-butanol at different weight ratios of decane and Fox Creek crude oil.....	46
Fig.3.5—Effect of NaCl concentration on phase behaviors for 2.5 wt% AF 8-41S with Octane.	49
Fig.3.6—Equilibrium IFT as a function of electrolyte concentration (salinity scan) for the systems of extended surfactant for hexane (C6), octane (C8), decane (C10) and dodecane (C12).....	50
Fig.3.7—The plot of $\ln S^*$ vs. EACN for C6, C8, C10 and C12.	51
Fig.3.8—Equilibrium IFT as a function of electrolyte concentration (salinity scan) for the systems of extended surfactant for pentane (C5), heptane (C7) and tetradecane (C14).....	52

Fig.3.9—Comparison of $\ln S^*$ predicted by Eq. 3.7 with experimental data for C5, C7 and C14.....	53
Fig.3.10—Equilibrium IFT as a function of electrolyte concentration (salinity scan) for the systems of extended surfactant for different crude oils.....	54
Fig.4.1—Effect of NaCl concentration on the phase behaviors for 0.5 wt% C₁₂H₂₅-(PO)₆-SO₄Na and 3 wt% BC with decane at room temperature.	57
Fig.4.2—Effect of NaCl concentration on IFT for a mixture of 0.5 wt% C₁₂H₂₅-(PO)₄-(EO)₁-SO₄Na, 0.1 wt% Calfax 16L-35, and 3 wt% butyl carbitol and decane at room temperature.....	61
Fig.4.3—Effect of butyl carbitol concentration on IFT for a mixture of 0.5 wt% C₁₂H₂₅-(PO)₄-(EO)₁-SO₄Na, 0.1 wt% Calfax 16L-35, 18 wt% NaCl and decane at room temperature.....	62
Fig.4.4—Effect of different co-surfactants on IFT for a mixture of 0.5 wt % C₁₂H₂₅-(PO)₄-(EO)₁-SO₄Na, 3 wt% butyl carbitol, 16 wt% NaCl and decane at room temperature.	63
Fig.4.5—Effect of different extended surfactants on IFT for a mixture of 0.1 wt % Calfax 16L-35, 3 wt % butyl carbitol, 16 wt % NaCl and decane at room temperature.....	64
Fig.4.6—Optimal salinity for different extended surfactants and AOT.	67
Fig.4.7—$\ln S^*$ as a function of ACN for different extended surfactants in the presence of isobutanol.	68

Fig.5.1—Effect of concentration of the co-surfactants of Steol CS-460 and Calfax DB 45 (1:1 ratio) on the stability for the surfactant formulation at 46 °C for Miller 29.	71
Fig.5.2—Effect of concentration of co-surfactants of Steol CS-460 and Calfax DB 45 (1:1 ratio) on phase behaviors for surfactant formulation with crude oil at 46 °C for Miller 29.....	72
Fig.5.3—Effect of the concentration of Calfax DB-45 or Steol CS-460 with 1:1 ratio on IFT for Miller 29 brine and crude oil at 46 °C.	73
Fig.5.4—Effect of shear rate on the viscosity of the surfactant/polymer solution at 46 °C for Miller 29.....	74
Fig.5.5—Stability tests of the surfactant/polymer solution at 46 °C for Miller 29. 74	
Fig.5.6—Cumulative oil recovery of sand packed column test using 1 PV surfactant/polymer slug for Miller 29.....	75
Fig.5.7—Cumulative oil recovery of core flood test using 1 PV surfactant/polymer slug for Miller 29.	76
Fig.5.8—Effect of Steol CS-460 concentration on the stability of the surfactant formulation at 50 °C for Primexx.	77
Fig.5.9—Effect of Steol CS-460 concentration on the phase behaviors of the surfactant formulation with crude oil at 50 °C for Primexx.	78
Fig.5.10—Effect of Steol CS-460 concentration on IFT of the surfactant formulation with crude oil at 50 °C for Primexx.....	79
Fig.5.11—Effect of shear rate on the viscosity of the surfactant/polymer solution at 50 °C for Primexx.	79

Fig.5.12—Stability of the surfactant/polymer formulation at 50 °C for Primexx..	80
Fig.5.13—Cumulative oil recovery of sand packed column test using 0.5 PV	
surfactant/polymer slug for Primexx.....	81
Fig.5.14—Cumulative oil recovery of core flood test using 0.5 PV	
surfactant/polymer slug for Primexx.....	82
Fig.5.15—Effect of Steol CS-460 concentration on the stability of surfactant	
formulation at 36 °C for Litchfield.	83
Fig.5.16—Effect of Steol CS-460 concentration on the phase behavior of the	
surfactant formulation with crude oil at 36 °C for Litchfield.....	84
Fig.5.17—Effect of Steol CS-460 concentration on IFT of the surfactant	
formulation with crude oil at 36 °C for Litchfield.....	85
Fig.5.18—Viscosity as a function of shear rate for wormlike micelles at different	
concentrations of hexyl glucoside for Litchfield.	86
Fig.5.19—Stability of the wormlike micelles (left) and surfactant formulation	
(right) at 36 °C for Litchfield.....	86
Fig.5.20— Cumulative oil recovery of sand packed column test using 0.1 PV Pre-	
slug + 1.5 PV binary slug for Litchfield.....	88
Fig.5.21—Cumulative oil recovery of core flood test using 0.1 PV Pre-slug + 1.5 PV	
binary slug for Lichfield.	89
Fig.5.22—Correlation of Sor after chemical flood and capillary number for three	
sites.....	90
Fig.6.1— Round-bottom pressurized glass vials with crimp seals with inserted	
septa used for phase behavior test at high temperature in this study.	94

Fig.6.2—Effect of IOS 15-18 concentration on stability of the surfactant at 90 °C.	
.....	94
Fig.6.3—Effect of IOS 15-18 concentration on the phase behavior of the surfactant with dodecane at 90 °C.	
.....	95
Fig.6.4—Effect of HG concentration on stability of 0.5 wt% IOS 15-18 at 90 °C.	96
Fig.6.5—Effect of HG concentration on phase behavior of 0.5 wt% IOS 15-18 with dodecane at 90 °C.	
.....	97
Fig.6.6—Effect of IPA concentration on stability of 0.5 wt% IOS 15-18 at 90 °C.	98
Fig.6.7—Effect of IPA concentration on phase behavior of 0.5 wt% IOS 15-18 with dodecane at 90 °C.	
.....	98
Fig.6.8—Effect of IPA concentration on IFT of 0.5 wt% IOS 15-18 formulation with dodecane at 90 °C.	
.....	99
Fig.6.9—Effect of SB concentration on the stability of 0.5 wt% IOS 15-18 at 90 °C.	
.....	100
Fig.6.10—Effect of SB concentration on the phase behavior of 0.5 wt% IOS 15-18 with dodecane at 90 °C.	
.....	100
Fig.6.11—Effect of SB concentration on IFT of 0.5 wt% IOS 15-18 with dodecane at 90 °C.	
.....	101
Fig.6.12—Cumulative oil recovery of sand packed column test using 1 PV surfactant slug.	
.....	102
Fig.6.13—Cumulative oil recovery of core flood test using 1 PV surfactant slug.	102

Abstract

After the primary and secondary production, there is still a great potential of enhanced oil recovery (EOR). Currently, the high oil price, increase of oil demand and maturing oil fields and the improvement in surfactant performance are generating a new wave of interest in chemical flood. Chemical flood injects surfactants to reduce interfacial tension (IFT) between oil and brine to reduce capillary force to help release oil, and polymers to increase the viscosity of the displacing water for mobility control to increase macroscopic sweep efficiency.

There is a great amount of trapped oil underneath the lands of Oklahoma. The objective of chemical flood was to recover a percentage of the trapped oil. The formation brine in Oklahoma reservoir has a very high salinity (> 10 wt% TDS) with substantial hardness. Thus the main objective of this study was to develop surfactant/polymer formulation for chemical flood in high salinity reservoirs.

Chapter 1 introduces the background and motivation of this study. Chapter 2 introduces the materials and methods used in this study. Chapter 3 presents the characterization of crude oil equivalent alkane carbon number (EACN) for surfactant flooding design, Chapter 4 presents formulating low-IFT microemulsions for high salinity formations using extended surfactants, Chapter 5 presents surfactant/polymer formulation of chemical flood for three high salinity reservoirs. Chapter 6 presents surfactant formulation of chemical flood for a high salinity and temperature reservoir. Chapter 7 summarizes this study and proposes some future work to be done.

Phase behavior test was used to develop surfactant formulation for given oil and brine. Mobility control was achieved by increasing the viscosity of displacing water by using either polymer or wormlike micelles. Once a good and stable surfactant/polymer formulation was developed, sand packed column test and core flood test were used to evaluate the performance of the chemical formulations developed for chemical flood in the laboratory.

The EACN of crude oil determined was 6.0-11.3. This study successfully developed surfactant/polymer formulations for chemical flood for several high salinity reservoirs in the laboratory. The optimal injection strategy using these surfactant/polymer formulations recovered a significant amount (25-73%) of residual oil after water flood in both the sand packed column tests and the core flood tests in the laboratory.

Chapter 1. Introduction

1.1. Potential of Enhanced Oil Recovery (EOR)

Depending on the production life of a reservoir, oil recovery can be classified into three stages: primary, secondary, and tertiary (Fig. 1.1).

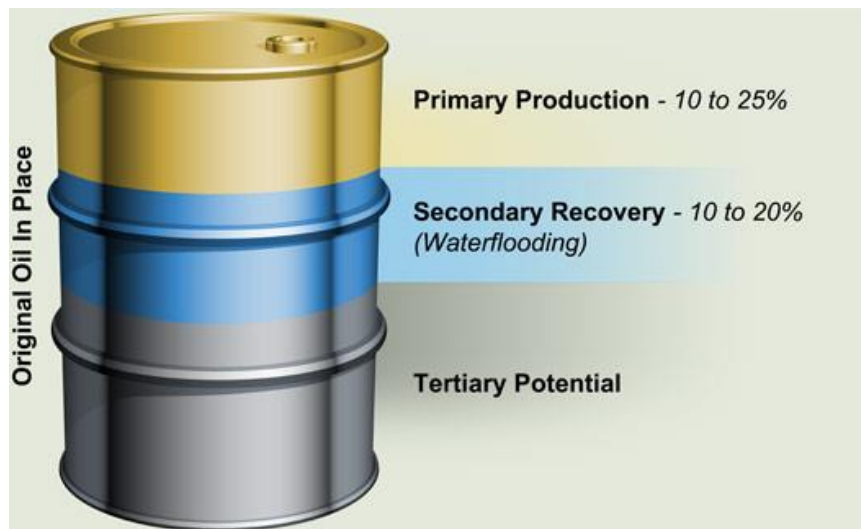


Fig.1.1—Three stages of oil production.

The first stage of oil recovery is primary recovery, which uses initially available natural energy in the reservoir. The natural energy includes natural water displacing oil downward into the well, expansion of the natural gas at the top of the reservoir and expansion of rock, expansion of initially dissolved gas in the crude oil, and gravity drainage resulting from the movement of oil within the reservoir from the upper to the lower parts where the wells are located. Typically, primary recovery attains 10% to 25% of the original oil in place (OOIP) in a reservoir (Green and Willhite 1998; Sheng 2010; Thomas 2008).

The second stage of oil recovery is secondary recovery, which begins when the well pressure falls until there is not enough subsurface pressure to force the oil to move up to the surface. Secondary recovery works by providing external energy into the reservoir to maintain or increase reservoir pressure. Secondary recovery methods include water injection, gas injection and gas (or artificial) lift. But the mainly secondary recovery method is water injection, also known as water flood. Typically a secondary recovery can recover additional 10% to 20% OOIP in a reservoir (Green and Willhite 1998; Sheng 2010; Thomas 2008).

The third stage of oil recovery is tertiary recovery, also known as enhanced oil recovery (EOR), which begins when secondary recovery is not enough to continue profitable extraction. EOR mainly tries to alter the properties of the oil to facilitate additional production by injecting special fluids such as thermal energy, miscible gases and chemicals. Accordingly, the three major types of EOR are thermal recovery (steam flood, in-situ combustion, and steam assisted gravity drainage) and miscible flood (CO₂, hydrocarbon and nitrogen injection), and chemical flood (surfactant, polymer, and alkaline flood). Thermal recovery, which injects heat to the reservoir to reduce the viscosity of the oil to improve its ability to flow, is most used to recover heavy oil. Miscible flood, which makes the gases expand, or mix with the oil to decrease viscosity to increase flow, is most often used to recover light oil. Chemical flood, which injects surfactants or alkali to reduce oil water interfacial tension (IFT) significantly to help release of oil, and polymers to increase the viscosity of the injected water for mobility control to increase macroscopic displacement efficiency, is applicable to a fairly wide

range of reservoirs. EOR can achieve another 5% to 15% OOIP in a reservoir depending on the methods used (Green and Willhite 1998; Sheng 2010; Thomas 2008).

Since oil price is often too low to make chemical flood economical on a large scale, large scale application of chemical flood is limited, even though chemical flood techniques have been around for several decades. However, currently, the high oil price, increase of oil demand and increase of maturing oil fields and the improvement in surfactant performance are generating a new wave of interest in chemical flood (Hirasaki et al. 2011).

1.2. Mechanisms of Chemical Flood

The macroscopic displacement efficiency is a measure of how well the displacing fluid has come in contact with the oil-bearing parts of the reservoir. The microscopic displacement efficiency is a measure of how well the displacing fluid mobilizes the residual oil once the fluid has come in contact with the oil. Microscopic displacement efficiency can be increased by reducing IFT between the displacing fluid and oil to reduce capillary forces. Macroscopic displacement efficiency can be increased by improving the mobility ratio by increasing the viscosity of the displacing fluid (Green and Willhite 1998).

1.2.1. Reduce IFT

Capillary pressure, which is the pressure difference across the interface between two immiscible fluids, is defined as the pressure difference between the non-wetting phase

and the wetting phase (Eq. 1.1). In oil and brine systems, brine is typically the wetting phase and oil is the non-wetting phase (Sheng 2010).

$$p_c = \frac{2\gamma \cos \theta}{r}, \dots \dots \dots (1.1)$$

Where p_c is capillary pressure, γ is the IFT between the two fluids; θ is the contact angle and r is the effective radius of the interface.

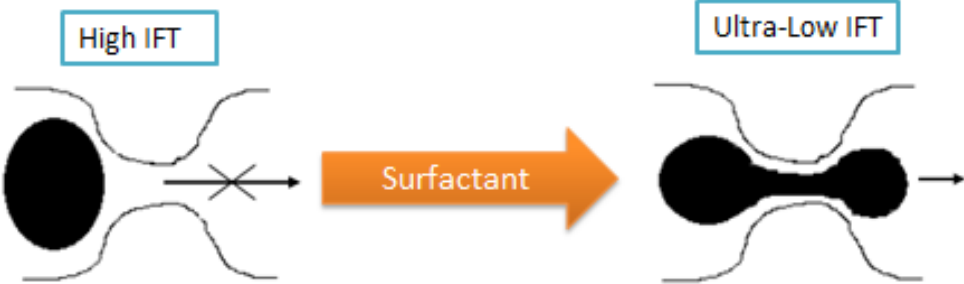


Fig.1.2—Use of surfactants to reduce IFT to reduce capillary force that traps oil.

In porous media, capillary pressure is the force necessary to squeeze an oil droplet through a pore throat by working against the IFT between oil and brine phases. From Eq. 1.1, we can see that capillary pressure is proportional to the IFT. At high IFT, the capillary forces are high and thus prevent oil from passing through the pore throat, which can cause injected water to bypass oil and leave behind a large quantity of oils in a waterflooded reservoir. But when surfactant is used to achieve ultralow IFT, the capillary forces are reduced to ultralow level, near zero, which can help dispersing oil in water to form thin and long oil drop to pass through pore throat easily and thus help recover oil (Fig. 1.2).

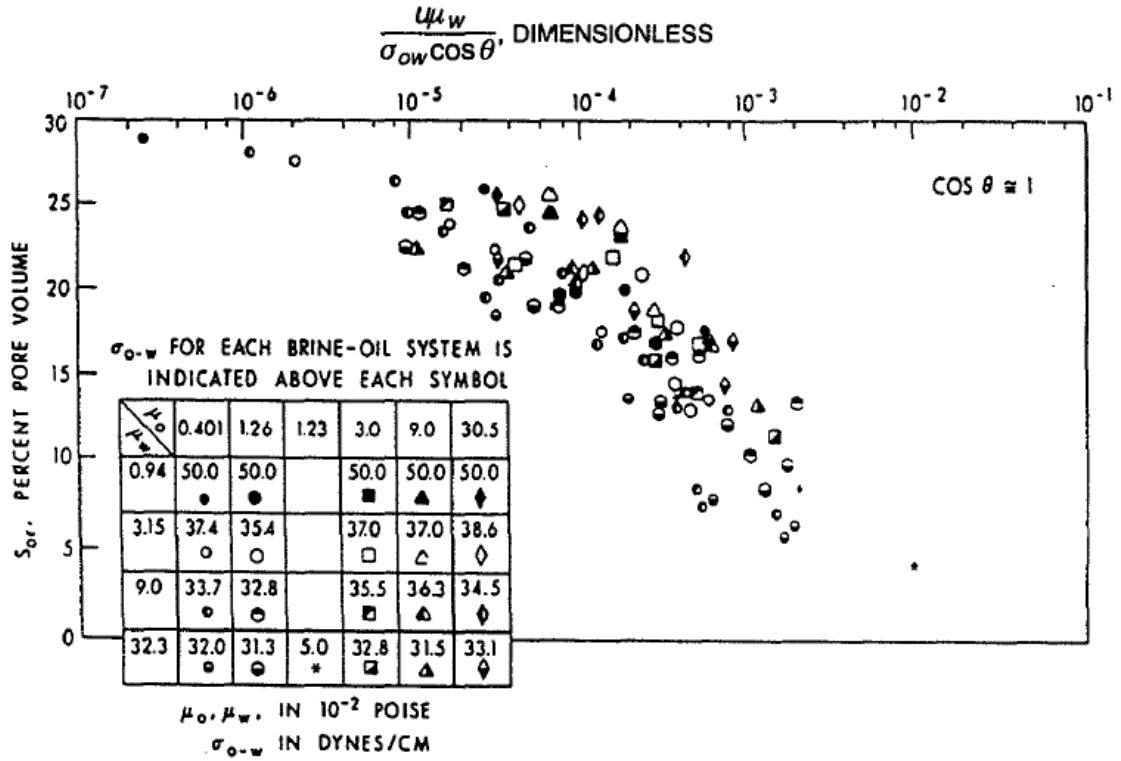


Fig.1.3—Schematic plot of correlation between the capillary number and residual oil saturation (Green and Willhite 1998).

There have been several studies investigating the effect of viscous forces and interfacial force on the mobilization of residual oil, which results in the correlations between the capillary number (N_c) and the fraction of oil recovered. The capillary number is the ratio of viscous forces, which mobilizes oil, to capillary (interfacial) force, which traps oil (Sheng 2010):

$$N_c = \frac{v\mu}{\gamma}, \dots\dots\dots(1.2)$$

Where v is the Darcy velocity, μ the viscosity of displacing fluid, γ is the IFT between water and oil.

Fig. 1.3 is a schematic plot of the correlation between the capillary number and residual oil saturation (S_{or}). The correlation shows that S_{or} decreases with increasing the capillary number. The capillary number can be increased by increasing the viscous forces or decreasing the IFT using surfactants, which is the most effective and practical way to increase the capillary number. It is shown that at typical reservoir velocities, IFT between crude oil and brine should be reduced from 20-30 mN/m to 0.001-0.01 mN/m to achieve high oil recovery.

1.2.2. Mobility Control

The mobility (λ) of a fluid is defined as the ratio of its effective permeability to its viscosity. Mobility ratio (M) is the ratio of the mobility of the displacing phase (brine) to the mobility of the displaced phase (oil).

$$M = \frac{\lambda_w}{\lambda_o} = \frac{\frac{k_w}{\mu_w}}{\frac{k_o}{\mu_o}}, \dots\dots\dots(1.3)$$

Where k_o and k_w are the effective permeability of oil and brine, respectively, and μ_o and μ_w are the viscosities of oil and brine, respectively.

The mobility control in chemical flood is primarily based on maintaining a favorable mobility ratio to improve sweep efficiency (Albonico and Lockhart 1993). From Eq. 1.3, it is evident that when $M \leq 1$, the displaced fluid is more mobile than the displacing fluid. When $M > 1$, the displaced fluid is less mobile than the displacing fluid, thus viscous fingering could occur, and this can bypass a significant amount of oil (Hirasaki and Pope 1974). Fig. 1.4 provides an example of displacement efficiency improvement

by mobility control over conventional water flood. In a conventional water flood, if the mobility ratio is unfavorable ($M > 1$), the water tends to finger by the oil and to move by the shortest path to the production well. Thus, mobility control is needed to reduce viscous fingering to develop a more uniform macroscopic sweep of the reservoir to improve oil recovery. Thus mobility control is required for a high oil recovery in a chemical flood (Green and Willhite 1998). When accurate effective permeability data are not available, the required mobility can be achieved by increasing the viscosity of water based on that of the crude oil.

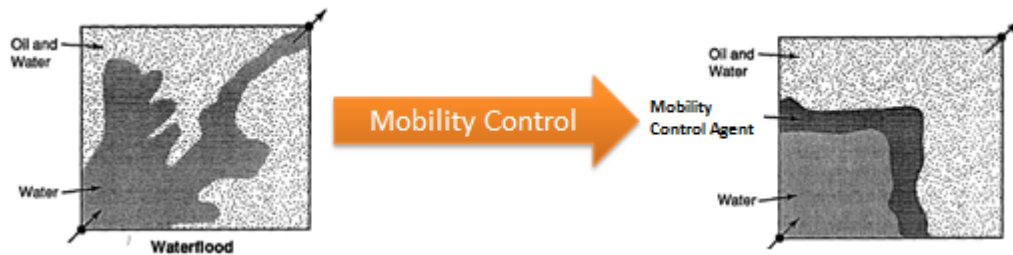


Fig.1.4—Mobility control for chemical flood (Green and Willhite 1998).

1.3. Surfactants

Surfactants are composed of a hydrophobic hydrocarbon tail and a hydrophilic head, thus they are soluble in both oil and brine. Surfactants can reduce the surface tension of a liquid, and the IFT between two liquids significantly (Salager et al. 2005).

Anionic surfactants are most widely used in chemical flood because they exhibit relatively low adsorption at neutral to high pH on both sandstones and carbonates, can be tailored to a wide range of conditions, and are widely available at relative low cost. Two widely used anionic surfactants in chemical flood are sulfates and sulfonates.

Alcohol ether sulfate is one of the most used sulfates for chemical flood at low temperature. Internal olefin sulfonate (IOS), alpha olefin sulfonate (AOS), and petroleum sulfonate (PS) are the most used sulfonates for chemical flood at high temperatures (Sheng 2010).

1.3.1. Micelles and Wormlike Micelles

Micelles are aggregate of surfactant molecules dispersed in a liquid colloid. The concentration of surfactants above which micelles form and all additional surfactants added to the system go to micelles is called the critical micelle concentration (CMC) (Fig. 1.5) (Salager et al. 2013a; Salager et al. 2013b).

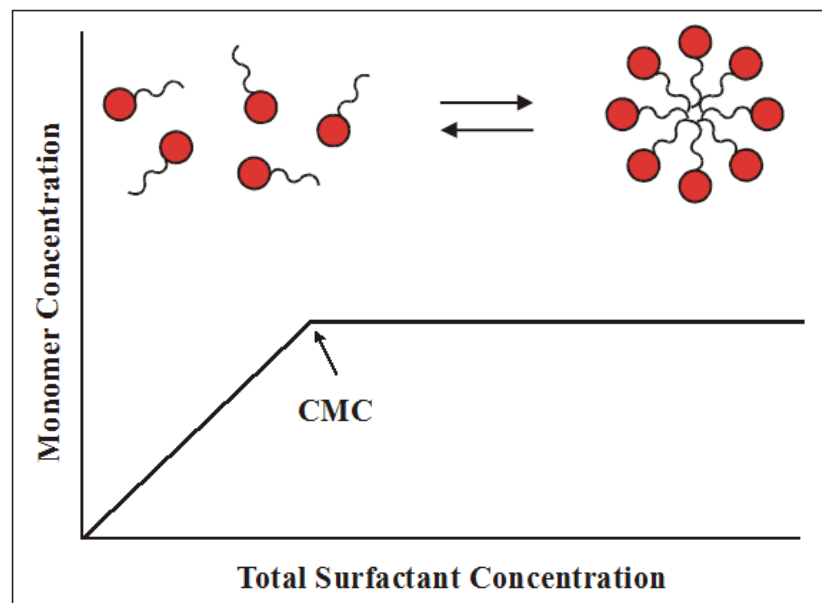


Fig.1.5—Definition of critical micelle concentration (CMC).

Normal micelles form in water solutions, with hydrophobic hydrocarbon groups in the interior and hydrophilic head groups exposed to the external aqueous solution. Reverse micelles form in nonpolar solvents, with hydrophilic head groups oriented in the

interior, and hydrophobic hydrocarbon groups exposed to the similar groups of the surrounding solvent (Salager et al. 2005).

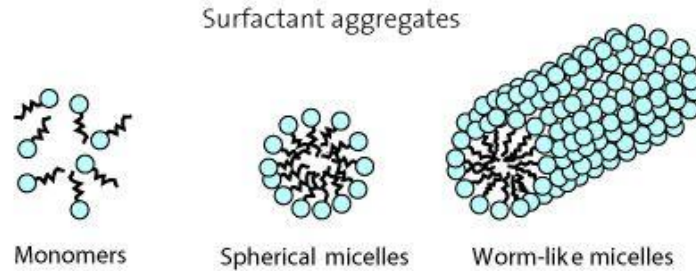


Fig.1.6—Schematic diagram of wormlike micells.

Wormlike micelles are elongated and semi-flexible surfactant aggregates, which results from the self-assembly of surfactant molecules in aqueous solutions. The self-assembly of surfactant monomers due to non-covalent bonds or intermolecular attractions can form spherical micelles at low surfactant concentrations, while it can form larger aggregates called wormlike micelles at higher surfactant concentrations (Fig. 1.6) (Raj 2013; Yang 2002; Yu et al. 2009).

The entangled wormlike micelles form a network that exhibits viscoelastic properties, which results in increase in the viscosity of fluids like polymer. Even in lower surfactant concentration, the addition of salt, co-surfactant or co-solvent can cause the transition from spherical micelle to wormlike micelles. This makes it especially suitable for high salinity reservoir because the viscosity is not that much affected by salinity as polymers. In addition, wormlike micelles have a higher tolerance to harsh conditions such as high temperature. Thus wormlike micelles would be a good mobility control agent for chemical flood in high salinity and high temperature reservoirs.

Traditionally polymer is used as the main mobility control agent by increasing the viscosity of the injected fluid. However, polymer is susceptible to high shear rate, because it can lose viscosity at high shear rate. Recently, it is reported that wormlike micelles, a special kind of surfactant aggregates that show viscoelastic properties similar to polymers, can be used as a potential alternative to polymer as mobility control agent in chemical flood, because they have the advantage of breaking and reforming under varying shear stress and thus maintaining the viscosity under changeable shear rate (Awang et al. 2012). Thus they are especially suitable for tight reservoirs, because high viscosity polymer can cause low injectivity and even plugging in tight formation.

1.3.2. Microemulsions

Phase behavior test is widely used to design surfactant formulations to achieve ultralow IFT between a given oil and brine. The phase behavior among oil, water and surfactant, which depends on many parameters such as the types and concentrations of surfactants, co-surfactants, co-solvents, oil, water salinity, and temperature, can be classified into Winsor Type I, II, and III microemulsions (Fig. 1.7).

Microemulsions are thermodynamically stable, clear and isotropic liquid mixtures of oil, water and surfactant. Winsor Type I microemulsions are oil in water microemulsions, in that oil is solubilized in normal micelles in the water phase. Winsor Type II microemulsions are water in oil microemulsion, in that water is solubilized in reverse micelles in the oil phase. Both Winsor Type I and II microemulsions are difficult to achieve ultralow IFT, thus they should be avoided in surfactant formulation for chemical flood. Winsor Type III microemulsions, which are also called middle

phase microemulsions, are water and oil swollen micelles in a bi-continuous structure of surfactant at the oil and brine interface, where equal amount of oil and brine are solubilized into the bi-continuous structure of surfactant. Winsor Type III microemulsions can achieve ultralow IFT, which is desired surfactant formulation for chemical flood.

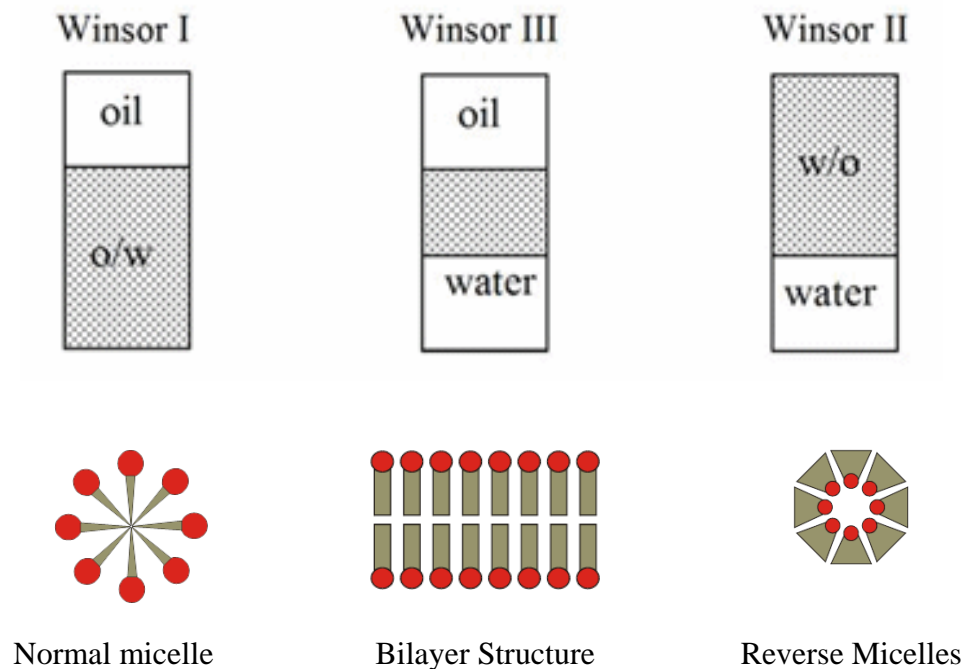


Fig.1.7—Types of microemulsions.

With increasing hydrophobicity of the surfactant formulation by increasing salinity, the microemulsion system changes from Winsor Type I, to Type III and to Type II and the oil/water IFT goes through a minimum value at optimal condition in Winsor Type III region. Salinity and IFT at optimal conditions are denoted as S^* and IFT^* . For a given oil and brine, Winsor Type III microemulsions can be obtained by adjusting the hydrophobicity of the surfactant formulation by changing the type and concentration of

co-surfactant or co-solvent, which has been proved successful in both laboratory, pilot and field tests for chemical flood design.

1.3.3. Hydrophilic-Lipophilic Deviation

Phase behavior of water, oil and surfactant is one of the most important factors that determine the efficiency of chemical flood using surfactants (Acosta and Bhakta 2009; Acosta et al. 2003; Acosta et al. 2008; Hirasaki and Zhang 2004; Huh 1979). Early experimental studies have shown that the optimal salinity for a water, oil and surfactant is a function of the alkane carbon number (ACN) for normal alkanes, or equivalent alkane carbon number (EACN) for a mixture of hydrocarbons or non-alkyl hydrocarbons (Anton et al. 1997; Baran et al. 1994; Bouton et al. 2010; Hammond and Acosta 2010; Han et al. 2009; Wu and Sabatini 2000).

The ACN characterizes the hydrophobicity of alkane-type hydrocarbons, with compounds with higher ACN being more hydrophobic. For a mixture of hydrocarbons or non-alkyl hydrocarbons, such as crude oil, EACN is used. The EACN assigns a single alkane analog to represent the behavior of a mixed hydrocarbon system. The EACN concept provides a simplified characteristic of crude oil by quantifying its hydrophobicity (Aoudia et al. 1995; Cayias et al. 1976; Roshanfekar and Johns 2011; Wade et al. 1977).

A hydrophilic-lipophilic deviation (HLD) concept has been proposed to describe microemulsion systems containing hydrocarbons, anionic surfactant, alcohol and brine (Salager et al. 1979).

$$\text{HLD} = \ln S - K * \text{EACN} - f(A) + C_c - \alpha_T \Delta T, \dots \dots \dots (1.4)$$

Where S is salinity as wt% NaCl, K is a characteristic parameter of the anionic surfactant, EACN is equivalent alkane carbon number for a mixture of hydrocarbons or non-alkyl hydrocarbons, and alkane carbon number for normal alkanes, C_c is the characteristic curvature of the surfactant, the value of the C_c reflects the tendency of the surfactant to form normal micelles (negative values of C_c) or reverse micelles (positive values of C_c) for a given oil/water, f(A) is a function of the alcohol type and concentration, α_T is a temperature parameter for anionic surfactant, ΔT is the temperature deviation measured from a certain reference temperature (25 °C). Negative, zero, or positive HLD values indicate the formation of Winsor Type I, Type III or Type II microemulsions, respectively.

When using anionic surfactants, the optimal condition also known as the optimal salinity (S*) can be obtained by varying the salt concentration. At S*, the HLD value is zero. Thus HLD can be rewritten as:

$$\ln S^* = K * \text{EACN} + f(A) - C_c + \alpha_T \Delta T, \dots \dots \dots (1.5)$$

If we conduct the phase behavior tests at room temperature in the absence of any alcohol, Eq. 1.5 is simplified to:

$$\ln S^* = K * \text{EACN} - C_c, \dots \dots \dots (1.6)$$

If we know the salinity and EACN of crude oil for a reservoir, and f(A) and α_TΔT, we can try different surfactants with different K and C_c to check if their parameters can satisfy Eq. 1.5. If not, we can try different surfactant combination to satisfy these

equations. For a surfactant mixture, we can estimate parameters of K and Cc using the following linear mixing rules (Witthayapanyanon et al. 2008). Thus the HLD equation can aid surfactant formulation for chemical flood.

$$C_{c_{mix}} = \sum x_i C_{c_i} \dots \dots \dots (1.7)$$

$$K_{mix} = \sum x_i K_i \dots \dots \dots (1.8)$$

Where x_i represents the mole fraction of surfactant i in the surfactant mixture.

1.4. Polymers

A polymer is a large molecule composed of many repeated unit of monomers. Water soluble polymer can increase the solution viscosity and thus provide mobility control for chemical flood. The two widely used polymers for chemical flood are partially hydrolyzed polyacrylamide and xanthan gum. The most widely used polymer for chemical flood is hydrolyzed polyacrylamide (HPAM) (Fig. 1.8).

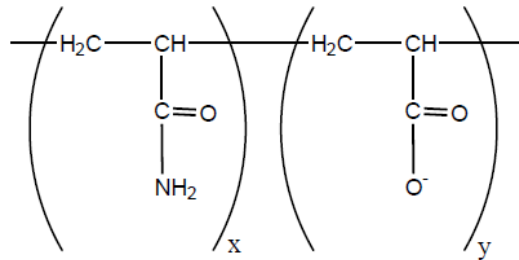


Fig.1.8—Partially hydrolyzed polyacrylamide.

HPAM is formed by reacting polyacrylamide with a base to convert some of the amide groups (CONH₂) to carboxyl groups (COO⁻) to reduce adsorption, which introduces negative carboxyl groups to the polymer chains of HPAM, and this has a large impact

on the rheological properties of the polymer solution depending on the salinity of the brine. At low salinity, the negatively charged carboxyl groups on the polymer chain repel each other and cause the polymer chains to stretch, which results in high viscosity. However, at high salinity, the repulsive forces are shielded by a double layer of electrolytes, thus the stretch of HPAM flexible chains is reduced, which results in low viscosity. HPAM has low tolerance to high temperature and high salinity, thus HPAM is a good polymer candidate for chemical EOR in a reservoir with low temperature and low salinity, but it can be used up to 90 °C depending on the brine hardness (Green and Willhite 1998).

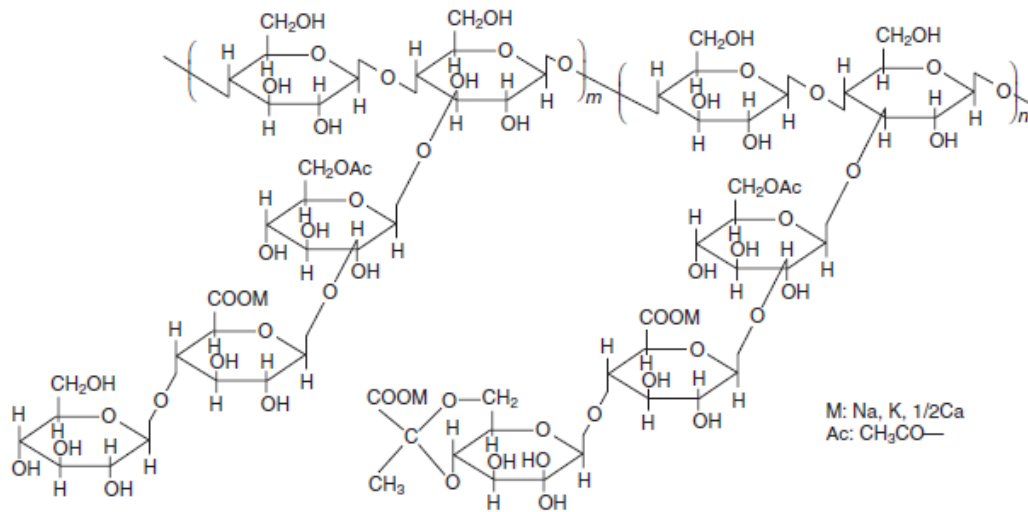


Fig.1.9—The structure of a xanthan gum.

Another widely used polymer for chemical flood is a biopolymer, xanthan gum, which is made up of polysaccharide, produced by the fermentation of the bacteria genus *Xanthomonas campestris*. The structure of a xanthan gum is shown in Fig. 1.9.

Since xanthan gum acts like a semi-rigid rod, it has a very high resistance to mechanical degradation (Littmann et al. 1992). Xanthan gum has certain tolerance for salinity, but it is not tolerant to extreme pH, hardness and bacterial attack. Its temperature tolerance changes with water composition, but thermal degradation starts to take place around 90 °C (Sheng 2010). In general, HPAM is much more sensitive to salinity than xanthan gum. Viscosity loss could occur for HPAM, but not for xanthan gum at high shear rate. The average molecular weights of xanthan gum used for chemical flood is from 1 million to 15 million Daltons (Seright et al. 2011; Thomas 2008).

1.5.Motivation

The OOIP underneath the lands of Oklahoma is 84 billion barrels of oil (BBO) (Fig. 1.10). By 2008, only 14.78 BBO has been produced, with remaining reserves of 0.53 BBO, which means that 68.7 BBO (81.8% of OOIP) are trapped (Boyd 2008). The objective of EOR is to recover a percentage of the trapped oil.

By now, 90% of the wells in Oklahoma, which produce less than 10 barrels of oil per day, are considered as marginal wells, which are good candidates for EOR. Currently, each year, 750 to 1000 marginal wells are being abandoned in Oklahoma. Once a field is abandoned, an EOR project becomes much more difficult and expensive to conduct, which can make potential reserves lost. If a candidate field is waterflooded, existing water flood infrastructure can be readily used for a chemical flood, which makes it ideal for companies who already use water flood to produce trapped oil (Fig. 1.11) (Puerto et al. 2010; Sanz and Pope 1995; Wellington and Richardson 1997, Xia et al. 2008; Zhang et al. 2006; Zhang et al. 2008). In addition, chemical flood does not have depth or

pressure limitation, or environmental issues, in that they have already been used in fracturing fluids and environmental remediation projects. Moreover, chemical flood has the advantages of high degree of residual oil mobilization (Hsu et al. 2012).

The Target – Unlocking Trapped Oil

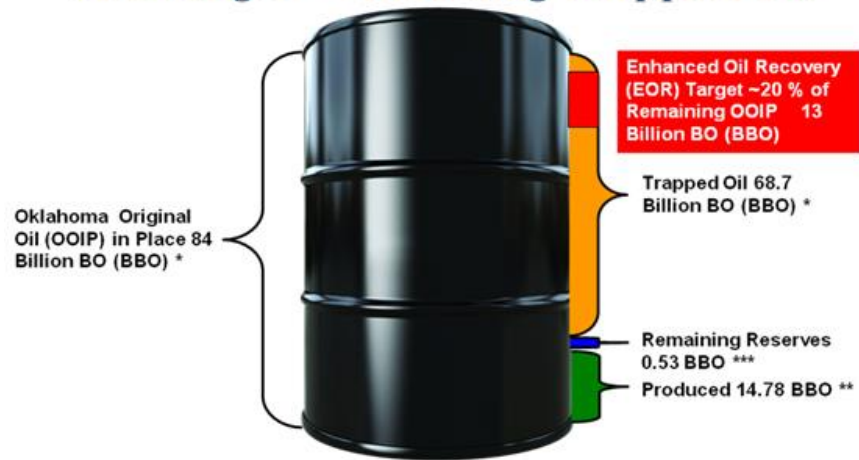


Fig.1.10—The trapped oil in Oklahoma (Boyd 2008).

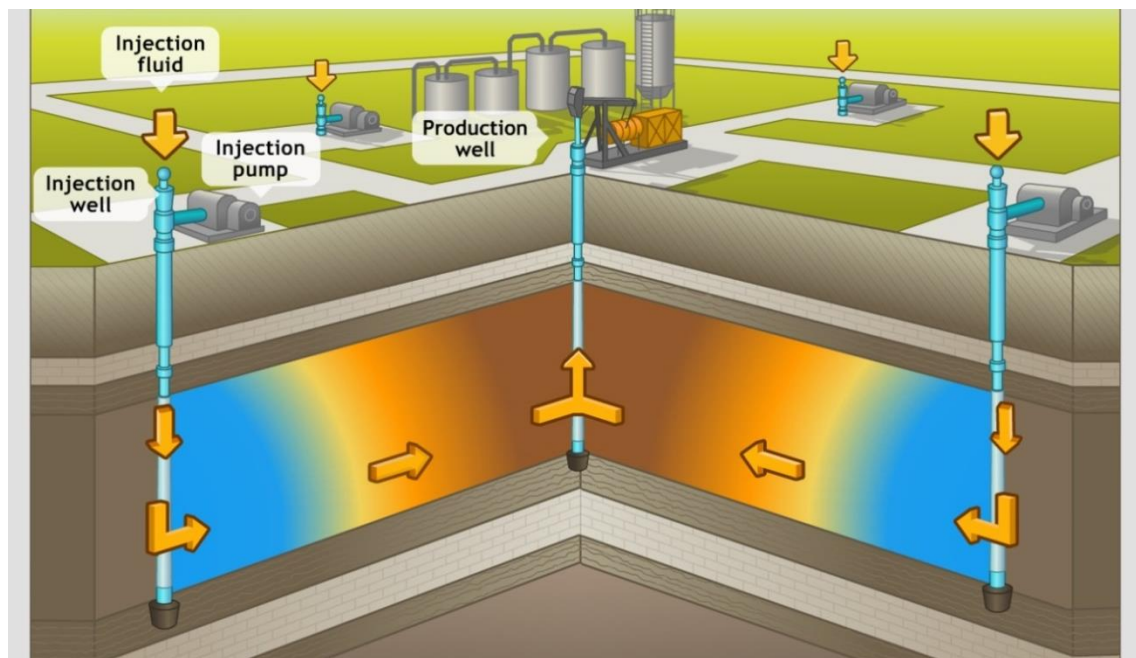


Fig.1.11—Water flood infrastructure.

The formation brine in Oklahoma reservoir has a very high salinity (> 10 wt% TDS) with substantial hardness (Hsu et al. 2012). In fact, many reservoirs that are suitable for chemical flood have high salinity and/or high temperatures. Such reservoirs may have brine with TDS up to 20 wt% and substantial hardness, and the temperatures up to 120 °C (Barnes et al. 2008a; Barnes et al. 2008b). These conditions are challenging for chemical flood design because injected surfactants or polymers must remain chemically stable at reservoir conditions for the duration of the project, which could last for years. Otherwise hydrolysis due to high temperature and precipitation of surfactants due to high salinity especially hardness, can make surfactants lose activity. Moreover, surfactant phase separation could result in a more viscous surfactant rich phase, which flows more slowly in the reservoirs, resulting in poor contact with the oil. All these can fail the surfactants to develop ultralow IFT with crude oil at reservoir conditions, resulting in low oil recovery. The polymer degradation due to high temperature and precipitation due to high salinity especially hardness can result in considerable viscosity loss, which can fail the mobility control, resulting in low oil recovery (Elraies et al. 2010; Flaaten et al. 2009; Flaaten et al. 2010; Veedu et al. 2010). Thus, it is still challenging to use chemical flood in reservoirs with high temperature and high salinity. However, so far most of the studies for chemical flood have focused on the chemical flood at low salinity and/or low temperature (Vermolen et al. 2011). Since many reservoirs that are suitable for chemical flood have high salinity and/or high temperatures, thus it is of great importance to investigate the use of chemical flood for such reservoirs. The main objective of this study is to design chemical flood for high salinity reservoir.

1.6. Hypothesis

The targeted formation brine has a very high salinity (> 10 wt% TDS) with some substantial hardness. The high salinity would reduce the solubility of surfactants in such brines. Thus when developing an effective surfactant/polymer formulation, we have to find a method to increase the solubility of the surfactant in the high salinity brine. One method to develop stable surfactant formulation for chemical flood is to use surfactants with a high affinity to water, such as extended surfactants with EO group. In addition, we can also use co-solvents such as isopropanol (IPA), sec-Butanol (SB) or hydrophilic linker to increase the salt tolerance of surfactant formulation to prevent surfactant phase separation or precipitation. Extended surfactants and co-solvents or hydrophilic linkers were used to aid the development of stable surfactant formulation for high salinity reservoirs.

1.7. Research Plan

1.7.1. Characterization of Crude Oil EACN for Surfactant Flooding Design

Early EOR efforts in the literature had shown that the optimal brine salinity developed for a specific brine/oil/surfactant mixture was largely related to the alkane carbon number (ACN, the number of carbons in a straight alkane chain) for normal alkanes, or so called equivalent alkane carbon number (EACN) for a mixture of hydrocarbons or non-alkyl hydrocarbons.

The ACN concept satisfactorily characterizes the hydrophobicity of alkane-type hydrocarbons, with higher ACN compounds being more hydrophobic. For a mixture of

hydrocarbons or rather complex hydrocarbons, such as crude oil, the EACN is conveniently used for surfactant formulation design purposes. The EACN assigns a single “alkane analog” to represent the behavior of a complicate hydrocarbon mixture. The EACN concept thus provides a useful tool to simplify the characterization of the crude oil even without sophisticated compositional analysis to determine its hydrophobicity for the screening tests.

Eq. 1.5 shows there exists a very good linear relationship between $\ln S^*$ and EACN. For a given well studied anionic surfactant, if we know the parameters (K , $f(A)$, C_c and α_T) in Eq. 1.5, the EACN of a crude oil can be calculated from Eq. 1.5 once we obtain the optimal salinities for the targeted oils with unknown carbon number and the same surfactant solution to obtain these parameters (K , $f(A)$, C_c and α_T).

For a new generation (anionic) surfactant, if we do not know the parameters (K , $f(A)$, C_c and α_T) in the equation, we can first find these parameters in Eq. 1.5 by determining the optimal salinities for the selected oils with known carbon number and the surfactant solution with a linear regression technique. The EACN of crude oil can then be calculated from Eq. 1.5 once we obtain the optimal salinities for the system of oils with unknown carbon number and the same surfactant solution, where the values of K , $f(A)$, C_c and α_T been calculated.

The EACN of a mixture of alkanes or alkanes and non-alkyl hydrocarbons have been determined in many earlier studies based on Eq. 1.5 using conventional surfactants. In more recent studies, anionic extended surfactants (Fig. 1.12), which have intermediate-polarity groups such as propylene oxide (PO) and/or ethylene oxide (EO) groups

inserted between the surfactant hydrophilic head and hydrocarbon tail, have been shown to generate middle phase microemulsions with greater solubilization and lower IFT without sacrificing their water solubility. Thus, due to these attractive properties that are highly desirable for practical uses, multiple extended surfactants with different functionalities have received great attentions and have been investigated for many practical applications lately. The estimated EACN for a mixture of alkanes or alkanes and non-alkyl hydrocarbons have been documented recently based on Eq. 1.5 using some of the extended surfactants (Castellino et al. 2011; Do et al. 2009; Kiran et al. 2009; Phan et al. 2010a; Witthayapanyanon et al. 2006; Witthayapanyanon et al. 2008; Wu et al. 2000).

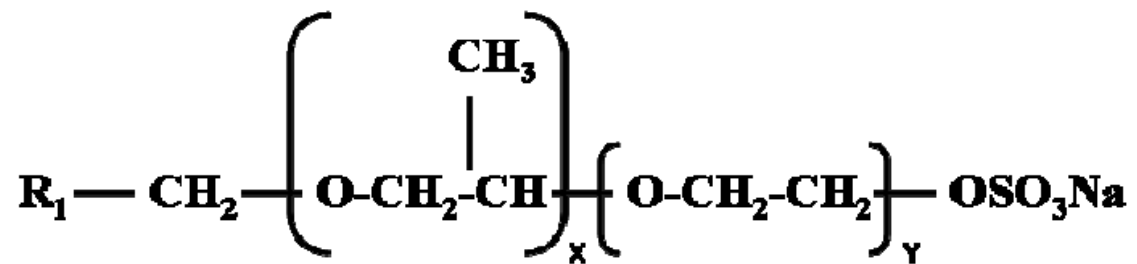


Fig.1.12—Basic structure of extended surfactants.

However, only a limited number of studies have focused on determining the EACN of crude oils, which is an important tool for designing surfactant flooding. In addition, to the best of our knowledge, there are no studies reporting the determination of the EACN of crude oils using extended surfactants.

Thus, in this study, the EACNs for crude oils from a dozen field sites (Miller 29, Fox Creek, Woods, War Party, Albert Barney 13, Litchfield 76, Stewart Fee 56, Lm Jones

46 Lm Jones 52, Mullendore-Berry 34, Earlsboro, Albert Barney 18, SE Hewitt, Litchfield and Primexx) were measured based on the above equations (Eq. 1.5) using a convenient technique developed for both conventional EOR surfactants and the selected anionic extended surfactants.

1.7.2. Formulating Low-IFT Microemulsions for High Salinity Formations Using Extended Surfactants

According to the classical Winsor R-concept, equally increasing the interactions of surfactant toward both oil and water phases can generate middle phase microemulsions with greater solubilization capacity and lower IFT (Phan et al. 2010b). One approach to enhance these oil/surfactant and water/surfactant interactions is to increase both the hydrophilicity of the surfactant head group(s) and the chain length of the hydrocarbon (or hydrophobic) tail; however, with increasing the tail group length, the surfactant molecules tend to lose their aqueous solubility, which can severely restrain its application (Do and Sabatini 2010; Kayali et al. 2010; Panswad et al. 2011).

To overcome the solubility issues and increase the flexibility of formulation, extended surfactants, which have intermediate-polarity groups such as propylene oxide (PO) and/or ethylene oxide (EO) groups inserted between the surfactant hydrophilic head and hydrocarbon tail, are introduced and have been shown to successfully achieve the middle phase microemulsions with much better solubilization and lower IFT at wider range of salt conditions without sacrificing their performance and aqueous solubility (Arpornpong et al. 2010; Charoensaeng et al. 2008; Charoensaeng et al. 2009; Fernandez et al. 2005a; Fernandez et al. 2005b).

Since extended surfactants have moderate polarity functional groups in their structures, some of these compounds not only have a longer hydrocarbon tail, but also exhibit a much smoother transition from the polar aqueous regime to the nonpolar oil regime near the oil/water interfaces. Not surprisingly, middle phase microemulsions with higher solubilization capacity and lower IFT can be formulated with the boost of different extended surfactants for a wide range of oils. In last decade, due to their attractive properties that are desirable for practical uses, extended surfactants have received a lot of attentions and have been systemically investigated for various applications (Klaus et al. 2010a; Klaus et al. 2010b; Klaus et al. 2011; Phan et al. 2011; Velasquez et al. 2010; Watcharasing et al. 2009; Witthayapanyanon et al. 2010).

However, few studies have reported the effects of co-solvent, co-surfactants, different extended surfactants and temperature on the middle phase microemulsion formations. Specifically, the comparisons of different extended surfactants with a conventional surfactant, sodium dioctyl sulfosuccinate (AOT) for middle phase microemulsion formations in the presence of a co-solvent, and the effect of alkane carbon number on the optimal salinity for the extended surfactant systems in the presence of a co-solvent.

As part of the designing tasks for field pilot chemical EOR trial in this study, different extended surfactants were first studied to determine the effects of co-solvent, co-surfactants, and different reservoir temperatures on the middle phase microemulsion formations. In parallel tests, the optimal salinities of several extended surfactants and AOT in the presence of a co-solvent were also compared. Lastly, the effect of alkane carbon number on the optimal salinity for the extended surfactant systems in the presence of a co-solvent was studied using an empirical equation.

1.7.3. Surfactant/Polymer Formulation of Chemical Flood for Three High Salinity Reservoirs

This study attempted to develop a surfactant/polymer formulation for three high salinity reservoirs. Table 1.1 shows the properties of three high salinity reservoirs. Once a good and stable surfactant/polymer formulation is developed, sand packed column test and core flood test were used to assess chemical flood in the laboratory to evaluate the performance of the chemical formulations developed.

Sites	Miller 29	Primexx	Litchfield
Reservoir temperature, °C	46	50	36
Average permeability, mD	50	75	17
Brine salinity, wt% TDS	18.5	13.0	16.4
Crude oil EACN	10.7	6.0	10.3
Crude oil viscosity at reservoir temperature, cp	5.0	2.3	10.4

1.7.4. Surfactant Formulation of Chemical Flood for a High Salinity and Temperature Reservoir

This study attempted to develop the surfactant formulation for a high salinity (15 wt% NaCl) and high temperature (90 °C) reservoir. Dodecane (EACN =12) was used as the oil. Once a good and stable chemical formulation was developed, sand packed column test and core flood test were used to assess chemical flood in the laboratory to evaluate the performance of the chemical formulations developed.

1.8. Summary

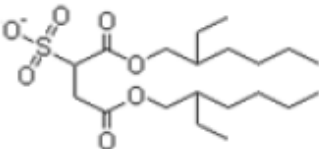
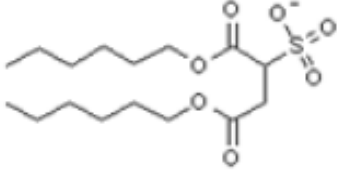
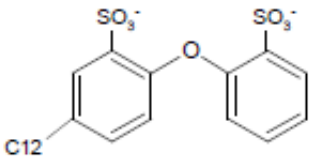
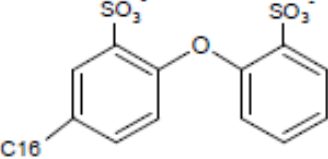
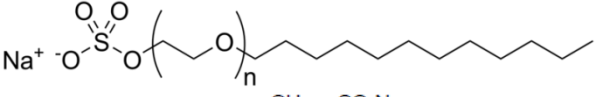
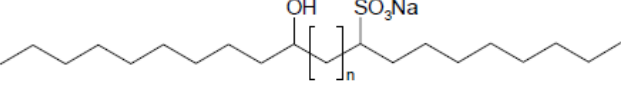
Chemical flood injects surfactants to IFT between oil and brine to reduce capillary force to help release of oil, and polymers to increase the viscosity of the displacing water for mobility control to increase macroscopic sweep efficiency.

There is a great amount of trapped oil underneath the lands of Oklahoma. The objective of chemical flood was to recover a percentage of the trapped oil. The formation brine in Oklahoma reservoir has a very high salinity (> 10 wt% TDS) with substantial hardness, which are challenging for chemical flood design because injected surfactants or polymer must remain chemically stable at reservoir conditions. Thus the main objective of this study was to develop surfactant/polymer formulation for chemical flood in high salinity reservoirs. The objectives of this study included characterization of crude oil EACN for surfactant flooding design, formulating low IFT microemulsions for high salinity formations using extended surfactants, surfactants/polymer formulation of chemical flood for three high salinity reservoirs (Miller 29, Primexx and Litchfield), and surfactant formulation of chemical flood for a high salinity and temperature reservoir.

Chapter 2. Materials and Methods

2.1. Materials

Conventional surfactants used in this study were sodium dioctyl sulfosuccinate (AOT), sodium dihexyl sulfosuccinate (AMA), sodium hexadecyl diphenyl oxide disulfonate (Calfax 16L-35), sodium dodecyl diphenyl oxide disulfonate (Calfax DB-45), and sodium laureth sulfate (Steol CS-460).

Surfactant	Structure
AOT	
AMA	
Calfax DB-45	
Calfax 16L-35	
Steol CS-460	
IOS 15-18	

n = 0 - 2

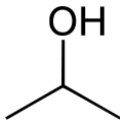
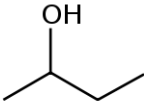
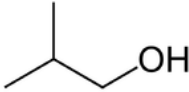

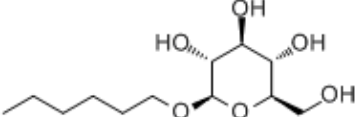
Both AMA (80 wt%) and AOT (70 wt%) were purchased from Fisher Scientific. Calfax 16L-35 (35 wt%) and Calfax DB-45 (45 wt%) were purchased from Pilot Chemical (Cincinnati, OH). Steol CS-460 (60 wt%) was purchased from Stepan Company (Northfield, IL). Internal Olefin Sulfonate IOS 15-18 (33 wt%) was provided by Shell Chemical Company (Houston, TX). The molecular structures of the above mentioned surfactants are summarized in Table 2.1.

The extended surfactants evaluated in this work contained various numbers of PO and/or EO groups between the sulfate head and hydrocarbon tail [R-(PO)_x-(EO)_y-SO₄Na] (Table 2.2). These extended surfactant samples were provided by Sasol North American Inc. (Lake Charles, LA).

Extended Surfactant	Hydrocarbon Chain Length	PO #	EO #	Active, wt %
C ₈ H ₁₇ -(PO) ₄ -SO ₄ Na	8	4	-	33.0
C ₈ H ₁₇ -(PO) ₄ -(EO) ₁ -SO ₄ Na	8	4	1	32.3
C ₁₀ H ₂₁ -(PO) ₄ -(EO) ₁ -SO ₄ Na	10	4	1	32.2
C ₁₂ H ₂₅ -(PO) ₄ -SO ₄ Na	12	4		32.3
C ₁₂ H ₂₅ -(PO) ₄ -(EO) ₁ -SO ₄ Na	12	4	1	30.2
C ₁₂ H ₂₅ -(PO) ₆ -SO ₄ Na	12	6	-	31.3
C ₁₂ H ₂₅ -(PO) ₄ -(EO) ₃ -SO ₄ Na	12	4	3	26.67
C ₁₂ H ₂₅ -(PO) ₃ -(EO) ₄ -(PO) ₃ -SO ₄ Na	12	6	4	26.27
C ₁₂ H ₂₅ -(PO) ₃ -(EO) ₄ -SO ₄ Na	12	3	4	28.08
C _{12,13} H _{25,27} -(PO) ₃ -(EO) ₄ -SO ₄ Na (Branched)	12-13	3	4	28.27
C _{12,13} H _{25,27} -(PO) ₈ -SO ₄ Na	12-13	8	0	86.35

Butyl carbitol (BC), isobutanol, isopropanol (IPA), sec-Butanol (SB) and hexyl glucoside (HG) were used as co-solvents in this study. Butyl carbitol (BC) (99 %), isobutanol (99 %), isopropanol (IPA) (99 %), sec-Butanol (SB) (99 %) were purchased from Sigma-Aldrich (Saint Louis, MO) and hexyl glucoside (75 wt%) was purchased

from Stepan Company (Northfield, IL). The molecular structures of the above mentioned co-solvents are summarized in Table 2.3.

TABLE.2.3—MOLECULAR STRUCTURE OF SOME CO-SOLVENT USED IN THIS STUDY	
Chemicals	Structure
Isopropanol (IPA)	
sec-Butanol (SB)	
Isobutanol	
Butyl carbitol (BC)	
Hexyl glucoside (HG)	

Sodium chloride (99 wt%), pentane (99 wt%), hexane (95 wt%), heptane (99 wt%), octane (99 wt%), decane (99 wt%), dodecane (99 wt%) and tetradecane (99 wt%) were purchased from Sigma-Aldrich (Saint Louis, MO).

Sudan Black is a non-fluorescent, relatively thermo stable fat-soluble dye. For the sand packed column tests and core flood tests using dodecane, Sudan Black was used to dye the dodecane to make the oil visible. Sudan Black was purchased from Fisher Scientific.

The crude oils and field brines (Miller 29, Fox Creek, Woods, War Party, Albert Barney 13, Litchfield 76, Stewart Fee 56, Lm Jones 46, Earlsboro, Albert Barney 18, SE Hewitt and Primexx) were collected from field sites in Oklahoma and New Mexico, USA. All

the field brines were filtered by filter paper (Particle Retention > 20-25 μm) before usage.

This high salinity field brines were not stable after filtration, because there were some precipitations overnight. A chelating agent, sodium gluconate ($\text{C}_6\text{H}_{11}\text{NaO}_7$) was found to stabilize the brine (Albonico and Lockhart 1993). It was showed that after adding 300 ppm sodium gluconate, the brine became stable for over extended time (Fig. 2.1). Sodium gluconate (100 wt%) was bought from PMP Fermentation Products, Inc.

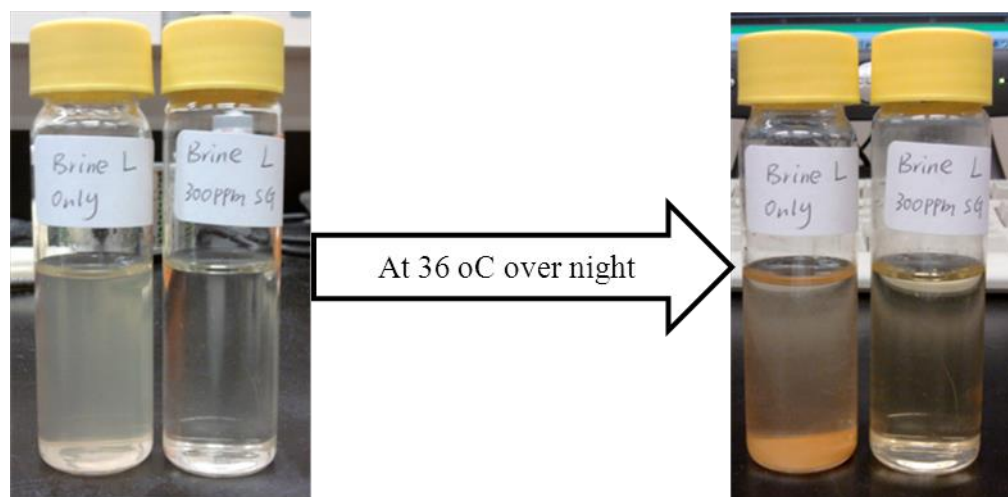


Fig.2.1—Effect of adding 300 ppm sodium gluconate on the stability of field brine at 36 °C.

The polymers used in this study were partially hydrolyzed polyacrylamide (SUPERPUSHER) and it was provided by SNF Inc. (France). Another polymer used in this study was xanthan gum (XG). The powders of xanthan gum (100 wt%) were provided by Kelco Oil Field Group (Houston, TX).

2.2. Methods

2.2.1. Phase Behavior Test

Phase behavior test was performed in flat-bottom glass vials with Teflon-lined screw caps using standard methods (Witthayapanyanon et al. 2006). A 1:1 water/oil ratio was used for the phase behavior tests to obtain the middle phase microemulsions (Fig. 2.2). The middle phase microemulsions were obtained by varying the salinity of the water or the ratio of surfactant/co-surfactant/co-solvent of a surfactant formulation. Phase behavior tests were equilibrated at predetermined temperatures.

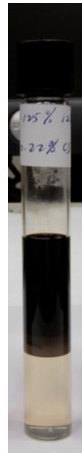


Fig.2.2—Flat-bottom glass vials with Teflon-lined screw caps used for phase behavior test at low temperature in this study.

Phase behavior tests with crude oil were conducted with surfactant formulation in field brine collected from the target formation. The presence of a middle phase microemulsion with crude oil was not easy to identify by visual observation because of the dark color of the crude oil, thus IFT measurement was used to verify the optimal surfactant formulation.

2.2.2. Screening Criteria for Chemical Flood

High permeability is favorable to chemical flood, and it is critical to polymer flood. Low permeability formation will have low injectivity or plugging issues. According to Taber et al. (1997a), the reservoir permeability for chemical flood projects should be over 10 mD. Heterogeneities and anisotropy of an oil-bearing formation have a significant effect on the macroscopic displacement efficiency. The movement of fluids through the reservoir will not be uniform if there are large variations in porosity and permeability. Fluids will be inclined to travel through the high permeability zone. This may lead to substantial bypassing of residual oil. Heterogeneous reservoirs are good candidates for polymer flood because the polymer solution has a tendency to divert toward unswept reservoir areas or areas where water flood resulted in an unsatisfactory sweep, which can improve both the vertical and areal sweep efficiency. For polymer flood, sufficient vertical permeability is required to allow polymer to induce cross flow in reservoir. While for surfactant flood, homogeneous formation is preferred (Falls et al. 1994; Levitt et al. 2006).

Oil viscosity is critical to polymer flood because it will directly affect the mobility of oil and thus affect the choice of polymer. According to Taber et al. (1997a), oil viscosity should be no more than 35 cp for surfactant flood, while for polymer flood; it can be as high as 150 cp.

An effective and economic surfactant formulation for chemical flood should achieve ultralow IFT between brine and oil, be chemically stable at reservoir conditions, be free

of viscous phases with fast coalescence rate and have low surfactant adsorption (Aparna et al. 2013; Glover et al. 1979; Shiau et al. 2010; Shiau et al. 2012).

One of the critical designing factors for surfactant formulation for chemical flood is to choose an appropriate surfactant formulation that can reduce the IFT between oil and brine to ultralow level (10^{-2} mN/m or less) to mobilize residual oil, because ultralow IFT is required to recover residual oil.

At the same time, the surfactant formulation must be chemically stable at reservoir conditions (salinity and temperature) without precipitation or phase separation. Otherwise precipitation of surfactants due to high salinity especially hardness, can make surfactants lose activity. Moreover, surfactant phase separation could result in a more viscous surfactant rich phase, which flows more slowly in the reservoirs, which can make the surfactant have a poor contact with the oil. All these can fail the surfactants to develop ultralow IFT with crude oil at reservoir conditions, which can result in low oil recovery. One method to prevent surfactant precipitation is to use a co-solvent such as isopropanol (IPA) and sec-Butanol (SB) to increase the salt tolerance of surfactant formulation. When there are a lot of divalent ions in the formation water, a chelating agent such as tripolyphosphate, EDTA and sodium gluconate can be used to chelate such divalent ions to prevent surfactant precipitation (Sheng 2010).

The surfactant formulation should also have minimal propensity to form viscous phases such as liquid crystals, gels, or macroemulsions, which are difficult to pump through perforation, reducing the injectivity. The high viscous phase can prevent the coalescence of the oil drops forming an oil bank. Therefore, a very high viscous phase

should be prevented when designing a surfactant formulation. One of the methods to prevent viscous phase is to add a co-solvent such as an alcohol. Coalescence rate describes how fast a microemulsion is formed in equilibrium with oil and brine. The surfactant formulation should have rapid coalescence rate to form microemulsion, because slow coalescence indicates problems with viscous phases.

In addition, surfactant adsorption can reduce surfactant activity and even make a chemical flood fail. Thus control of surfactant adsorption in chemical flood is of great importance to achieve a successful chemical flood project (Novosad, 1982). The ionic attraction between positively charged mineral surface and the negatively charged surfactant anion results in the adsorption of anionic surfactants on sandstone and carbonate formation. Thus one of the effective methods to reduce anionic surfactant adsorption onto minerals surface is to increase the pH of the reservoir fluid to make the mineral surface negatively charged by adding some alkali such as sodium hydroxide, sodium carbonate and sodium orthosilicate. However, alkali cannot be used in formation with high hardness in the brine, because alkali can form precipitation with divalent ions (Solairaj et al. 2012).

2.2.3. Critical Factors Affecting Design of Slug Size of Surfactant

Once a good surfactant formulation is designed for a targeted reservoir, we can then design the chemical flood strategies such as the slug size of surfactant for a chemical flood. Initially, the oil recovery increases with increasing the slug size of surfactant, and then reaches a plateau with further increasing the slug size. However, the cost of surfactant also increases linearly with increasing the slug size and can limit the slug size

that can be used to achieve profitable oil recovery. Therefore, a good balance should be made between the cost of surfactant and the potential oil that can be recovered. Based on the targeted oil recovery and cost of surfactants, an economic slug size of surfactant can be determined for a targeted reservoir (Hsu et al. 2012).

2.2.4. IFT Measurement

The IFT between oil and surfactant formulation was measured at predetermined temperatures using a spinning drop tensiometer (Fig. 2.3).



Fig.2.3—Grace instrument M6500 spinning drop tensiometer.

Equilibrium IFT was measured between the excess water and excess oil phases of microemulsions. The excess water phase of a microemulsion was added into the spinning drop glass tube. Then 1-3 μL of the excess oil phase was injected into the same glass tube. Dynamic IFT was measured between the brine and oil that was not contacted with each other before IFT measurement. The water phase was added into the spinning

drop glass tube. Then 1-3 μL of the oil phase was injected into the same glass tube. The IFT measurement was recorded after 15 min of spinning. The glass tube was then spun at increasing RPM values until the oil droplet expanded sufficiently such that its length is four times greater than its width. At that point, the interfacial tension (γ) was calculated as follows (Kiran et al. 2009).

$$\gamma = \Delta\rho \cdot \omega^2 \cdot r^3 / 4, \dots \dots \dots (2.1)$$

Where $\Delta\rho$ is the difference in density between the heavy and light phase, ω is the angular velocity of the motor, and r is the half width of the oil droplet.

2.2.5. Determination of EACN of Crude Oil

The method using a conventional surfactant formulation (2.2 wt% AOT and 8 wt% isobutanol) to determine EACN of crude oil in this study was adopted from the method of Wu et al. (2000). This method determined the EACN of the crude oil by first determining the optimal salinity for a mixed oil (a mixture of the crude oil and decane) and a surfactant of known values of K , $f(A)$, C_c and α_T and then applying the correlation. Based on the EACN of decane and the mixed oil, the EACN of the crude oil was determined using the ideal mixing rule. This method was referred as the indirect method to determine EACN of crude oil in this study.

For another method using the same conventional surfactant formulation to determine EACN of crude oil in this study, the optimal salinity for crude oil and the surfactant formulation was obtained to calculate EACN by the correlation. This method was referred as the direct method to determine EACN of crude oils in this study.

For the method using extended surfactant to determine EACN of crude oil in this study, the optimal salinity for oils of known EACN (hexane, octane, decane and dodecane) and the extended surfactant (2.5 wt% AF 8-41S) was first obtained to determine K and Cc using linear regression and then the optimal salinity for the crude oil and the same extended surfactant was obtained to calculate EACN.

2.2.6. Preparation of Polymer Solutions or Wormlike Micelles



Fig.2.4—Magnetic stirrer for the preparation of polymer solution.



Fig.2.5—Blender for the preparation of polymer solution.

To prepare SNF polymer solution, the polymer powders were added slowly into the brine or surfactant solution to achieve desired concentrations of polymer solution, which was then mixed by magnetic stirrer (MAGNE 4, MAGNETIC STIRRER, Cole-Parmer Instrument Co.) overnight for complete hydration (Fig. 2.4). The polymer solutions were then kept at predetermined temperature for further analysis.

To prepare the xanthan gum solution, xanthan gum powers were added into the brine or surfactant solution to achieve desired concentrations of polymer solution, which was then mixed by Blender (Model 38BL54, Waring Laboratory) for 10 min (Fig. 2.5). The polymer solutions were then kept at predetermined temperature for further analysis.

Wormlike micelles (Steol CS-460/Hexyl glucoside) were prepared by varying hexyl glucoside concentration, from 0 to 0.5 wt%, while keeping the concentration of Steol CS-460 at 1 wt%. The wormlike micelles were then kept at predetermined temperature for further analysis.

2.2.7. Viscosity Measurement

Brookfield dial reading viscometer (Brookfield Engineering Laboratories, Inc.) was used in this study to measure the viscosity of the solutions at predetermined temperatures (Fig.2.6).

2.2.8. Stability Test

The surfactant/polymer solutions or wormlike micelles were kept at predetermined temperatures for over extended time and then the appearance of the solutions was

observed. The presence of precipitate and phase separation was assessed by visual observation.



Fig.2.6—Brookfield dial reading viscometer.

2.2.9. Sand Packed Column Test

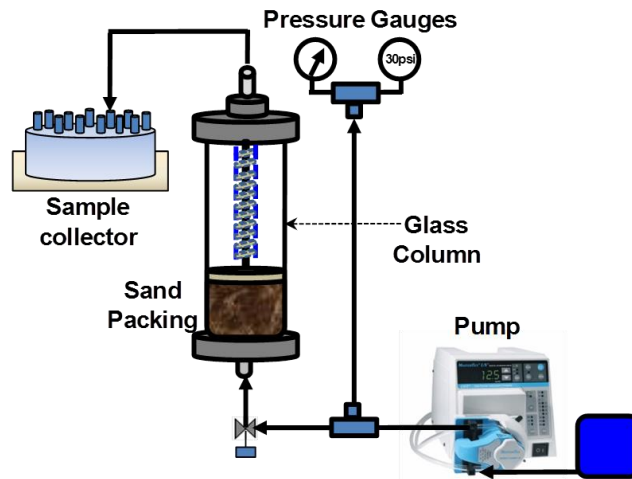


Fig.2.7— Schematic diagram of sand packed column test.

Sand packed column test was used to evaluate the performance of the chemical formulations developed to recover oil in the laboratory and to optimize the chemical

injection strategies. Column test was used to simulate one-dimensional reservoir flow (Wellington and Richardson 1997). Fig. 2.7 showed a schematic diagram for sand packed column test.



Fig.2.8—The apparatus for sand packed column test used in this study.

Fig. 2.8 showed the apparatus for column test used in this study. Crushed Berea sandstone or Ottawa sand (F-95) was packed into the column. The porosity of the crushed sand and Ottawa sand (F-95) was measured to be 0.35 and 0.38, respectively. A vertically oriented jacked Kontes chromatography column (1 inch of diameter) was used in this study. A flow adaptor was used to adjust the length of the sand pack inside the column. The fluids were delivered through the column from bottom to top. The temperature of the jacked column was controlled by circulating water from a water bath that was maintained at reservoir temperature. The fluids were injected by syringe pump at predetermined rate. The column was first saturated with brine and then a predetermined amount of oil was injected into the column. Continuous brine solution was injected until there was no oil coming out from the sand pack. The volume

difference of the injected oil and collected oil from water flood was the residual oil remaining in the sand pack. Then a chemical slug was injected, pushed by water drive to improve oil recovery. The recovered oil by chemical flood was collected. The oil recovery was calculated by dividing the amount of oil recovered by chemical flood by the amount of the remaining oil left in the sand pack after water flood (Hsu et al. 2012). All the solution was injected at 0.3 ml/min, unless otherwise specified.

2.2.10. Core Flood Test

Core flood test was used to further evaluate the performance of the optimal injection strategies from sand packed column test to recover oil at reservoir conditions in the laboratory. Fig.2.9 showed a schematic diagram of a core flood test.

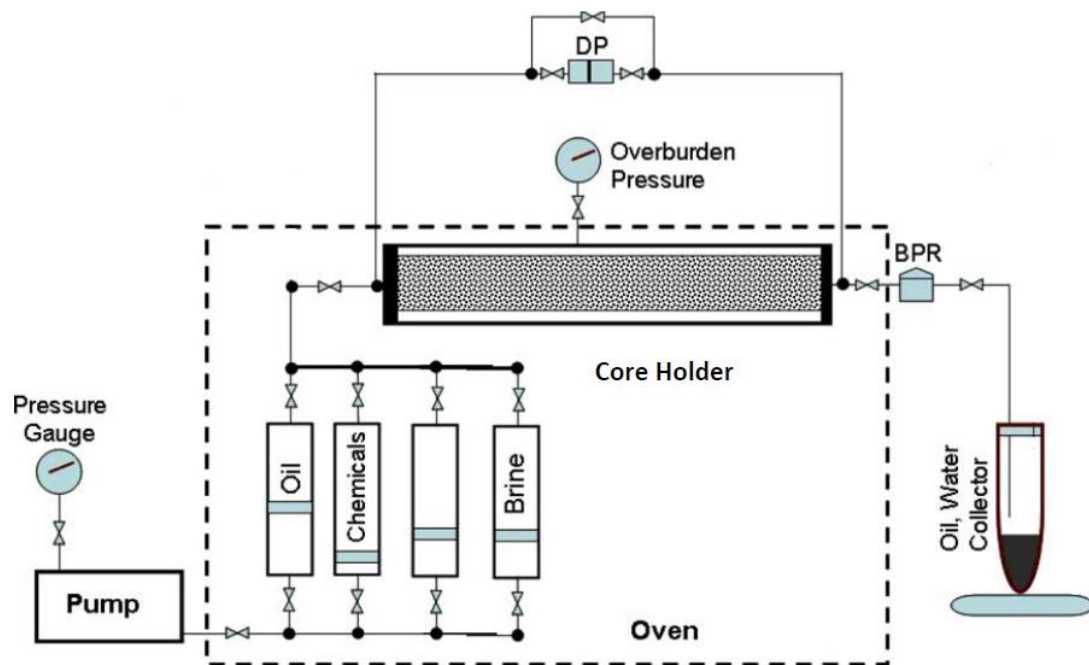


Fig.2.9— Schematic diagram of core flood apparatus.

Fig.2.10 showed the apparatus for the core flood test used in this study. The typical dimension of the Berea core was 1-3 inch long and one inch of diameter with permeability close to the average reservoir permeability to mimic the targeted reservoir condition. The back pressure on the core was set at 500 psi and the overburden pressure was set at 1200 psi.



Fig.2.10—The apparatus for core flood test used in this study.

Before running core flood, the dry weight of the core was measured and then the core was loaded into the core holder and flooded with brine overnight. The core was then taken out and the weight of the brine saturated core was measured. The difference between the weight of the brine saturated core and that of the dry core, was then divided by the brine density to obtain the effective pore volume (PV). The core was then flooded with 6 PV of oil and subsequently flooded with 6 PV of formation brine to

simulate the water flood. The volume difference of the injected oil and collected oil from water flood was the residual oil remaining in the core. Then a chemical slug was injected, pushed by water drive to improve oil recovery. The recovered oil by chemical flood was collected. The oil recovery was calculated by dividing the amount of oil recovered by chemical flood by the amount of the remaining oil left in the core after water flood. All the solution was injected at 0.3 ml/min, unless otherwise specified.

2.3.Summary

Phase behavior test was used to develop surfactant formulation for given oil and brine. Mobility control was achieved by increasing the viscosity of displacing water by using either polymer or wormlike micelles. Once a good and stable surfactant/polymer formulation was developed, sand packed column test and core flood test were used to evaluate the performance of the chemical formulations developed for chemical flood in the laboratory.

Chapter 3. Characterization of Crude Oil EACN for Surfactant

Flooding Design

In this chapter, the EACNs for crude oils from a dozen field sites (Miller 29, Fox Creek, Woods, War Party, Albert Barney 13, Litchfield 76, Stewart Fee 56, Lm Jones 46, Earlsboro, Albert Barney 18, SE Hewitt and Primexx) were measured based on the above equation (Eq. 1.5) using a convenient technique developed for both conventional EOR surfactants and the selected anionic extended surfactants.

3.1. Indirect Method to Determine EACN of Crude Oils Using AOT and Isobutanol

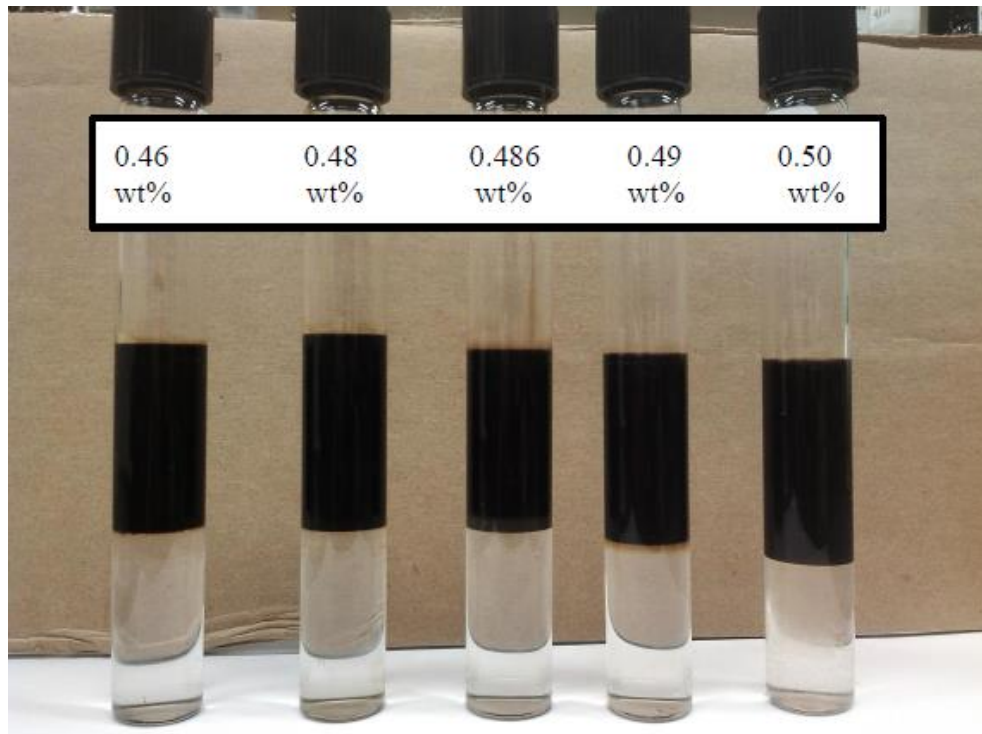


Fig.3.1—Effect of NaCl concentration on phase behaviors for the mixture of AOT and isobutanol with Fox Creek crude oil.

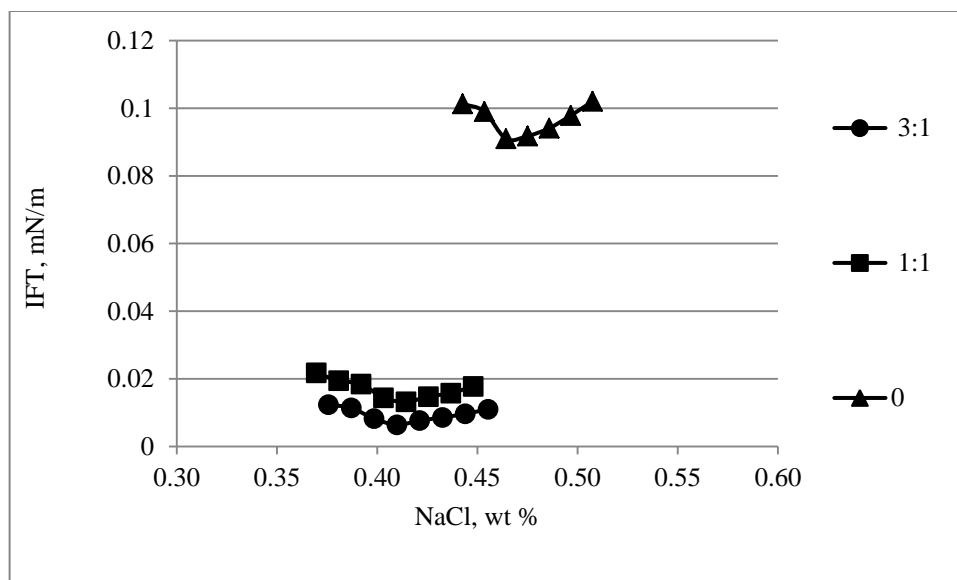


Fig.3.2—Equilibrium IFT as a function of electrolyte concentration (salinity scan) for the systems of AOT and iso-butanol at different weight ratios of decane and Miller 29 crude oil.

The method of scanning the mixed oils and inferring the EACN of the crude oil from the EACN of the mixture, as discussed above, was used to estimate the EACN for three crude samples retrieved from Miller 29, Fox Creek, and Woods sites. Decane was chosen as the surrogate oil (a known EACN = 10) added into a series of oil mixtures. In theory, the molecular weight of individual crude oil is required in order to apply the ideal mixing rules (see Eqs. 3.1 to 3.6 below). To overcome this, two separate salinity scans were conducted independently to match the number of unknowns and the total number of equations to solve these parameters. In these separate salinity scans, the ratios of decane to the crude oil were varied. Fig. 3.1 showed the effect of NaCl concentration on phase behaviors for the mixture of 2.2 wt% AOT and 8 wt% isobutanol with Fox Creek crude oil. The presence of a middle phase microemulsion

with crude oil is not easy to identify by visual observation because of the dark color of the crude oil, thus IFT measurements were used to verify the optimal surfactant formulation. Figs. 3.2-3.4 depict equilibrium IFT as a function of electrolyte concentration (salinity - NaCl scan) for the systems of AOT and isobutanol at different weight ratios of decane and crude from three sites (Miller 29, Fox Creek, and Woods), respectively.

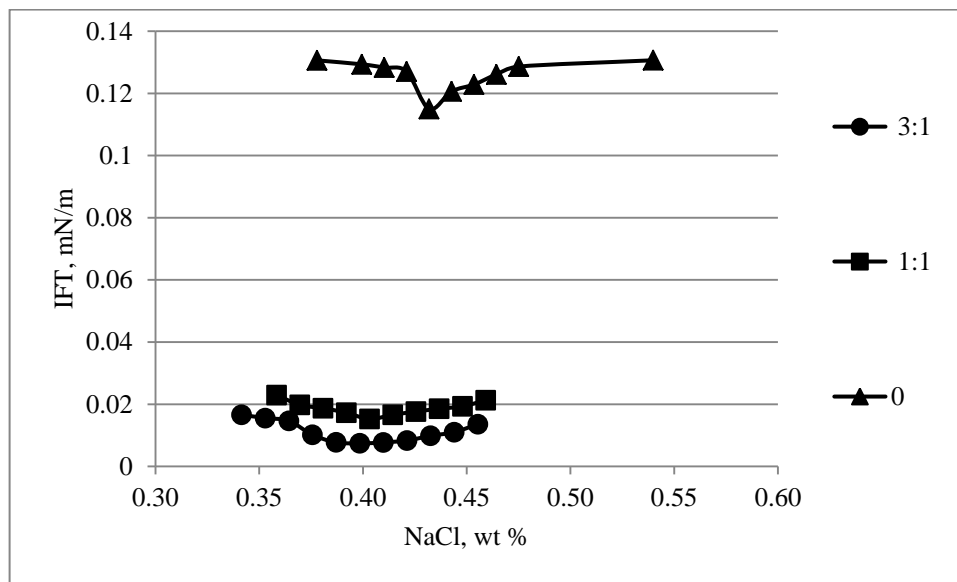


Fig.3.3—Equilibrium IFT as a function of electrolyte concentration (salinity scan) for the systems of AOT and iso-butanol at different weight ratios of decane and Woods crude oil.

Figs. 3.2-3.4 clearly showed that the IFT values first decreased with increasing the NaCl concentration at lower salt conditions and then slowly increased with further increase of NaCl concentrations. This is because increase of electrolyte concentration for ionic surfactants causes the surfactant molecules to become more hydrophobic and thus partitioning more toward the regime of oil-water interfaces, thereby reducing the film

curvature of normal micelles and IFT. The IFT of the system reaches a minimum value at conditions where the net curvature of the surfactant membranes at oil-water interface approaches zero when equal amount of oil and water are solubilized in the middle phase microemulsions.

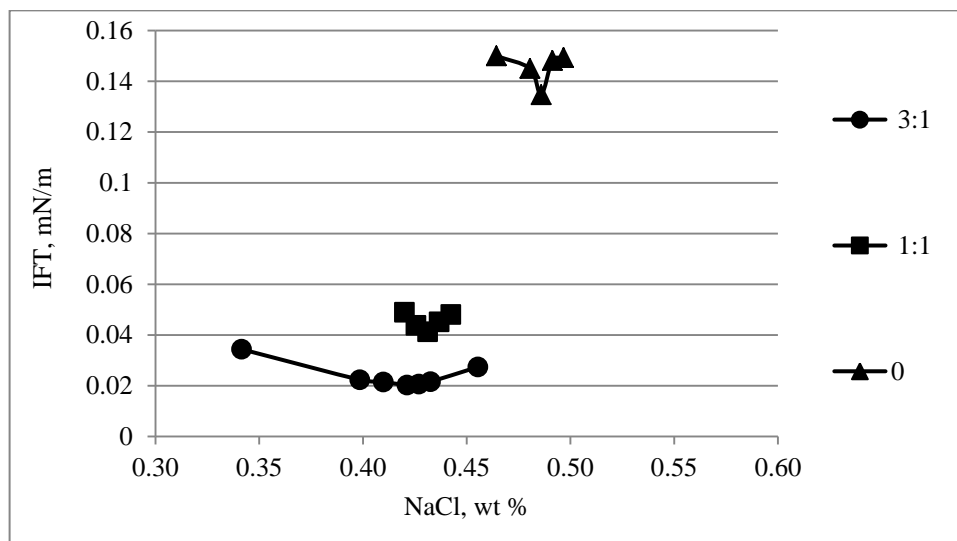


Fig.3.4—Equilibrium IFT as a function of electrolyte concentration (salinity scan) for the systems of AOT and iso-butanol at different weight ratios of decane and Fox Creek crude oil.

Table 3.1 lists the compositions of decane and crude mixtures and the corresponding optimal salinity for three crude oil samples investigated.

TABLE 3.1—SUMMARY OF OPTIMAL NAACL CONCENTRATION USED TO DETERMINE EACN OF CRUDE OIL					
Method	System	Weight ratio of decane and crude oil	Optimal salinity, wt %		
			Miller 29	Woods	Fox Creek
Direct		0	0.464	0.432	0.486
Indirect	a	3:1	0.410	0.398	0.421
	b	1:1	0.414	0.403	0.431

For the salinity scans for the two systems, the following six equations were constructed:

$$\ln S^*(a) = K * EACN(\text{mix.}, a) + f(A) - Cc + \alpha_T \Delta T, \dots \dots \dots (3.1)$$

$$\ln S^*(b) = K * EACN(\text{mix.}, b) + f(A) - Cc + \alpha_T \Delta T, \dots \dots \dots (3.2)$$

$$EACN(\text{mix.}, a) = EACN(\text{Decane}) * x(a) + EACN(\text{Oil}) * [1 - x(a)], \dots \dots \dots (3.3)$$

$$EACN(\text{mix.}, b) = EACN(\text{Decane}) * x(b) + EACN(\text{Oil}) * [1 - x(b)], \dots \dots \dots (3.4)$$

$$x(a) = \frac{\frac{W(\text{Decane}, a)}{MW(\text{Decane})}}{\frac{W(\text{Decane}, a)}{MW(\text{Decane})} + \frac{W(\text{Oil}, a)}{MW(\text{Oil})}}, \dots \dots \dots (3.5)$$

$$x(b) = \frac{\frac{W(\text{Decane}, b)}{MW(\text{Decane})}}{\frac{W(\text{Decane}, b)}{MW(\text{Decane})} + \frac{W(\text{Oil}, b)}{MW(\text{Oil})}}, \dots \dots \dots (3.6)$$

Where $S^*(a)$ and $S^*(b)$ are the actual optimal salinities in systems a and b, respectively (where a and b refer to the two different ratios of binary oil systems-see Table 3.1). Based on previous studies done by others (Wu et al. 2000), the K value is 0.16 for AOT; $EACN(\text{mix.}, a)$ and $EACN(\text{mix.}, b)$ are EACNs of mixed oils in systems a and b, respectively; the $f(A)$ value of iso-butanol is -0.87; the Cc value of AOT is 2.21. Since the parameters listed above for these equations were for the systems conducted at 15 °C, while the optimal salinity for each system in this study was determined at room temperature (i.e., 25 ± 1 °C), thus before applying Eqs. 3.1-3.2, the temperature correction factor ($\alpha_T \Delta T = 0.5462$) was determined by comparing the optimal salinity of the decane-only system determined at room temperature and the optimal salinity calculated from Eq. 1.5.

The EACN of Decane is equal to 10; $x(a)$ and $x(b)$ are the mole fractions of decane in the binary oil mixtures in systems a and b, respectively; EACN(Oil) is the EACN of crude oil; MW(Decane) is the molecular weight of Decane which is 142 g/mol; MW(Oil) is the molecular weight of crude oil; W(Decane, a) and W(Decane, b) are masses of decane in systems a and b, respectively; and W(Oil, a) and W(Oil, b) are the mass of crude oil in systems a and b, respectively.

TABLE 3.2—SUMMARY OF EACN DETERMINED FOR THREE CRUDE OILS				
Method	Parameters	Miller 29	Woods	Fox Creek
Direct	EACN	11.0	10.6	11.3
Indirect	EACN	10.7	10.3	11.2
	MW(g/mol)	159.6	159.1	160.0

Eqs. 3.1 and 3.2 are direct applications of the Salager relationship (Eq. 1.5) with the salinity scan results of the mixed oil systems. Eqs. 3.3 and 3.4 use the ideal mixing rules to estimate the EACN values of mixed oil systems. Eqs. 3.5 and 3.6 calculate the molar fractions of the decane in the mixtures. Solving these six equations simultaneously obtained the results of EACN for three crude oils and their MWs (Table 3.2).

The MW determined by the indirect method is consistent as much as the determined EACN is concerned. For example, For Fox Creek crude oil, the MW for an alkane with EACN of 11.2 is 158.8 g/mol, which is very close to the determined MW of 160.0 g/mol. These MWs also indicated that these crude oil samples might not contain elevated levels of heavy end compounds (e.g., asphaltenes and resins), though additional tests will be required to confirm these assumptions.

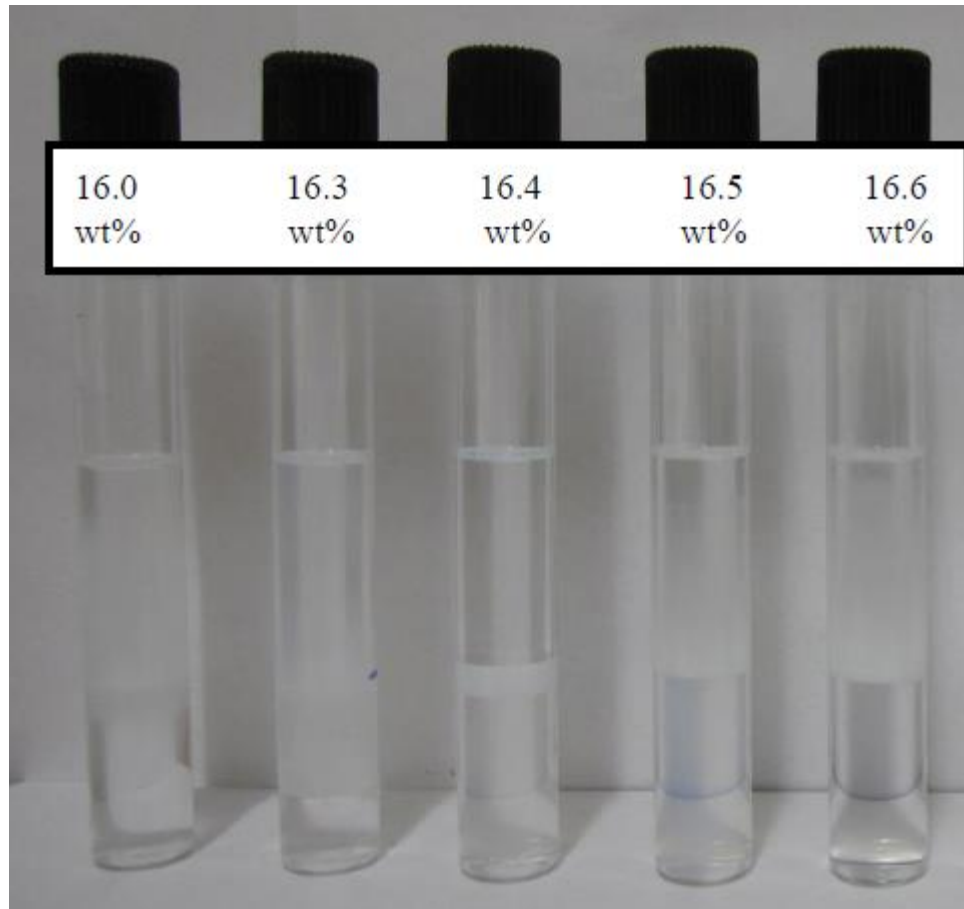


Fig.3.5—Effect of NaCl concentration on phase behaviors for 2.5 wt% AF 8-41S with Octane.

3.2. Direct Method to Determine EACN of Crude Oils Using Conventional EOR

Surfactant: AOT and Isobutanol System

Table 3.1 also showed the results of direct method measurements of the optimal salinity for each crude oil. Table 3.2 summarized the EACN for each crude oil determined by applying Eq. 1.5 and the direct method. From Table 3.2, we can see that EACNs for the three crude oils were 10.3-11.3 and EACNs determined by two separate methods appeared very close. In addition, for the direct method, only one parameter (unknown

EACN) needs to be determined, thus it is much simpler for conducting fewer experiments and solving equations as compared to the indirect method.

3.3. Determination of EACN of Crude Oils Using Extended Surfactant Systems

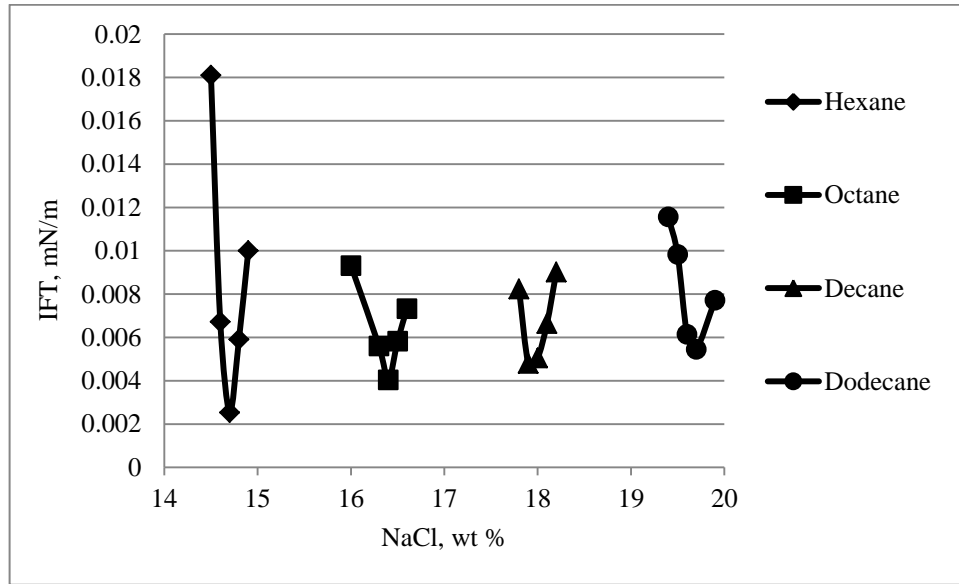


Fig.3.6—Equilibrium IFT as a function of electrolyte concentration (salinity scan) for the systems of extended surfactant for hexane (C6), octane (C8), decane (C10) and dodecane (C12).

The optimal salinities for various oils with known carbon number (e.g., hexane, C6; octane, C8; decane, C10; and dodecane, C12) and the pre-selected extended surfactant solution (i.e., AF 8-41S) were first determined by phase behavior study. Fig.3.5 showed the effect of NaCl concentration on phase behaviors for 2.5 wt% AF 8-41S with octane. Figure 3.6 showed equilibrium IFT as a function of electrolyte concentration (salinity scan) for the systems of extended surfactant for C6, C8, C10, and C12. Figure 3.6

showed that the optimal salinity increases with increase of EACN, which is consistent with the Eq. 1.5 and similar to others observations for conventional EOR surfactants.

Based on these data, the $\ln S^*$ vs. EACN was re-plotted in Fig. 3.7 and we can obtain an empirical expression of Eq. 1.6 as provided in Eq. 3.7 using a linear regression approach.

$$\ln S^* = 0.0478 * \text{EACN} + 2.4075, \dots \dots \dots (3.7)$$

Since the regression coefficient was very close to 1 for this set of data, there exhibited a reasonable linear relationship between $\ln S^*$ and EACN. Previously, a very good linear relationship between $\ln S^*$ and EACN had been reported in literature using different types of extended surfactants (Do et al. 2009; Phan et al. 2010a; Witthayapanyanon et al. 2006).

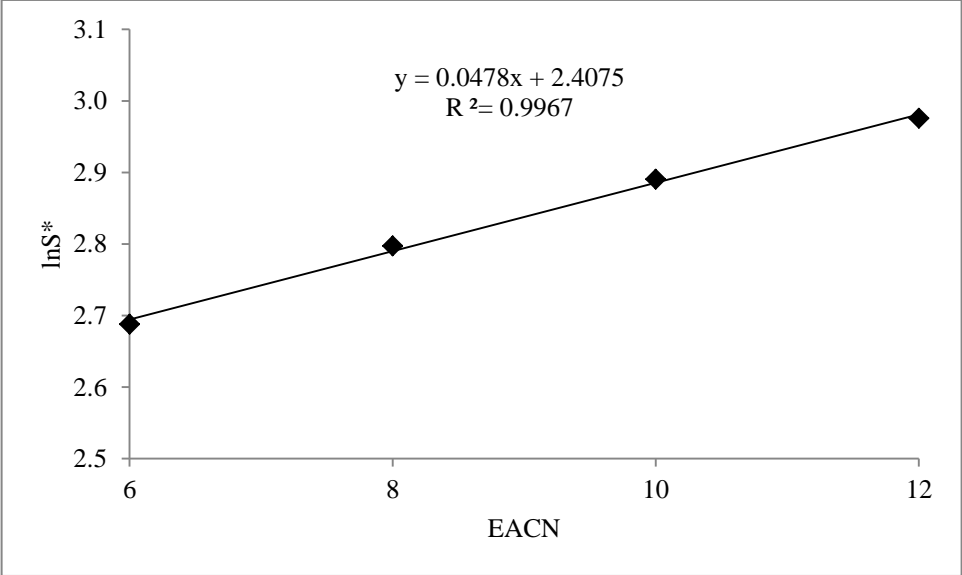


Fig.3.7—The plot of $\ln S^*$ vs. EACN for C6, C8, C10 and C12.

To verify the validity of Eq. 3.7 obtained in this study, the optimal salinities for additional oil systems, including pentane (C5), heptane (C7), and tetradecane (C14) were explored. Fig. 3.8 showed equilibrium IFT as a function of electrolyte concentration (salinity scan) for the target extended surfactant for different oils, C5, C7 and C14. For comparisons, the resulting optimal salinities for the systems with C5, C7 and C14 were plotted along those S^* values as predicted from Eq. 3.7, as depicted in Fig. 3.9. From Fig. 3.9, we can clearly see that the optimal salinities for the systems with C5, C7 and C14 measured experimentally were almost identical to the predicted values by Eq. 3.7. This provides a great confidence that the resulted parameters (K , C_c) and Eq. 3.7 was a valid description of $\ln S^*$ as a function of EACN for the selected extended surfactant, AF 8-41S.

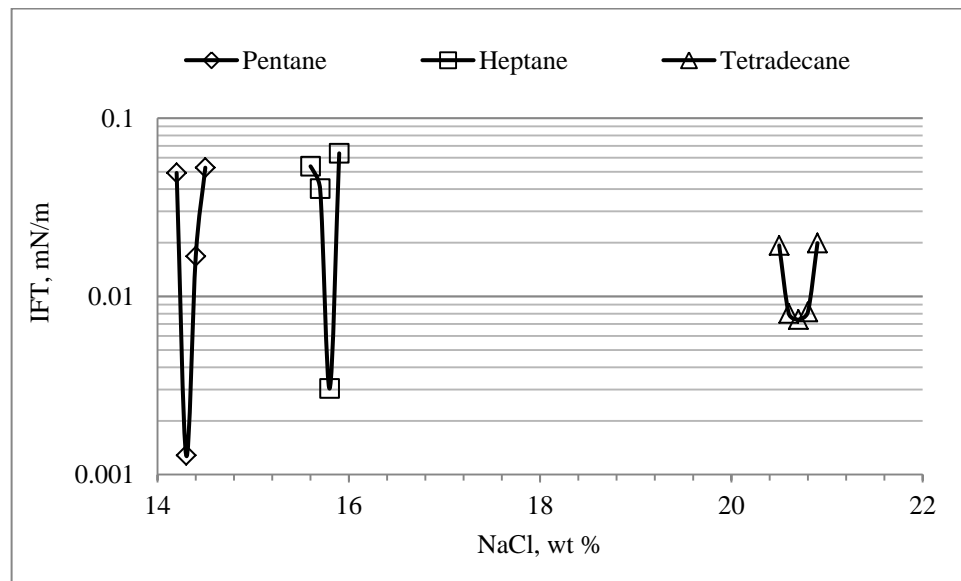


Fig.3.8—Equilibrium IFT as a function of electrolyte concentration (salinity scan) for the systems of extended surfactant for pentane (C5), heptane (C7) and tetradecane (C14).

Table 3.3 summarized the comparison of K and Cc values obtained in this study with those reported in the literature. From Table 3.3, we can see that the K and Cc values for different extended surfactants reported in the literature are 0.053 to 0.13 (of K) and -3.1 to -0.031 (of Cc), respectively, depending on the type of extended surfactants investigated. The K for the extended surfactant determined in this study was 0.048, which was slightly lower than that of most extended surfactants reported previously, yet it was comparable for the reported K value (0.053) for one extended surfactant investigated. The Cc for the extended surfactant determined in this study was -2.41, which falls into the range of -3.1 to -0.031 reported in the literature (Do et al. 2009; Phan et al. 2010; Witthayapanyanon et al. 2006; Witthayapanyanon et al. 2008).

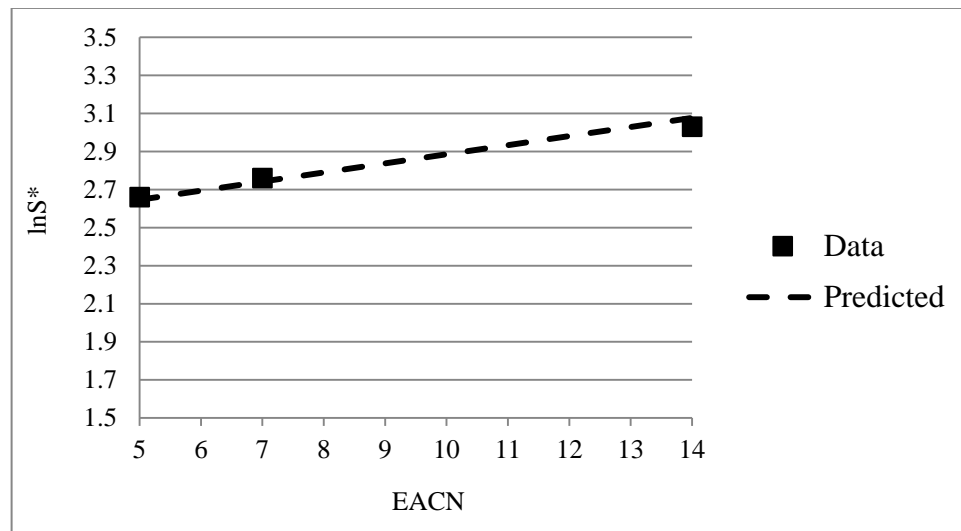


Fig.3.9—Comparison of $\ln S^*$ predicted by Eq. 3.7 with experimental data for C5, C7 and C14.

Fig. 3.10 showed equilibrium IFT as a function of electrolyte concentration (salinity scan) for the systems of extended surfactant for different crude oils tested (a total of 12 crudes). Table 3.4 summarized the resulted optimal salinities for the system of crude

oils and the surfactant solution. The EACN of crude oil was calculated based on Eq. 3.7, as shown in Table 3.4. The EACNs for these crude oils were between 6.0 to 11.3.

TABLE 3.3—COMPARISON OF K AND CC OBTAINED IN THIS STUDY WITH THOSE REPORTED IN THE LITERATURE			
Extended surfactant	K	Cc	Reference
$C_8H_{17}-(PO)_4^-(EO)_1-SO_4Na$	0.0478	-2.4075	This Study
$C_{12,15}H_{25,31}-(EO)_2-SO_4Na$	0.062	-2.97	Witthayapanyanon et al. (2008)
$C_{12,13}H_{25,27}-(PO)_8-SO_4Na$	0.087	-0.784	Witthayapanyanon et al. (2008)
$C_{12}H_{25}-(PO)_{12}-(EO)_2-SO_4Na$	0.104	-0.031	Do et al. (2009)
$C_{12}H_{25}-(PO)_{14}-(EO)_2-SO_4Na$	0.069	-3.1	Witthayapanyanon et al. (2006)
$C_{14,15}H_{29,31}-(PO)_8-SO_4Na$	0.13	-0.11	Phan et al. (2010)
$C_{14,15}H_{29,31}-(PO)_8-SO_4Na$	0.053	-0.52	Witthayapanyanon et al. (2006)

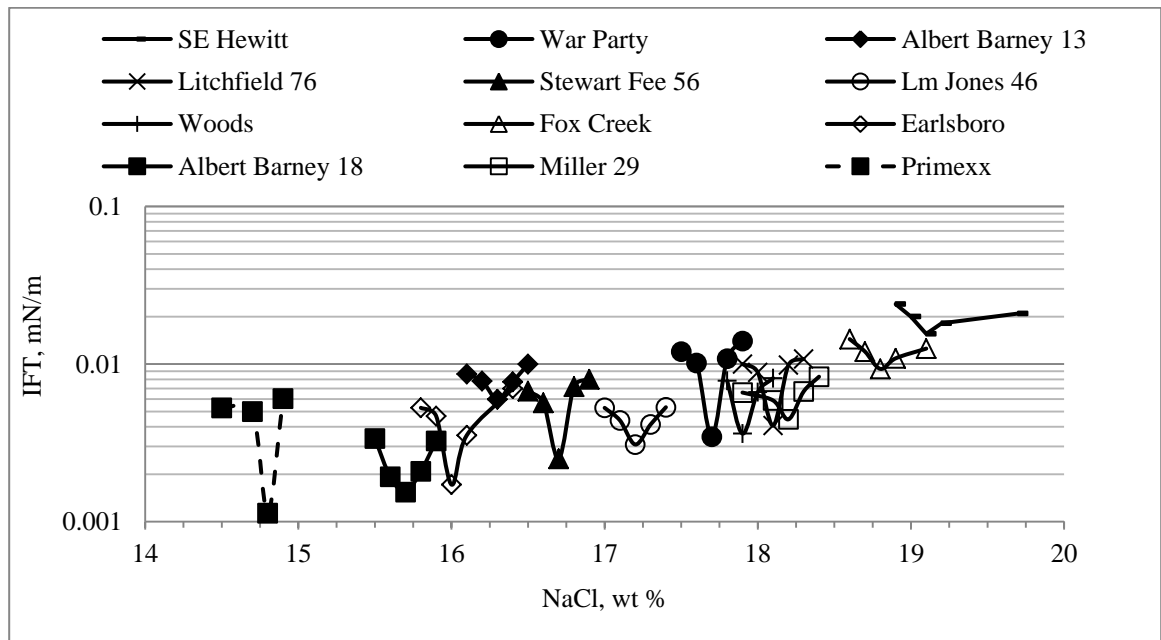


Fig.3.10—Equilibrium IFT as a function of electrolyte concentration (salinity scan) for the systems of extended surfactant for different crude oils.

From the above analysis, the EACN of crude oils from field sites was determined as 6.0-11.3 using both the conventional AOT/Iso-butanol and anionic extended surfactant in this study. EACN of crude oils from eight field sites determined by Cayias et al.

(1976) was 6.2-8.6, which is comparable with those reported in this study. In addition, the EACNs for Miller 29, Woods and Fox Creek were also determined using an extended surfactant and the results are very close to those determined by conventional surfactants, as shown in Table 3.4. However, the using of extended surfactant to determine EACN of crude oil does not need co-solvent, thus it is simpler than conventional surfactant to determine EACN of crude oil.

Crude Oil	S*, wt % NaCl	EACN
War Party	17.7	9.8
Albert Barney 13	16.3	8.0
Litchfield 76	18.1	10.2
Stewart Fee 56	16.7	8.5
Lm Jones 46	17.2	9.2
Woods	17.9	10.0(10.3)
Fox Creek	18.8	11.0(11.2)
Earlsboro	16.0	7.6
Albert Barney 18	15.7	7.2
Miller 29	18.2	10.3(10.7)
SE Hewitt	19.1	11.3
Primexx	14.8	6.0

EACN in parenthesis is determined by the indirect method using conventional surfactant

3.4. Summary

The EACN of crude oil determined by using salinity scan of crude oil and conventional surfactant (a mixture of 2.2 wt% AOT and 8 wt% isobutanol) (direct method) was very close to those determined by using the salinity scan of the mixed oil (a mixture of crude oil and decane) and the same conventional surfactant (indirect method). However, the direct method only needed to conduct one set of salinity scan, thus it is much simpler than the indirect method to determine EACN of crude oil. The EACN of crude oil

determined by using the extended surfactant (2.5 wt% AF 8-41S) were very close to those determined by using conventional surfactant. However, the method of using extended surfactant to determine EACN of crude oil does not need co-solvent, thus it is simpler than conventional surfactant to determine EACN of crude oil. The EACN of crude oil determined was 6.0-11.3.

Chapter 4. Formulating Low-IFT Microemulsions for High Salinity Formations Using Extended Surfactants

As part of the designing tasks for field pilot chemical EOR trial in this study, different extended surfactants were first studied to determine the effects of co-solvent, co-surfactants, and different reservoir temperatures on the microemulsion formations. In parallel tests, the optimal salinities of several extended surfactants and AOT in the presence of a co-solvent were also compared. Lastly, the effect of alkane carbon number on the optimal salinity for the extended surfactant systems in the presence of a co-solvent was studied using an empirical equation.

4.1. Effects of Co-Solvent and Co-surfactants on the Formation of Middle Phase Microemulsion

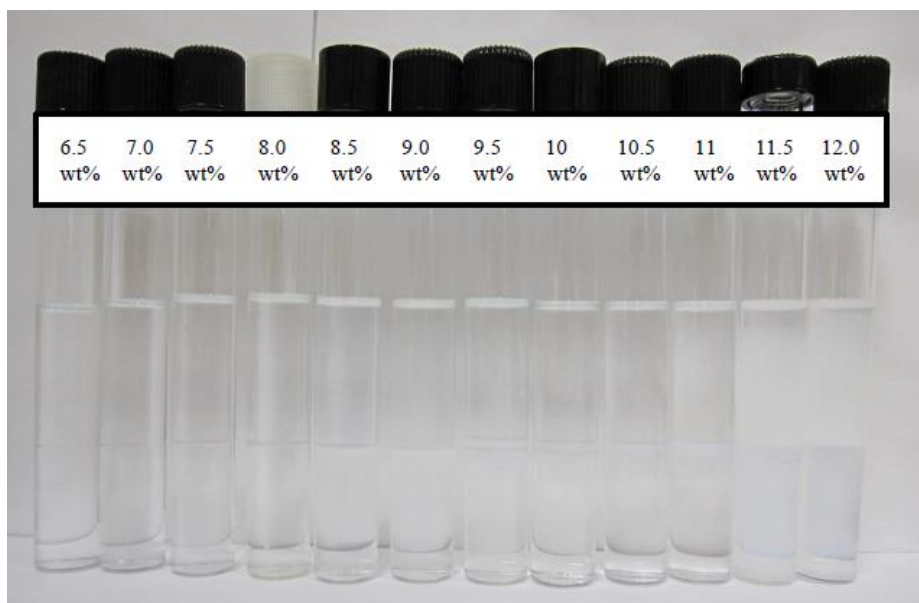


Fig.4.1—Effect of NaCl concentration on the phase behaviors for 0.5 wt% $C_{12}H_{25}-(PO)_6-SO_4Na$ and 3 wt% BC with decane at room temperature.

Three of the selected extended surfactants, $C_{12}H_{25}-(PO)_4-SO_4Na$ (C12P4), $C_{12}H_{25}-(PO)_4-(EO)_1-SO_4Na$ (C12P4E1) and $C_{12}H_{25}-(PO)_6-SO_4Na$ (C12P6), were used to determine the effects of different co-surfactants and one co-solvent on the formation of middle phase microemulsions. A series of salinity scans were conducted for measuring the optimal salinity for creating the middle phase microemulsions using in general the pre-set compositions and conditions: 3 extended surfactants (C12P4, C12P4E1, C12P6), 0.5 wt %; 3 co-surfactants (Calfax 16L-35, Steol CS-460, AMA), 0, 0.1 wt%; co-solvent, butyl carbitol (BC), 0, 1, 2 and 3 wt %; oil, decane; 2 temperatures, room temperature (RT) (25 ± 1 °C), 46 °C. Fig. 4.1 showed the effect of NaCl concentration on the phase behaviors for 0.5 wt% $C_{12}H_{25}-(PO)_6-SO_4Na$ and 3 wt% BC with decane at room temperature. From this figure, we can see that middle phase microemulsions can be formed under optimal salinity. Tables 4.1-4.2 summarized the effects of co-solvent and co-surfactants on the formation of middle phase microemulsions for different extended surfactants under the pre-set conditions.

TABLE 4.1—EFFECTS OF CO-SOLVENT AND CO-SURFACTANTS ON MIDDLE PHASE MICROEMULSION WINDOW AT ROOM TEMPERATURE

0.5 wt% Extended surfactant	0.1 wt% Co-surfactant	Middle phase microemulsion window (with coalescence time < 5 min), wt % NaCl			
		No BC*	1 wt% BC	2 wt% BC	3 wt% BC
$C_{12}H_{25}-(PO)_4-SO_4Na$	-	-(-)	12.5(-)	12.5-13(-)	12-15.5(13)
	Calfax 16L-35	-(-)	16(-)	15-19.5(16)	14-19.5(15-19.5)
	Steol CS-460	-(-)	13.5-14(-)	13.5-14(14)	13.5-17.5(13.5-14)
	Aerosol MA	-(-)	-(-)	12-14(-)	11.5-16.5(14-15.5)
$C_{12}H_{25}-(PO)_4-(EO)_1-SO_4Na$	-	-(-)	-(-)	13-13.5(-)	13-16(13)
	Calfax 16L-35	18(-)	16-18(-)	15.5-19.5(-)	15-21.5(16-20)
	Steol CS-460	-(-)	14-14.5(-)	14-14.5(14.5)	14-18(14.5-16)
	Aerosol MA	-(-)	12.5-13(-)	12.5-14(13)	12-17(13-14)
$C_{12}H_{25}-(PO)_6-SO_4Na$	-	-(-)	9.5(-)	9.5-10(-)	9-11(10)
	Calfax 16L-35	-(-)	-(-)	13-17(14)	12.5-18(14-18)
	Steol CS-460	-(-)	11.5(-)	11.5-12(11.5)	11-14(11.5-12)
	Aerosol MA	-(-)	10-10.5(-)	10-11(10)	10-13(10-11)

BC = Butyl carbitol, -=Not available

TABLE 4.2—EFFECTS OF CO-SOLVENT AND CO-SURFACTANTS ON MIDDLE PHASE WINDOW AT 46 °C

0.5 wt% Extended surfactant	0.1 wt% Co-surfactant	Middle phase microemulsion window (with coalescence time < 5 min), wt % NaCl			
		No BC	1 wt% BC	2 wt% BC	3 wt% BC
C ₁₂ H ₂₅ -(PO) ₄ -SO ₄ Na	-	-(-)	-(-)	-(-)	10(-)
	Calfax 16L-35	-(-)	-(-)	14(-)	12-14(13-14)
	Steol CS-460	-(-)	-(-)	-(-)	10(-)
	Aerosol MA	-(-)	-(-)	-(-)	10-12(10-11.5)
C ₁₂ H ₂₅ -(PO) ₄ -(EO) ₁ -SO ₄ Na	-	-(-)	-(-)	-(-)	10(10)
	Calfax 16L-35	-(-)	-(-)	15.5(-)	12-15.5(14)
	Steol CS-460	-(-)	-(-)	-(-)	10(-)
	Aerosol MA	-(-)	-(-)	-(-)	10-12(10)
C ₁₂ H ₂₅ -(PO) ₆ -SO ₄ Na	-	-(-)	-(-)	-(-)	-(-)
	Calfax 16L-35	-(-)	-(-)	-(-)	10-12.5(-)
	Steol CS-460	-(-)	-(-)	-(-)	-(-)
	Aerosol MA	-(-)	-(-)	-(-)	9-9.5(-)

BC = Butyl carbitol, -=Not available

Tables 4.1-4.2 showed that, for both extended surfactant-only (single system) and binary surfactant mixtures (i.e., extended surfactant/co-surfactant), the middle phase microemulsion windows (i.e., NaCl concentration range where O/W/middle phase co-exist) became progressively bigger with increasing butyl carbitol concentrations. For example, for the single surfactant system of C12P4 (0.5 wt%, room temperature), there was no middle phase microemulsion detected in 0% butyl carbitol, but middle phase microemulsion successfully formed at 12.5 wt% NaCl at 1 wt% of butyl carbitol, the microemulsion window expanded to 12.5-13 wt% NaCl by adding 2 wt% butyl carbitol, and lastly this middle phase window increased to 12-15.5 wt% NaCl at 3 wt% butyl carbitol. Also, the middle phase microemulsion window concomitant with a fast coalescence time (< 5 min) appeared wider with increasing butyl carbitol concentration. Similarly, others found that butyl carbitol has an excellent coalescing and coupling power, which may promote the formation of middle phase microemulsion (Witthayapanyanon et al. 2010). Based on these data, formation of middle phase microemulsions could be realized at salinity up to 20 wt% NaCl under favorable

conditions. Thus these extended surfactants could be great candidates for surfactant-based chemical flood at high TDS formations, where half-a-dozen field single-well and inter-well trials would be held.

Tables 4.1-4.2 also showed that adding co-surfactants in these extended surfactant formulations could also facilitate the formation of middle phase microemulsions and expand the middle phase transition window. For example, in a mixture of 0.5 wt% C12P4E1 and 1 wt% butyl carbitol (at RT), no middle phase microemulsion was observed without co-surfactants added. Once adding the co-surfactants, middle phase microemulsions appeared for all three co-surfactants tested. It is likely that the mixed surfactant/co-surfactant micelles could aid the formation of microemulsions by varying the hydrophobicity of the surfactant formulation and increasing balance between different interactions near the regime of oil and water interface (Witthayapanyanon et al. 2010).

Fig. 4.2 showed the resulting IFT values against NaCl concentrations in a mixture of C12P4E1 (0.5 wt%), Calfax 16L-35 (0.1 wt%) and butyl carbitol (3 wt%) with decane at RT. Fig. 4.2 showed that the IFT first decreased with increasing the NaCl concentration and then increased with further increasing the NaCl concentration, as commonly observed in a salt scan test. Increase of electrolyte concentration for anionic surfactants and their mixtures causes the surfactant system to become more hydrophobic and thus segregate more towards the oil-water interface, thereby reducing the surfactant membrane curvature and IFT. The IFT of the system reaches a minimum value at conditions where the net curvature of the surfactant membrane at the oil-water interface is near zero when equal amounts of oil and water are solubilized in the middle

phase microemulsions. Similar IFT profiles were also observed when conducting salinity scans for extended surfactants with different oils (Phan et al. 2011; Witthayapanyanon et al. 2006; Witthayapanyanon et al. 2010).

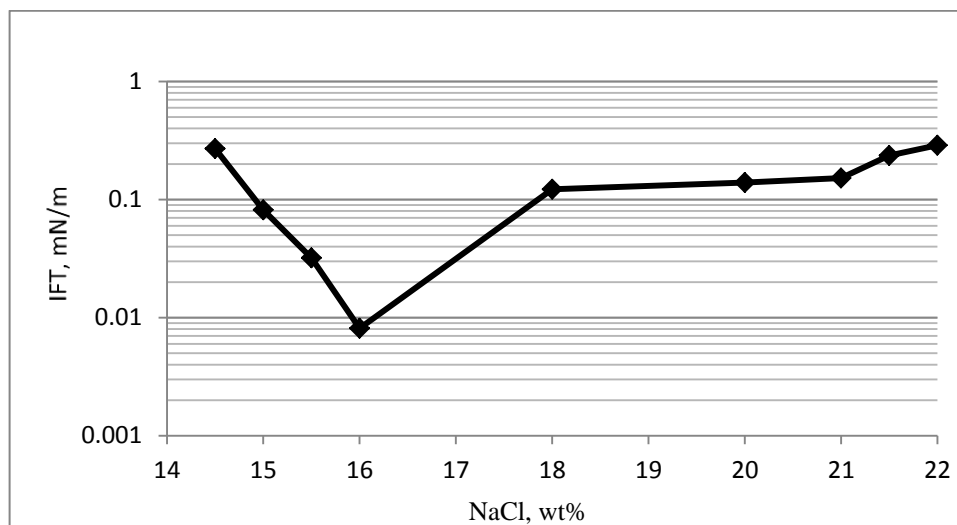


Fig.4.2—Effect of NaCl concentration on IFT for a mixture of 0.5 wt% $C_{12}H_{25}-(PO)_4-(EO)_1-SO_4Na$, 0.1 wt% Calfax 16L-35, and 3 wt% butyl carbitol and decane at room temperature.

Tables 4.1-4.2 also clearly revealed that the microemulsion window, as explained previously, tended to shift to lower salinity when increasing temperature from RT to 46 °C. For example, in a mixture of 0.5 wt% $C_{12}P_4$ and 3 wt% butyl carbitol, the middle phase microemulsion window was 12-15.5 wt% NaCl at RT, but the average window slightly shifted to 10 wt% NaCl at higher 46 °C. In general, increase of temperature can decrease the hydrophilicity of the extended surfactants, thus less salt would be required to increase the interactions of surfactant and water molecules to achieve middle phase microemulsions. A similar optimal salinity dependence on temperature was also observed for extended surfactants with different oils (Velasquez et al. 2010).

Fig. 4.3 depicted the resulting IFT versus co-solvent (butyl carbitol) concentration for one of the surfactant mixtures, containing C12P4E1 (0.5 wt%), Calfax 16L-35 (0.1 wt%) and decane at constant salt (18 wt% NaCl) and temperature (RT). The values of IFT increased slightly when increasing butyl carbitol concentrations. This is due to the presence of co-solvent could decrease the optimal solubilization parameter and thus slightly increase the IFT. However, the advantages of using alcohols for EOR can easily outweigh some of the disadvantages, because addition of alcohols can largely decrease the viscosity of microemulsions, gel formation and coalescence time (Flaaten et al.2009).

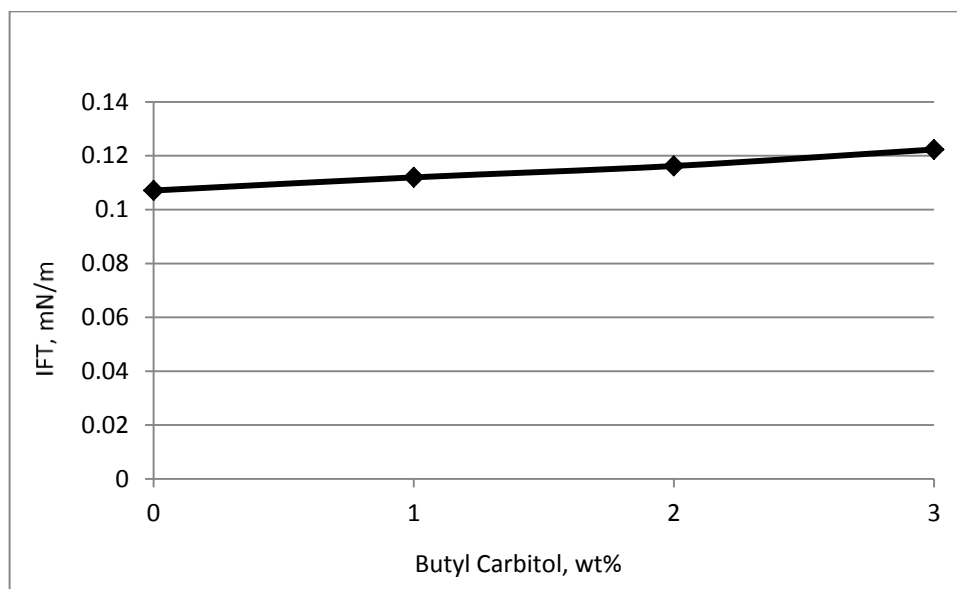


Fig.4.3—Effect of butyl carbitol concentration on IFT for a mixture of 0.5 wt% C₁₂H₂₅-(PO)₄-(EO)₁-SO₄Na, 0.1 wt% Calfax 16L-35, 18 wt% NaCl and decane at room temperature.

Fig.4.4 showed the examples of adding different co-surfactants affecting the IFT for a surfactant mixture of, C12P4E1 (0.5 wt %), butyl carbitol (3 wt%), with decane at RT

and constant salt (16wt% NaCl). Calfax 16L-35 exhibited the lowest IFT value among the three co-surfactants used (at the same 0.1 wt % concentration), followed by Steol CS-460 of intermediate IFT, and even higher IFT of AMA. This is likely due to the presence of 0.1 wt % Calfax 16L-35 (containing a mixture of different structural isomers) in the formulations could greatly improve the solubilization capacity of oil/water partitioning into the middle phase microemulsions.

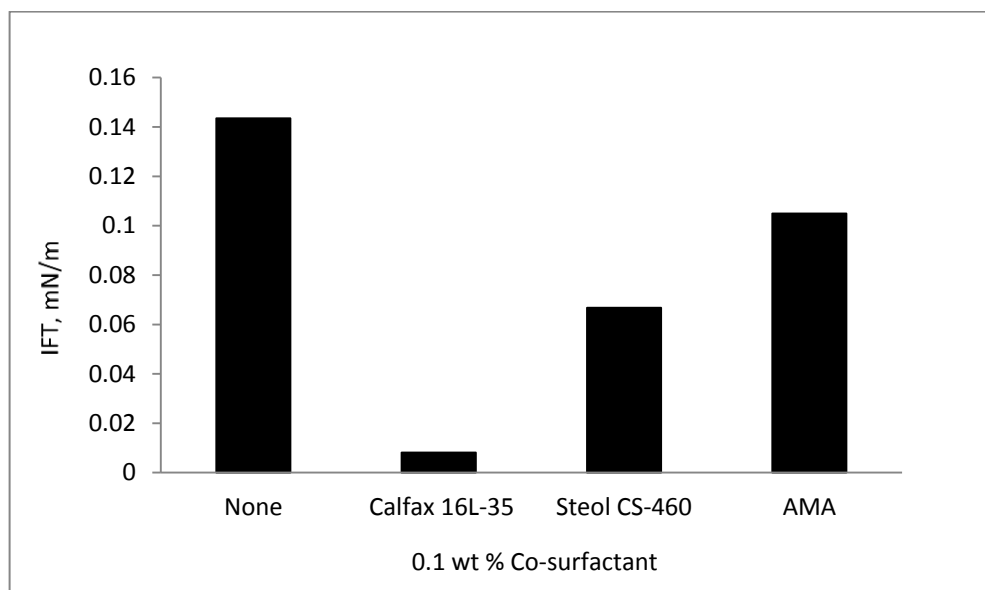


Fig.4.4—Effect of different co-surfactants on IFT for a mixture of 0.5 wt % $C_{12}H_{25}-(PO)_4-(EO)_1-SO_4Na$, 3 wt% butyl carbitol, 16 wt% NaCl and decane at room temperature.

Fig. 4.5 showed the results of different primary extended surfactants on IFT at a constant mixture of 0.1 wt % Calfax 16L-35, 3 wt % butyl carbitol, 16 wt % NaCl with decane oil at room temperature.

Fig. 4.5 showed that the surfactant formulation of 0.5 wt % C12P4E1 exhibited the lowest IFT among the three extended surfactants tested. In the case of C12P4E1 vs.

C12P4 and C12P6, the presence of one EO group in C12P4E1 molecules could improve the solubilization of oil/water in the middle phase microemulsion to help achieving lower IFT. Similarly, others reported that different extended surfactant structures could have significant impact on the formation of middle phase microemulsions and IFT with long-chain triglycerides (Phan et al. 2011).

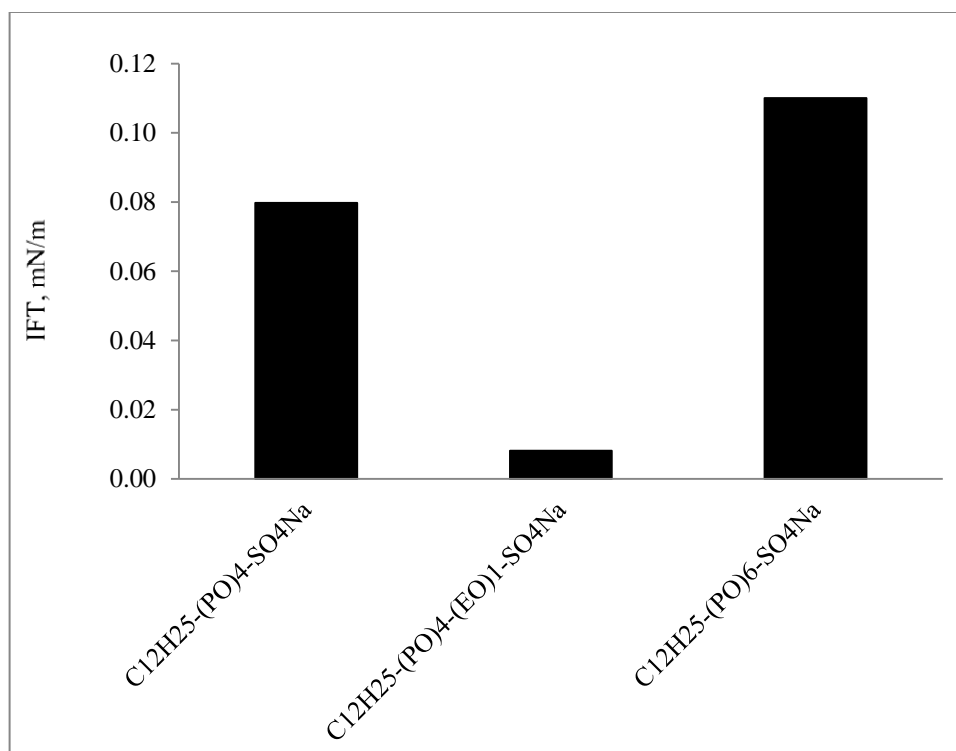


Fig.4.5—Effect of different extended surfactants on IFT for a mixture of 0.1 wt % Calfax 16L-35, 3 wt % butyl carbitol, 16 wt % NaCl and decane at room temperature.

4.2.Effect of Different Extended Surfactants on Middle Phase Microemulsion Formation at Various Temperatures

To further study the effect of additional extended surfactants on middle phase microemulsion formation at different temperatures, a series of salinity scans were

conducted for 2.5 wt % of individual extended surfactant-only system and decane (C10) at two different temperatures: RT and 46 °C.

Extended Surfactants	46 °C		Room temperature	
	Middle phase microemulsion window (with coalescence time < 5 min), wt % NaCl	Optimal salinity, wt % NaCl	Middle phase microemulsion window (with coalescence time < 5 min), wt % NaCl	Optimal Salinity, wt % NaCl
C ₈ H ₁₇ -(PO) ₄ -SO ₄ Na	14.1-17.9 (15.8-16.5)	16.4	17.7-18.9(17.8-18)	17.9
C ₈ H ₁₇ -(PO) ₄ -(EO) ₁ -SO ₄ Na	15.2-17.2(16.3-16.7)	16.6	17.8-18.5(17.9-18.3)	18
C ₁₀ H ₂₁ -(PO) ₄ -(EO) ₁ -SO ₄ Na	12-14.2(-)	13.9	14.7-15.6(-)	15.3
C ₁₂ H ₂₅ -(PO) ₄ -(EO) ₁ -SO ₄ Na	-(-)	-	-(-)	-
C ₁₂ H ₂₅ -(PO) ₃ -(EO) ₄ -SO ₄ Na	11-17.9(14.2-15.3)	14.7	17.3-19(17.5-18.1)	17.6
C _{12,13} H _{25,27} -(PO) ₃ -(EO) ₄ -SO ₄ Na	8.5-13.5(10.8-11.6)	10.9	13.1-14(13.2-13.4)	13.3
C ₁₂ H ₂₅ -(PO) ₃ -(EO) ₄ -(PO) ₃ -SO ₄ Na	12-17.5(15.5-16.6)	15.7	-(-)	-

-=Not available

Table 4.3 summarized the optimal salinity results of seven extended surfactants for the middle phase microemulsions at different temperatures. Table 4.3 showed that middle phase microemulsions formed at both temperatures (RT and 46 °C) for most extended surfactant systems tested, except C12P4E1. Among these, the surfactant formulation of C8P4E1 exhibits the highest optimal salinities (i.e., 18 wt% NaCl at room temperature and 16.6 wt% at 46 °C). Also, the middle phase windows and their optimal salinities shifted to lower levels of salinity by increase of temperature. Middle phase microemulsions could form at high salinity (> 10 wt% NaCl) for the selected surfactants under proper reservoir conditions. Thus applying these extended surfactants may be a viable approach for surfactant flood at high salinity formations.

Table 4.3 also showed that for both RT and 46 °C, the optimal salinity for C8P4E1 was slightly greater than that of C8P4, and was much higher than that of C10P4E1. This demonstrated that increase of the EO number or decrease of the hydrophobic chain

length in these extended surfactants would require larger optimal salinity for a particular oil. In general, increasing the number of EO group, or reducing the length of the hydrophobic tail would make the surfactant membranes become much more hydrophilic in aqueous solution, thus additional salt was required to balance the interactions of the surfactant/oil/water to form the middle phase microemulsions. For both RT and 46 °C, the optimal salinities of C12P3E4 were much higher than those of C12/13P3E4, a branched-tail surfactant. Not surprisingly, by adding branching hydrocarbon groups in the surfactant structure could decrease the optimal salinity for a given oil. This is in agreement with others' observations that adding branching in the hydrocarbon chain could make the surfactant much less hydrophilic, thus less amount of salt was needed to increase the interactions of surfactant with water attaining middle phase microemulsions (Phan et al. 2011).

4.3. Comparison of Performance of Different Extended Surfactants and AOT in the Presence of Co-Solvent

To compare the performance of different extended surfactants and AOT, systematical salinity scans were conducted at 2.2 wt % of individual surfactant, 8 wt % iso-butanol using different oils (hexane, decane or dodecane) at RT. Fig.4.6 depicted the results of optimal salinity for four extended surfactants (C12P4E1, C12P4E3, C12P3E4, C12/13P3E4) and AOT.

Fig. 4.6 showed that C12P3E4 exhibited the highest optimal salinity for the three oils investigated (C6, C10, C12). This is likely due to this extended surfactant has the highest EO group number and it has no branched tail, which makes the surfactant more

hydrophilic, thus excessive salt will be needed to balance the interactions of surfactant/oil/water for attaining middle phase microemulsions (Witthayapanyanon et al. 2006). In addition, the optimal salinities for these extended surfactants were much higher than that of AOT. It is anticipated that these extended surfactants have various EO groups (1 to 4) in their structures, which makes these extended surfactants much more hydrophilic than AOT, thus more salt was needed to form middle phase microemulsions compared with AOT, which has no EO group in its structure (Witthayapanyanon et al. 2006).

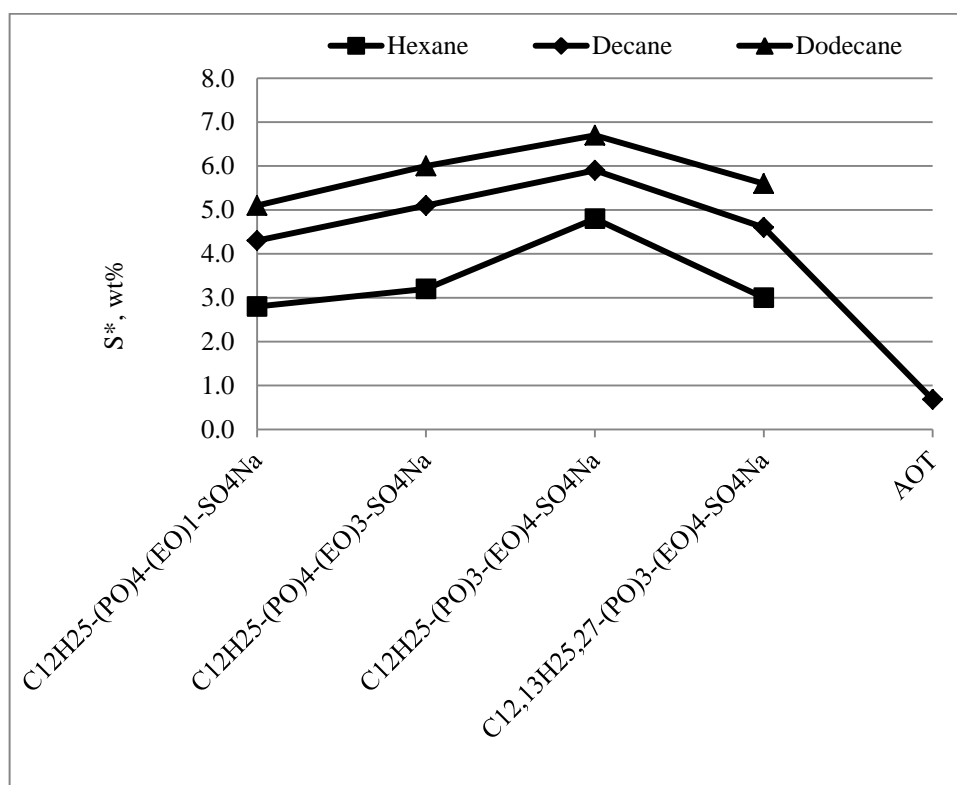


Fig.4.6—Optimal salinity for different extended surfactants and AOT.

4.4. Effect of ACN on Optimal Salinity Four Extended Surfactants with Oil in the Presence of Co-Solvent

To study the effect of ACN on optimal salinity for the surfactant formulation with four extended surfactants in the presence of co-solvent, salinity scan was conducted for 2.2 wt % of individual extended surfactant, 8 wt % iso-butanol, and oil (C6, C8, C10 and C12) at RT.

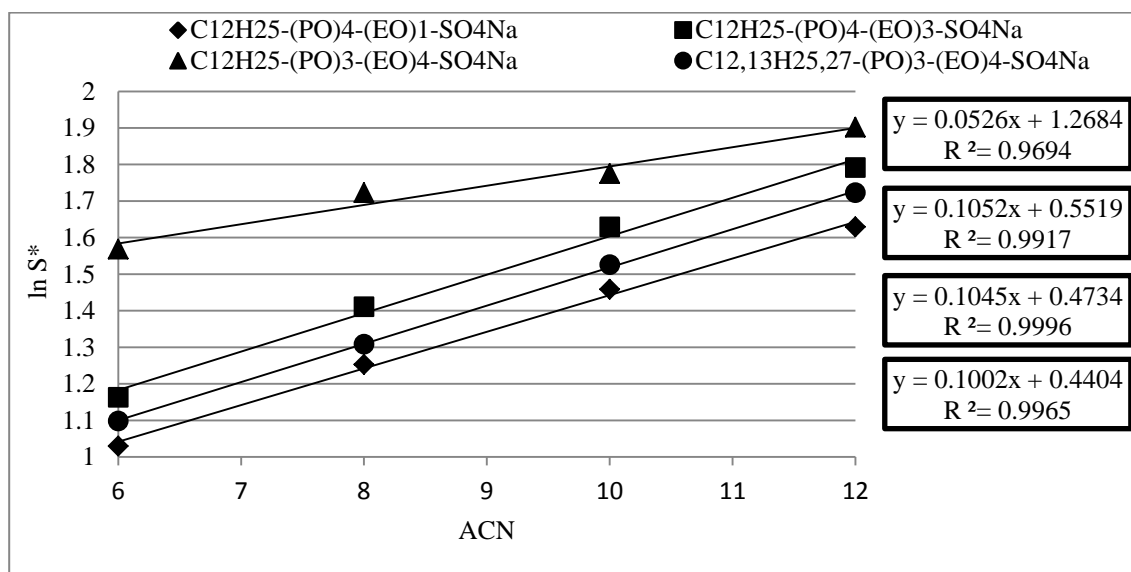


Fig.4.7—lnS* as a function of ACN for different extended surfactants in the presence of isobutanol.

Fig. 4.7 showed lnS* as a function of ACN for four extended surfactants in the presence of iso-butanol. Fig. 4.7 showed that lnS* increased almost linearly with increasing ACN. Similar lnS* dependences on ACN or EACN (Equivalent Alkane Carbon Number) were also observed for a variety of extended surfactants with different types of oil (Do et al. 2009; Witthayapanyanon et al. 2006; Witthayapanyanon et al. 2008; Velasquez et al. 2010). From the linear regression results using Eq. 1.5 (Fig. 4.7), we

concluded that there existed a very good linear relationship between $\ln S^*$ and ACN for each of the extended surfactant.

The K values for C12P4E1, C12P4E3 and C12/13P3E4 were around 0.1, which is the typical K value for alkyl sulfates. However, the K value for C12P3E4 was 0.0526, which was much lower than the typical K value for alkyl sulfates, but it was comparable for the reported K values (0.053 and 0.069) for two extended surfactants reported by others (Witthayapanyanon et al. 2006).

In addition, the intercept of the linear regression (of Eq. 1.5) is the value of $f(A) - C_c$, and in order to calculate $f(A)$ and C_c , the optimal salinity for 2.2% $C_{12}H_{25}-(PO)_3-(EO)_4-SO_4Na$ and decane in the absence of isobutanol was first determined to be 18.1 wt% at room temperature. Thus $f(A)$ was calculated to be -1.21. Then, the resulted C_c values for the four extended surfactants tested were calculated and tabulated in Table 4.4.

TABLE 4.4—PARAMETERS FOR FOUR EXTENDED SURFACTANTS		
Extended Surfactant	K	C_c
$C_{12}H_{25}-(PO)_4-(EO)_1-SO_4Na$	0.1002	-1.561
$C_{12}H_{25}-(PO)_4-(EO)_3-SO_4Na$	0.1052	-1.673
$C_{12}H_{25}-(PO)_3-(EO)_4-SO_4Na$	0.0526	-2.389
$C_{12,13}H_{25,27}-(PO)_3-(EO)_4-SO_4Na$	0.1045	-1.594

The value of C_c reflects the hydrophobicity of the surfactants: the smaller the C_c value (mostly negative values), the more hydrophilic the surfactant is (Kayali et al. 2010). From Table 4.4, we can see that C12P3E4 ($C_c = -2.39$) is significantly more hydrophilic than the other three extended surfactants investigated (C12P4E1, C12P4E3, C12/13P3E4).

4.5. Summary

Phase behavior tests using extended surfactants were investigated. For a given single or binary surfactants, the middle phase microemulsion window became wider and wider with increasing butyl carbitol concentration, even though IFT slightly increased when increasing butyl carbitol concentration. Co-surfactant could also help the formation of middle phase microemulsions. Middle phase microemulsions formed at both room temperature and 46 °C for most extended surfactant and the optimal salinity decreased with increasing the temperature. Middle phase microemulsions could form at salinity up to 20 wt% NaCl under favorable conditions. Thus extended surfactants may be good candidates for surfactant flood at high salinity. The presence of EO group, straight and shorter hydrocarbon chain could make the extended surfactants much more hydrophilic, thus more salt was needed to form middle phase microemulsion. The optimal salinity for the four extended surfactants investigated was much higher than that of AOT. $\ln S^*$ increased almost linearly with increasing ACN and there existed a very good linear relationship between $\ln S^*$ and ACN for the four extended surfactant studied.

Chapter 5. Surfactants/Polymer Formulation of Chemical Flood for Three High Salinity Reservoirs

This chapter attempted to develop a surfactant/polymer formulation for three high salinity reservoirs. Once a good and stable surfactant/polymer formulation was developed, sand packed column test and core flood test were used to assess chemical flood in laboratory to evaluate the performance of the chemical formulations developed.

5.1. Surfactants/Polymer Formulation of Chemical Flood for Miller 29 Site

5.1.1. Surfactant Formulation

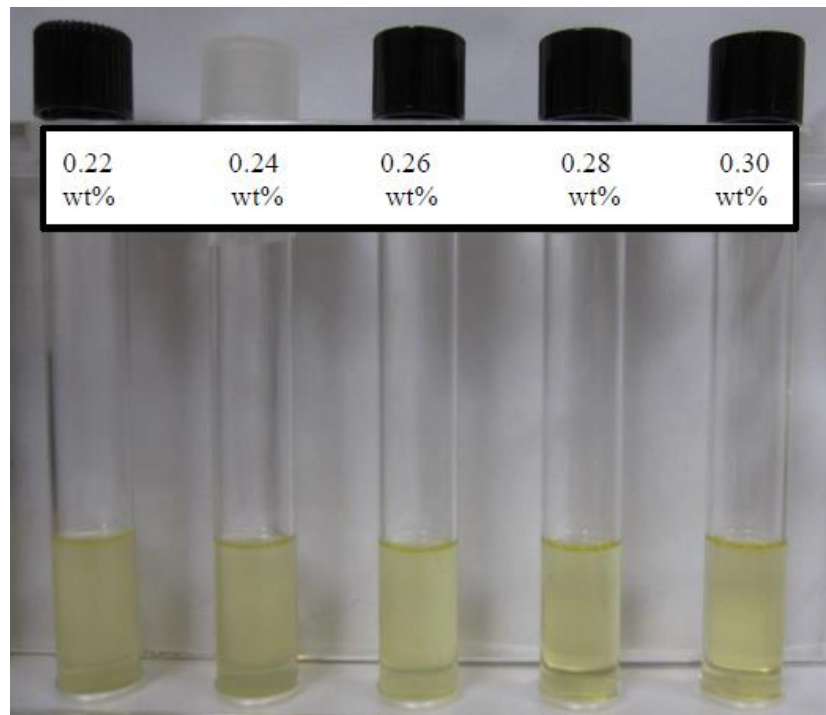


Fig.5.1—Effect of concentration of the co-surfactants of Steol CS-460 and Calfax DB 45 (1:1 ratio) on the stability for the surfactant formulation at 46 °C for Miller

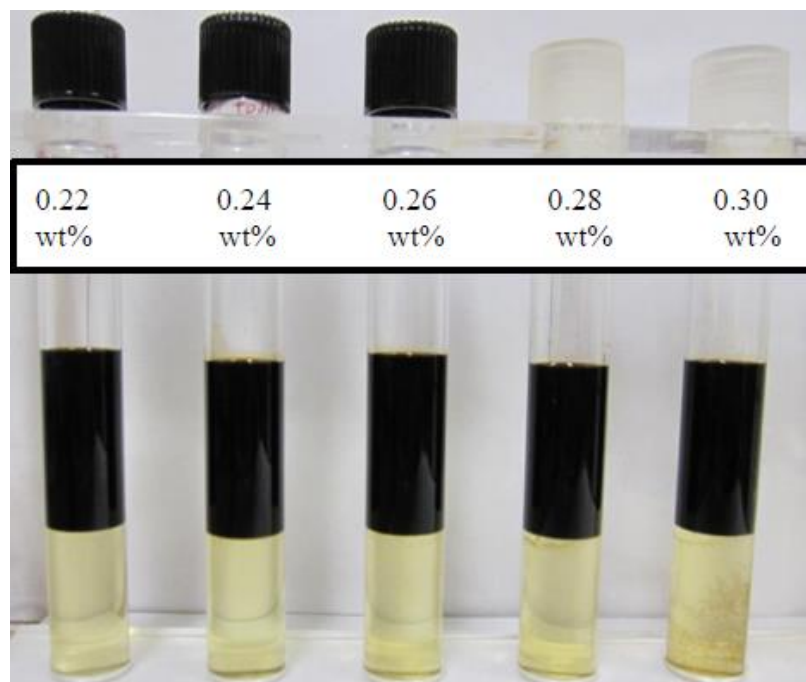


Fig.5.2—Effect of concentration of co-surfactants of Steol CS-460 and Calfax DB 45 (1:1 ratio) on phase behaviors for surfactant formulation with crude oil at 46 °C for Miller 29.

The surfactant formulation was developed by changing the concentration of co-surfactant to change the hydrophobicity of the surfactant formulation (Salager et al. 2005). The concentration of AOT was kept at 0.18 wt% and then it was scanned with 0.22-0.30 wt% total co-surfactants of Steol CS-460 and Calfax DB 45 (1:1 ratio). Fig. 5.1 and 5.2 showed the effect of co-surfactant concentration on the stability tests and phase behavior tests with crude oil for the surfactant formulation for Miller 29. From these figures, we can see that surfactant formulations were stable in the high salinity brine. IFT measurements were used to verify the optimal surfactant formulation, as shown in Fig. 5.3. The surfactant formulation with 0.18 wt% AOT, 0.12 wt% Steol CS-460 and 0.12 wt% Calfax DB 45 achieved ultralow IFT (0.006 mN/m). The coalescence

rate of the excess phases for all microemulsion samples were from several minutes to one hour.

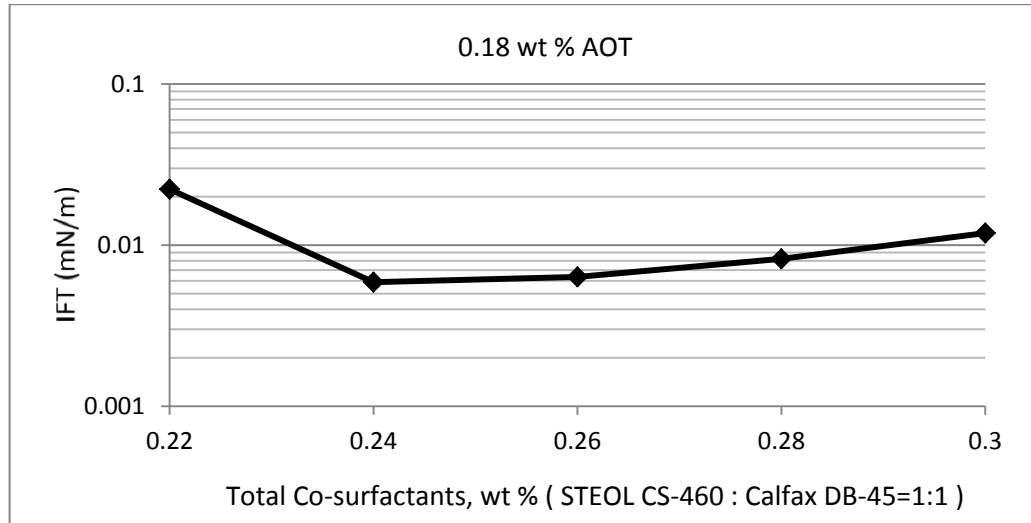


Fig.5.3—Effect of the concentration of Calfax DB-45 or Steol CS-460 with 1:1 ratio on IFT for Miller 29 brine and crude oil at 46 °C.

5.1.2. Mixed Surfactants/Polymer Formulation

A total of 3500 ppm SUPERPUSHER was added to the optimal surfactant formulation (0.18 wt% AOT, 0.12 wt% Steol CS-460 and 0.12 wt% Calfax DB 45) to prepare the surfactant/polymer solution. The IFT of the surfactant/polymer solution with crude oil is 0.008 mN/m. The viscosities of surfactant/polymer solution decreased with increasing the shear rate and were between 7 to 8 cp (Fig. 5.4). Since the oil viscosity is 5 cp at reservoir temperature (46 °C), the developed surfactant/polymer formulation (AOT/Steol/Calfax/SUPERPUSHER) provided enough viscosity for mobility control in this study.

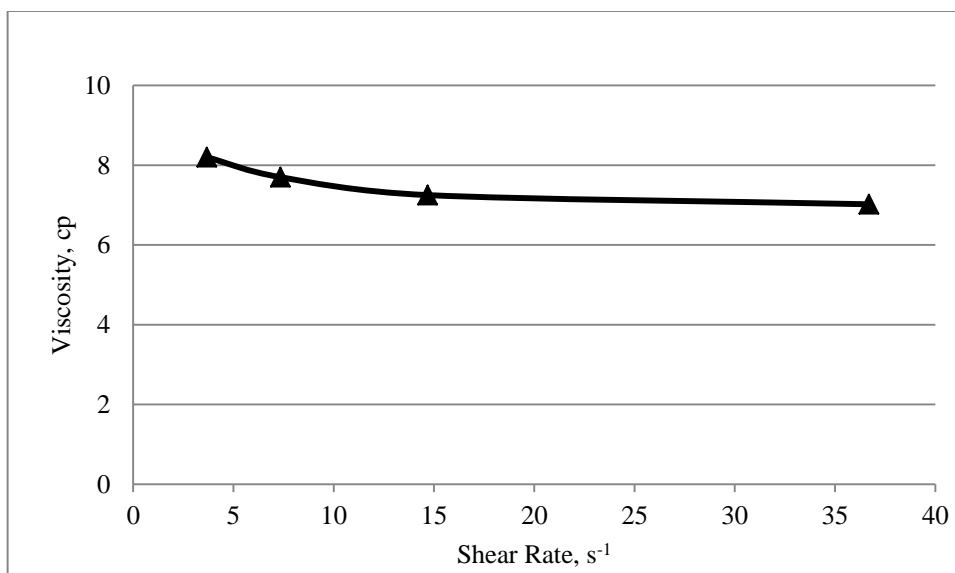


Fig.5.4—Effect of shear rate on the viscosity of the surfactant/polymer solution at 46 °C for Miller 29.

5.1.3. Stability Test



Fig.5.5—Stability tests of the surfactant/polymer solution at 46 °C for Miller 29.

In this study, the stability of the surfactant/polymer formulation was tested at the reservoir temperature of 46 °C. Fig. 5.5 showed the stability of the surfactant/polymer solution at 46 °C for Miller 29. No precipitation or phase separation was observed from the stability test over extended period (6 months), thus the stability of surfactant/polymer solution was verified at 46 °C.

5.1.4. Sand Packed Column Test

Test #	Slug	Oil recovery, %
1	0.5 PV	26
2	0.75 PV	38
3	1 PV	44

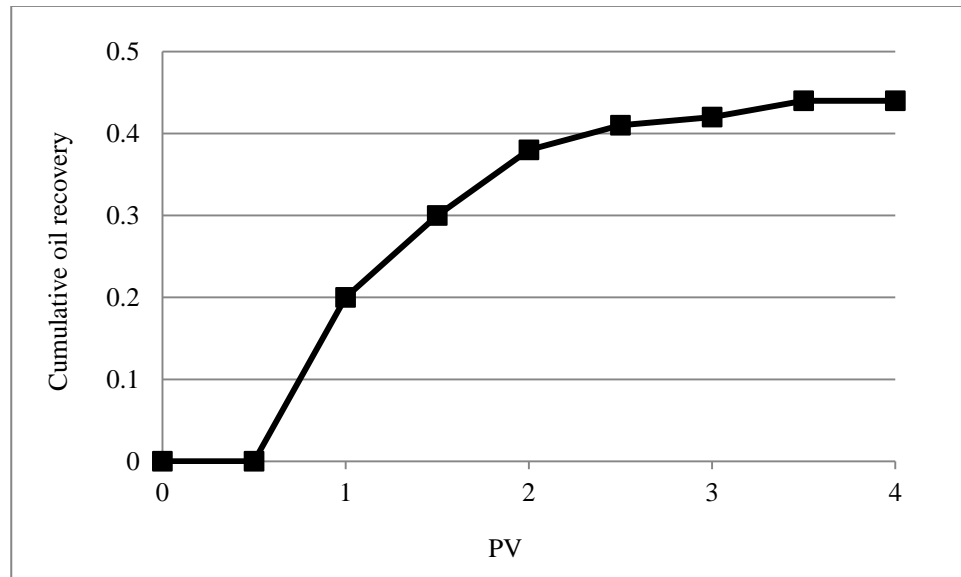


Fig.5.6—Cumulative oil recovery of sand packed column test using 1 PV surfactant/polymer slug for Miller 29.

The ternary surfactant/polymer mixtures (AOT, 0.18 wt%, Steol CS-460, 0.12 wt%, Calfax DB 45, 0.12 wt%, SUPERPUSHER, 0.35 wt%) was tested in the 1-inch sand packed column using different chemical slug sizes. The PV of Berea sand pack was 4.5 ml and the porosity was 0.35. The residual saturation after water flood, S_{or} , was close to 30% (of PV). As the injected slug size of surfactant/polymer increased, the levels of oil recovered also increased (Table 5.1). Injection of 1 PV surfactant/polymer mixture recovered additional 44% residual oil from water flooded sand pack (Fig. 5.6), while only 26% oil recovered with 0.5 PV of surfactant/polymer injected.

5.1.5. Core Flood Test

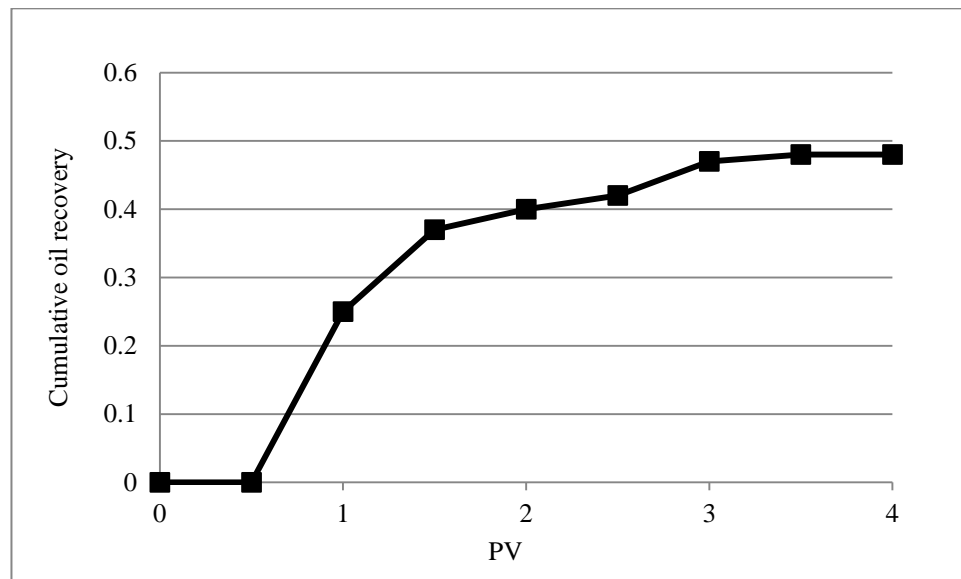


Fig.5.7—Cumulative oil recovery of core flood test using 1 PV surfactant/polymer slug for Miller 29.

Based on these encouraging results, the injection strategy of sand pack #3 was further evaluated in the core flood experiment. The dimension of the consolidated Berea core

plug was one inch long and one inch of diameter with a permeability of 50 mD. The PV of the core plug determined in this study was 3.2 ml and the porosity was 0.25. The Sor after water flood was 35% PV. A total of 48 % residual oil after water flood was recovered as a result of surfactant/polymer injection in the core test (Fig. 5.7). Pressure differences across the core were negligible and the core was not plugged during the core flood test.

5.2. Surfactant/Polymer Formulation of Chemical Flood for Primexx Site

5.2.1. Surfactant Formulation

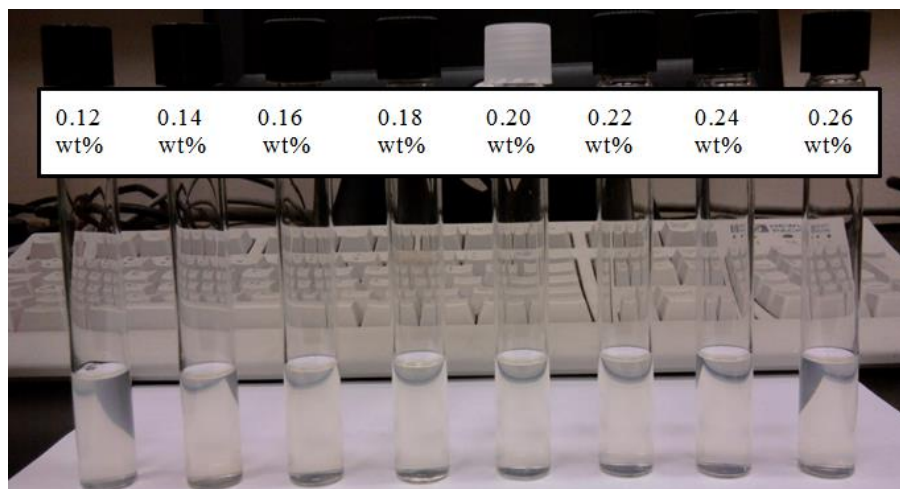


Fig.5.8—Effect of Steol CS-460 concentration on the stability of the surfactant formulation at 50 °C for Primexx.

The site-specific surfactant formulation was developed by changing the concentration of co-surfactant to change the hydrophobicity of the surfactant formulation prepared in the retrieved Primexx brine against the site crude. The concentration of AOT was kept at 0.1 wt% and the concentration of hexyl glucoside was kept at 0.02 wt%, then their

mixtures were scanned with 0.12-0.26 wt% Steol CS-460. Figs. 5.8 and 5.9 showed the effect of Steol CS-460 concentration on the stability and the IFTs with crude oil of the surfactant formulation at reservoir temperature of 50 °C for Primexx site.

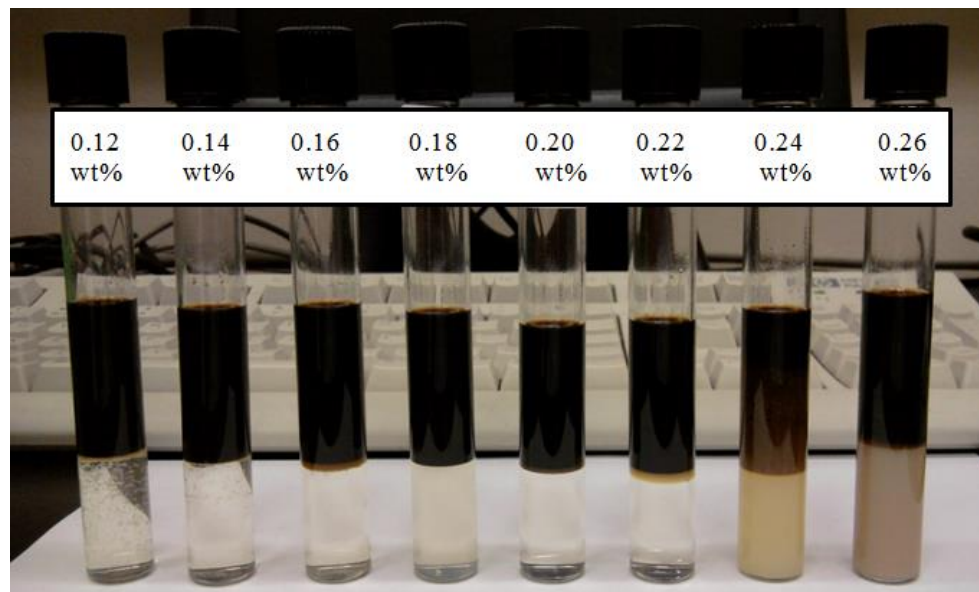


Fig.5.9—Effect of Steol CS-460 concentration on the phase behaviors of the surfactant formulation with crude oil at 50 °C for Primexx.

From these figures, it is clearly that the developed surfactant formulations were stable in the high salinity brine and successfully formed middle phase microemulsions with crude oil under favorable conditions. IFT measurement was used to verify the optimal surfactant formulation, as shown in Fig. 5.10. The optimal surfactant formulation was realized with 0.1 wt% AOT, 0.02 wt% hexyl glucoside and 0.22 wt% Steol CS-460 at ultralow IFT value of 0.002 mN/m. The coalescence rate of the excess phases for these middle phase microemulsions was from several minutes to one hour.

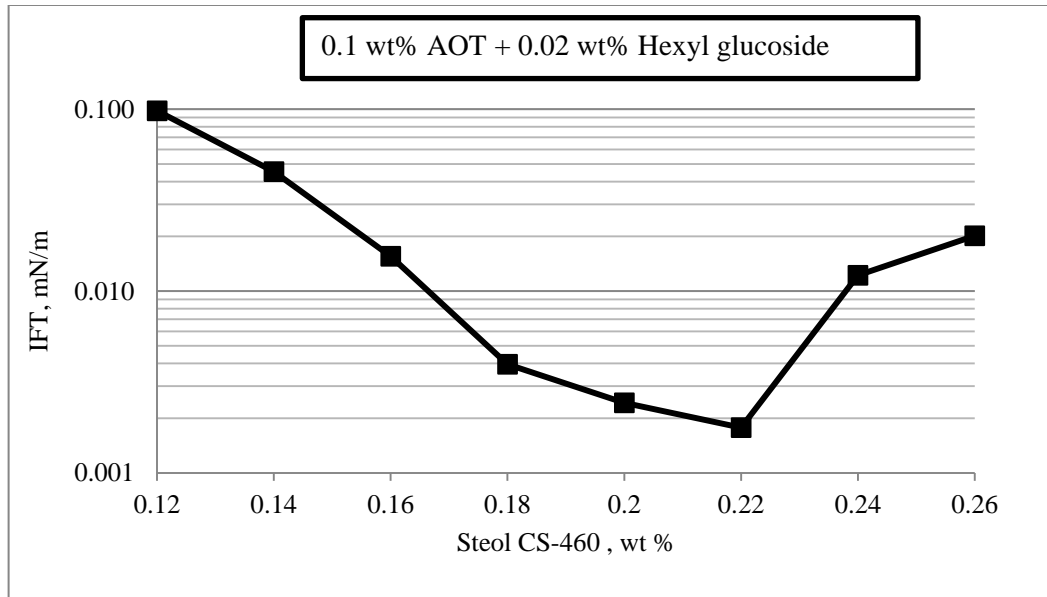


Fig.5.10—Effect of Steol CS-460 concentration on IFT of the surfactant formulation with crude oil at 50 °C for Primexx.

5.2.2. Mixed Surfactant/Polymer Formulation

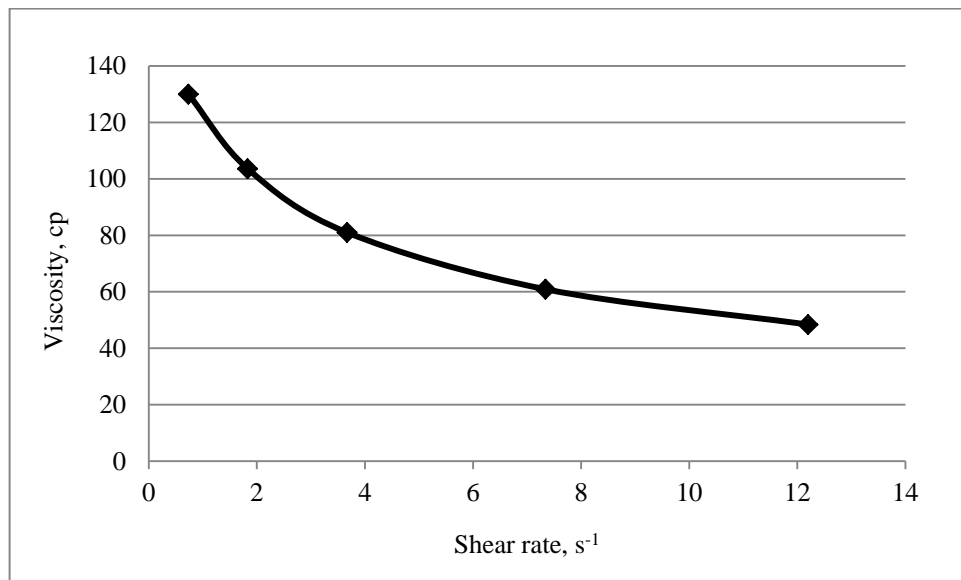


Fig.5.11—Effect of shear rate on the viscosity of the surfactant/polymer solution at 50 °C for Primexx.

A total of 1500 ppm (0.15 wt%) xanthan gum was introduced to the optimal surfactant formulation (0.1 wt% AOT, 0.02 wt% hexyl glucoside and 0.22 wt% Steol CS-460) to evaluate the performance of mixed surfactant/polymer solution. The IFT of the surfactant/polymer solution with crude oil increased slightly to 0.006 mN/m. The observed viscosities of surfactant/polymer mixture decreased with increasing the shear rate and were in the range of 48.4-130 cp (Fig. 5.11). Since the expected shear rate in reservoir floods falls within the range of 1 to 20 s⁻¹ (Awang et al. 2012) and the crude oil viscosity was 2.3 cp at reservoir temperature (50 °C), the binary surfactant/polymer formulation provided adequate viscosity for favorable mobility control in this study.

5.2.3. Stability Test



Fig.5.12—Stability of the surfactant/polymer formulation at 50 °C for Primexx.

In this study, the stability of the surfactant/polymer formulation was tested at the reservoir temperature of 50 °C. Fig. 5.12 showed the stability of the surfactant/polymer formulation at 50 °C for Primexx. Similarly, no precipitation or phase separation was observed from the stability test over extended period (6 months), thus the surfactant/polymer solution was stable at 50 °C.

5.2.4. Sand Packed Column Test

Test #	Slug	Oil recovery, %
1	0.1 PV	20
2	0.3 PV	35
3	0.5 PV	45

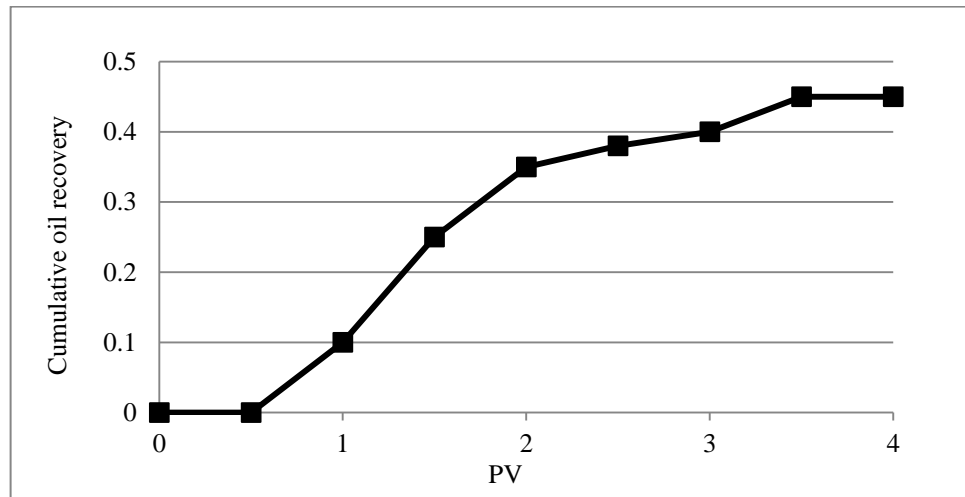


Fig.5.13—Cumulative oil recovery of sand packed column test using 0.5 PV surfactant/polymer slug for Primexx.

The surfactant/polymer solution of 0.1 wt% AOT, 0.02 wt% hexyl glucoside, 0.22 wt% Steol CS-460 and 0.15 wt% xanthan gum was used for the 1-inch sand pack tests by injecting three different slug sizes (PV = 0.1, 0.3, 0.5). The observed PV was 4.5 mL and the porosity was 0.35. As the slug size of surfactant/polymer increased, the oil recovery also increased (Table 5.2). The Sor after water flood was 30% PV. Injection of 0.5 PV surfactant/polymer slug recovered satisfactorily 45% residual oil from the sand packed column after water flood (Fig. 5.13).

5.2.5. Core Flood Test

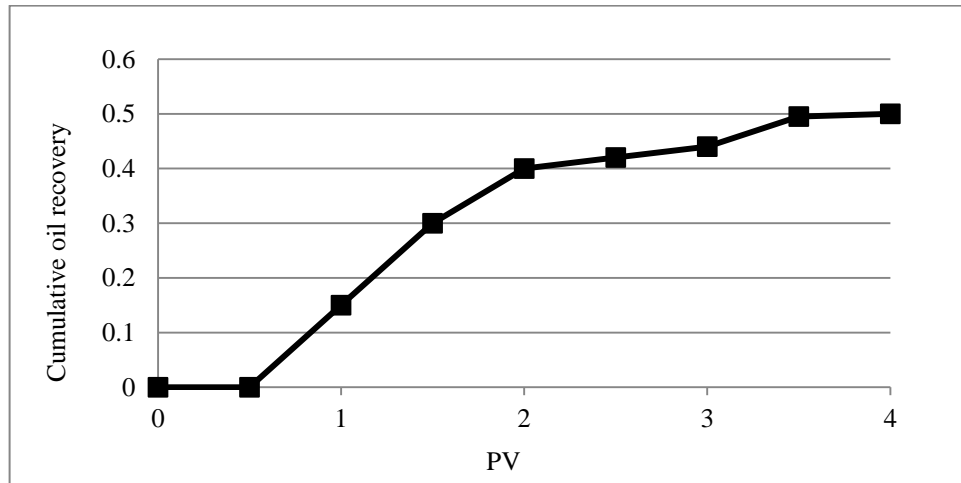


Fig.5.14—Cumulative oil recovery of core flood test using 0.5 PV surfactant/polymer slug for Primexx.

The injection strategy used in sand packed column No.3 was selected for the core flood test. The dimension of the Berea core was one inch long and one inch of diameter with a permeability of 50 mD. One PV was measured to be 3.2 ml and the porosity of the core was 0.25. Sor after water flood was around 35% PV. Based on the results, 50% residual oil of post water flooded in the core was recovered after injecting 0.5 PV surfactant/polymer slug (Fig. 5.14). Similar to the Miller 29 core tests, pressure differences across the core was basically negligible and the core showed no sign of plugging during the core flood.

5.3. Surfactant only Formulation of Chemical Flood for Litchfield Site

5.3.1. Surfactant Formulation

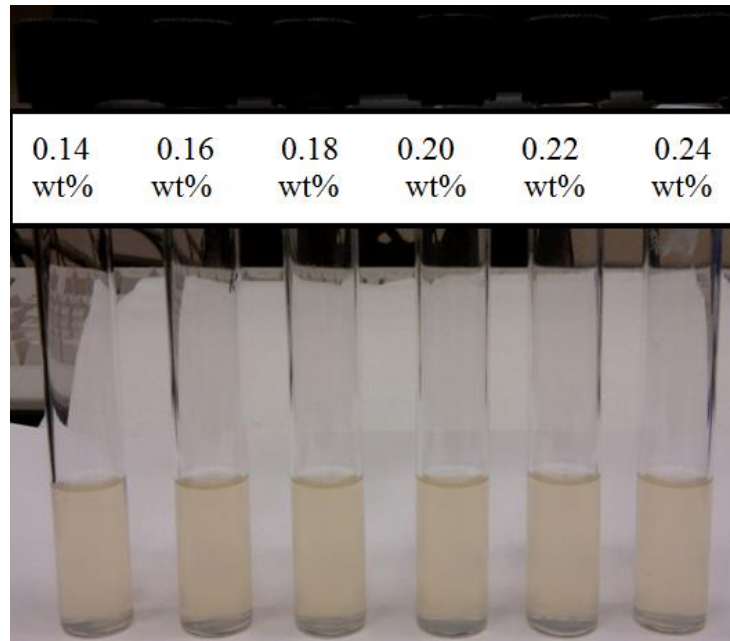


Fig.5.15—Effect of Steol CS-460 concentration on the stability of surfactant formulation at 36 °C for Litchfield.

The site-specific surfactant formulation was also developed for the target No. 3 Litchfield site using similar approach by changing the concentration of co-surfactant to change the hydrophobicity of the surfactant formulation. The concentration of anionic extended surfactant, AF 123-8S, was kept constant at 0.125 wt%, and then the formulation was scanned with different concentrations of Steol CS-460, between 0.14 and 0.24 wt%. Figs. 5.15 and 5.16 showed the effect of Steol CS-460 concentration on the stability and IFTs with Lichfield crude oil at reservoir temperature of 36 °C. From these figures, we observed that a binary mixture of AF 123-8S and Steol CS-460 can create middle phase microemulsions with Lichfield crude under proper conditions. The

IFT measurements were conducted to confirm the optimal surfactant formulation, as depicted in Fig. 5.17. The developed binary system surfactant system, 0.125 wt% AF 123-8S and 0.2 wt% Steol CS-460, exhibited ultralow IFT value of 0.006 mN/m. The resulting coalescence rate of the excess phases for these middle phase microemulsions were from several minutes to one hour.

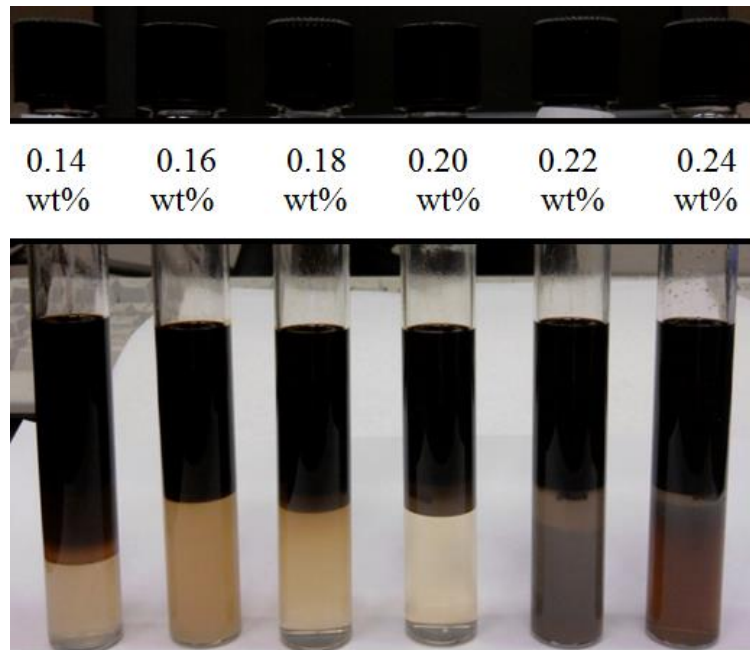


Fig.5.16—Effect of Steol CS-460 concentration on the phase behavior of the surfactant formulation with crude oil at 36 °C for Litchfield.

5.3.2. Wormlike Micelles Formulation for Litchfield Site

In addition to mixed surfactant formulation, viscous wormlike micelles system were also attempted using single surfactant system, including 1 wt% Steol CS-460 scanned with 0-0.5 wt% hexyl glucoside at reservoir conditions of 36 °C (Raj 2013). There was phase separation when the concentrations of hexyl glucoside were lower, < 0.1 wt%,

while there was no phase separation when the concentration of hexyl glucoside was much higher, between 0.2 to 0.5 wt%. This showed that it was highly desirable to add adequate hexyl glucoside (> 0.2 wt%) to maintain the stability of wormlike micelles system in the high salinity brine.

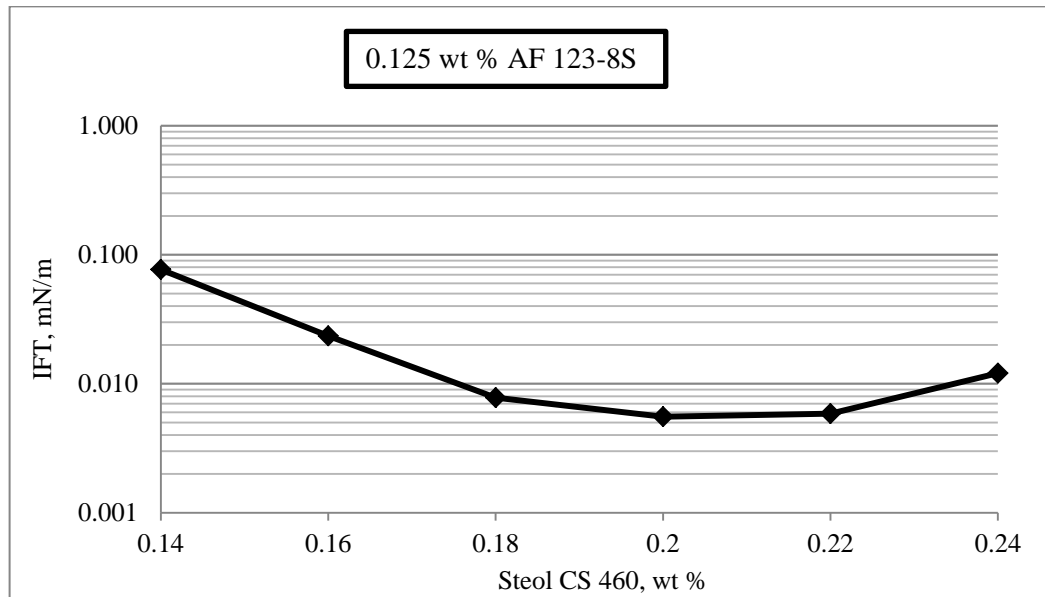


Fig.5.17—Effect of Steol CS-460 concentration on IFT of the surfactant formulation with crude oil at 36 °C for Litchfield.

The viscosity of the wormlike micelles tested was almost independent of the shear rates applied (Fig. 5.18), which provided further advantage to use wormlike micelles as the mobility control agent as compared to conventional polymers, mainly because there was almost no viscosity loss due to increase of shear rate. In addition, the wormlike micelles system of 1 wt% Steol CS-460 and 0.2 wt% hexyl glucoside exhibited the highest viscosity (close to 45 cp) observed in this study. The IFT of the wormlike micelles with crude oil at reservoir temperature was less impressive, equaled to 0.25 mN/m.

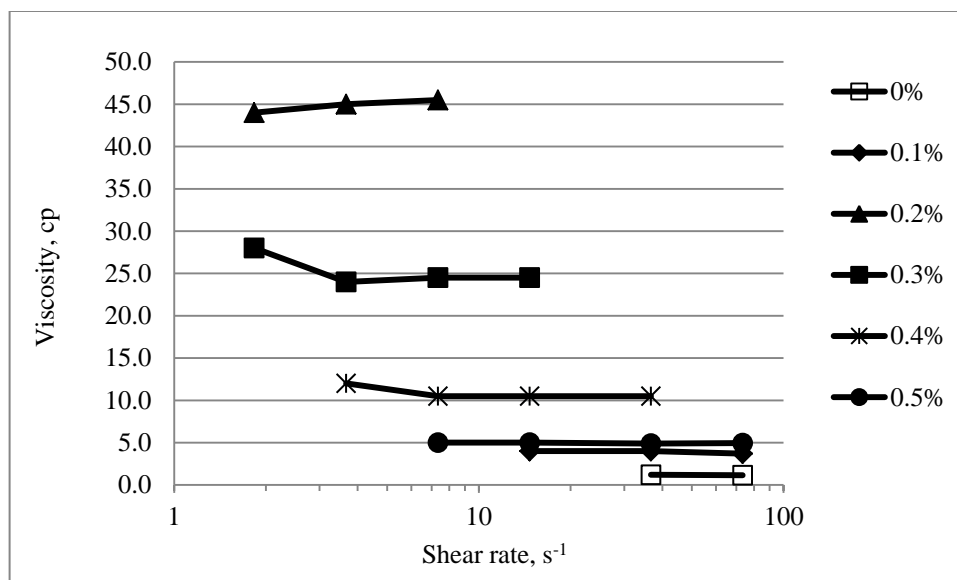


Fig.5.18—Viscosity as a function of shear rate for wormlike micelles at different concentrations of hexyl glucoside for Litchfield.

5.3.3. Stability Test

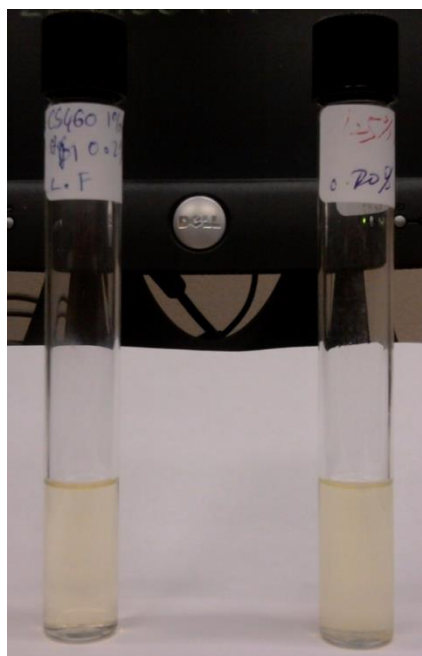


Fig.5.19—Stability of the wormlike micelles (left) and surfactant formulation (right) at 36 °C for Litchfield.

In this study, the solution stabilities of the mixed surfactant formulations of 0.125 wt% AF 123-8S and 0.2 wt% Steol CS-460, and the wormlike micelles system of 1 wt% Steol CS-460 and 0.2 wt% hexyl glycoside were both examined at the reservoir temperature of 36 °C. Fig. 5.19 showed the stability of the wormlike micelles and the surfactant formulation at 36 °C for Lichfield site. Since no precipitation or phase separation was observed over extended period (6 months), both mixed surfactant formulation and wormlike micelles system were stable at 36 °C.

5.3.4. Sand Packed Column Test

Table 5.3 summarizes the results of the sand pack tests for Lichfield.

Test #	Pre-slug, PV	Binary-slug, PV	Post-slug, PV	Oil recovery, %
1		1.5		13
2	0.1			8
3	0.5			8
4		1.5	0.5	13
5	0.1	1.5	0.4	25
6	0.1	1.5		25
7	0.1	0.5		17
8	0.1	1		21

The optimal surfactant formulation with 0.125 wt% AF 123-8S and 0.2 wt% Steol CS-460 was used for all 1 inch sand pack tests as the main chemical slug. In general, 1 PV was 4.5 ml and porosity was 0.35. Noted that the wormlike micelles of 1 wt% Steol CS-460 with 0.2 wt% hexyl glucoside was injected only as pre-slug or post-slug for mobility control purpose.

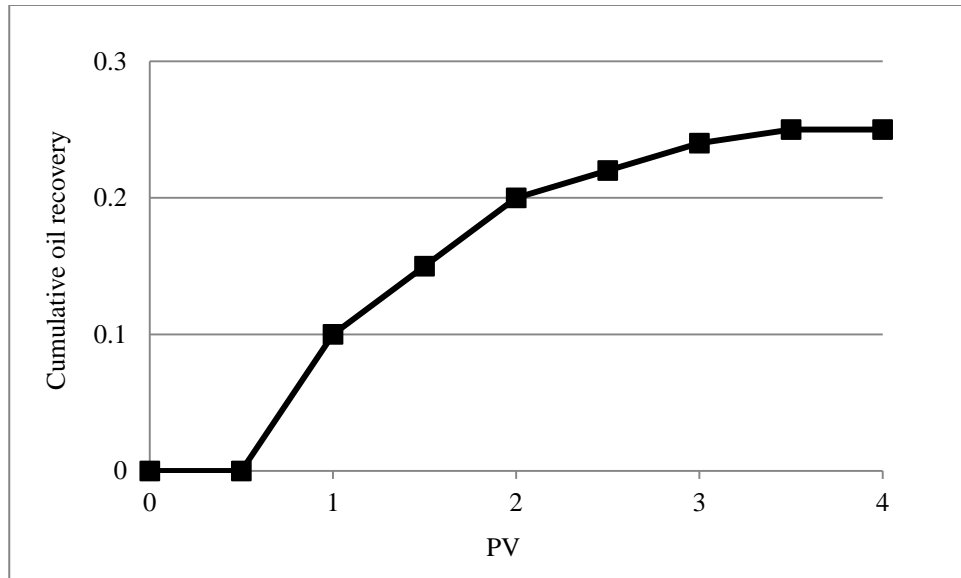


Fig.5.20— Cumulative oil recovery of sand packed column test using 0.1 PV Pre-slug + 1.5 PV binary slug for Litchfield.

The chemical injection strategy for the sand packed column test #1 was 1.5 PV binary main slug and 13% residual oil after water flood was recovered. As shown by sand pack tests #2 and #3, injecting 0.1 or 0.5 PV of wormlike micelles without Ultralow IFT main slug recovered only 8% of the residual oil, which was much less than the binary slug obtained by sand pack test #1. This indicated that the binary surfactant formulation (an Ultralow IFT system) was very effective to recover oil. To explore the impact of pre-slug or post-slug on recovery, applying pre-slug or/and post-slug steps was studied in sand packed column tests #4 and #5. The residual oil recovery was 25% when using 0.1 PV pre-slug, followed by 1.5 PV binary slug and 0.4 PV post slug (Sand pack No. 5). This showed that when surfactant-only slug was used without mobility control, it would follow the water channels through the formation formed during water flood, and thus the amount of oil recovered was compromised. When mobility control agent is

used, it can block water channels and seek out oil-bearing channels, thus can maximize oil recovery (Sheng 2010).

However, injection of 0.5 PV post-slug only after 1.5 PV main slugs had insignificant effects on oil recovery. In sand pack test #6 (Fig. 5.20), applying 0.1 PV pre-slug, followed by 1.5 PV binary slug, achieved almost identical oil recovery as that of sand pack test #5. In addition, further studies showed that increase of the main binary slug size can increase the oil recovery in the presence of 0.1 PV pre-slug (Sand pack #6 vs. #7 & #8). Overall, the sand packed column tests indicated that injection of 0.1 PV pre-slug, followed by 1.5 PV binary slug, achieved the highest oil recovery in the study for sand packed column tests.

5.3.5. Core Flood Test

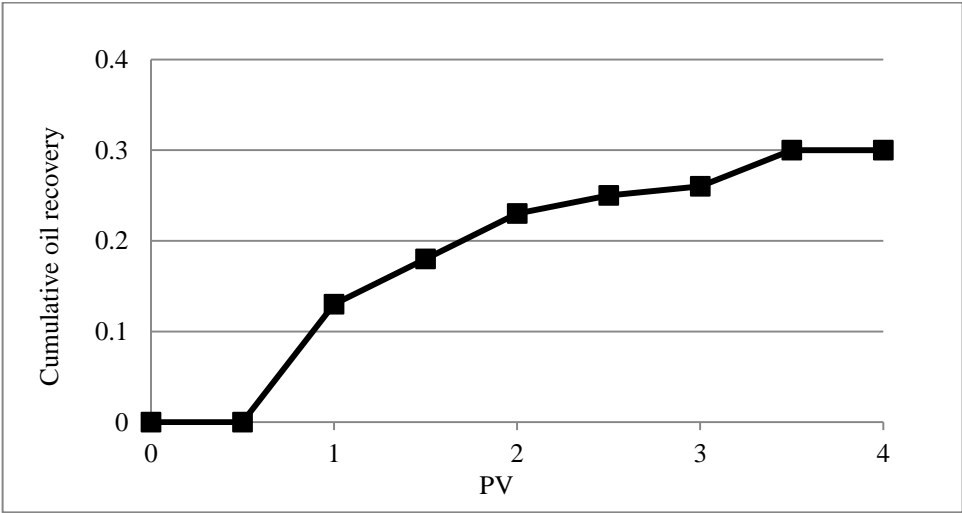


Fig.5.21—Cumulative oil recovery of core flood test using 0.1 PV Pre-slug + 1.5 PV binary slug for Lichfield.

The injection strategy of sand pack # 6 was selected for the core flood test. The dimension of the Berea core was one inch long and one inch of diameter with a permeability of 20 mD (close to site-specific conditions). For 20 mD core, 1 PV was equal to 2.1 mL with the observed porosity of 0.16. The Sor after water flooded was around 35% PV. A total of 30% residual oil after water flood was recovered in this core test (Fig. 5.21). Pressure across the core was negligible and the core was not plugged during the core flood.

5.4. Correlation of Sor after Chemical Flood and Capillary Number for Three Sites

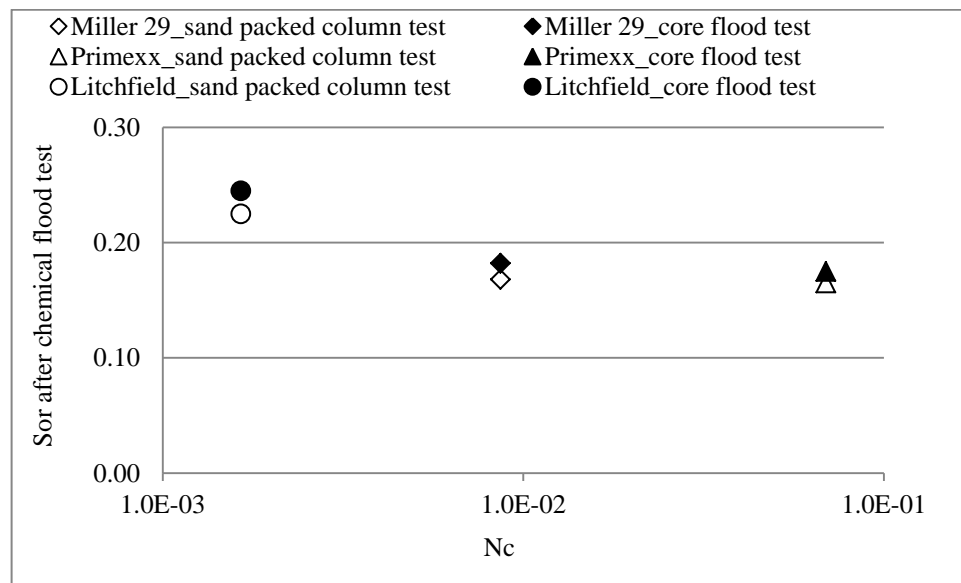


Fig.5.22—Correlation of Sor after chemical flood and capillary number for three sites.

The capillary numbers (N_c) for the chemical flood tests of the three sites were calculated according to Eq. 1.2 and then they were correlated with the Sor after chemical flood tests (Fig. 5.22). Fig. 5.22 showed that Sor tended to decrease with increasing the capillary number and similar correlations were reported in the literature

(Green and Willhite 1998). Since for a given site, the same injection rate was used for both the sand packed column test and core flood test, the Sor after the two tests using the same chemical injection strategy was very close to each other.

5.5. Summary

In this study, we successfully developed several potential surfactant/polymer formulations for three target high salinity formations.

For Miller 29 site, the surfactant formulation of 0.18 wt% AOT, 0.12 wt% Steol CS-460 and 0.12 wt% Calfax DB 45 achieved ultralow IFT (0.006 mN/m) with crude oil. The addition of 3500 ppm (0.35 wt%) SUPERPUSHER in the surfactant formulation gave reasonable low IFT (0.008 mN/m) and high viscosity (7.7 cp at shear rate of 7.34 s^{-1}). The developed surfactant/polymer formulation was stable at reservoir conditions. The injection strategy with 1 PV of the surfactant/polymer slug recovered 45% residual oil after water flood in the sand packed column test and recovered 48 % residual oil after water flood in the core flood test.

For Primexx site, the second surfactant formulation of 0.1 wt% AOT, 0.22 wt% STEOL CS-460 and 0.02 wt% hexyl glucoside exhibited ultralow IFT of 0.002 mN/m. The addition of 1500 ppm xanthan gum in the surfactant formulation gave ultralow IFT (0.006 mN/m) and high viscosity (60.9 cp at shear rate of 7.34 s^{-1}). The developed surfactant/polymer formulation remained stable at reservoir conditions. The injection strategy with 0.5 PV of the surfactant/polymer slug recovered 45% residual oil after water flood in the sand packed column test and recovered 50 % residual oil after water flood in the core flood test.

For Litchfield site, a mixed extended surfactant formulation of 0.125 wt% AF 123-8S and 0.2 wt% STEOL CS-460 achieved the ultralow IFT value of 0.006 mN/m with Litchfield crude oil. Addition of wormlike micelles with 1 wt% STEOL CS-460 and 0.2 wt% hexyl glucoside provided the required viscosity (around 45 cp). The developed chemical formulation was stable at reservoir conditions. The injection strategy with 0.1 PV of wormlike micelles and 1.5 PV binary surfactant slug recovered 25% residual oil after water flood in the sand packed column test and recovered 30% residual oil after water flood in the core flood test.

Chapter 6. Surfactant Formulation of Chemical Flood for a High Salinity and Temperature Reservoir

This chapter attempted to develop the surfactant formulation for a pre-determined high salinity (15 wt% NaCl) and high temperature (90 °C) reservoir conditions. Dodecane (EACN =12) was used as the representative oil. Once a good Ultralow IFT and stable chemical formulation was developed, flow-through sand pack tests and core flood experiment were conducted to assess chemical flood in the laboratory to evaluate the performance of the chemical formulations developed.

6.1. Challenges of Surfactant Formulation at High Temperature

Phase behavior test using flat-bottom glass vials with Teflon-lined screw caps works well for surfactant formulation at low temperature (< 60 °C). However, the high vapor pressures from water and oil at high temperature (> 60 °C) may cause the problem of rupture or explosion, thus the use of these vials for surfactant formulation at high temperature (> 60 °C) may be problematic from a laboratory safety standpoint. Thus for surfactant formulation using phase behavior test at high temperature (> 60 °C), specifically designed test tube is required to prevent possible rupture or explosion (Barnes et al. 2008a). In this study, round-bottom pressurized glass vials with crimp seals with inserted septa were purchased from CEM Corporation (Matthews, NC) (Fig. 6.1). Preliminary tests at 90 °C and 120 °C using these vials with dodecane and/or water showed that they did not have the problem of rupture or explosion at both temperatures for at least one month. Thus they were used to develop surfactant formulation at 90 °C in this study.

Internal olefin sulfonate (IOS 15-18) was first selected and studied at a series of concentrations (0.3, 0.4, 0.5, 1, 2 wt%) to develop surfactant formulation for the high salinity and high temperature reservoir (Figs.6.2 and 6.3). The results showed that middle phase microemulsions were formed for all the tests, even though the aqueous solutions of single surfactant formulation appeared unstable under both high salinity and high temperature conditions. Thus, we further modified and tried several approaches to better control of stability of the surfactant formulations under harsh high salinity and high temperature conditions (Salager et al. 2005).

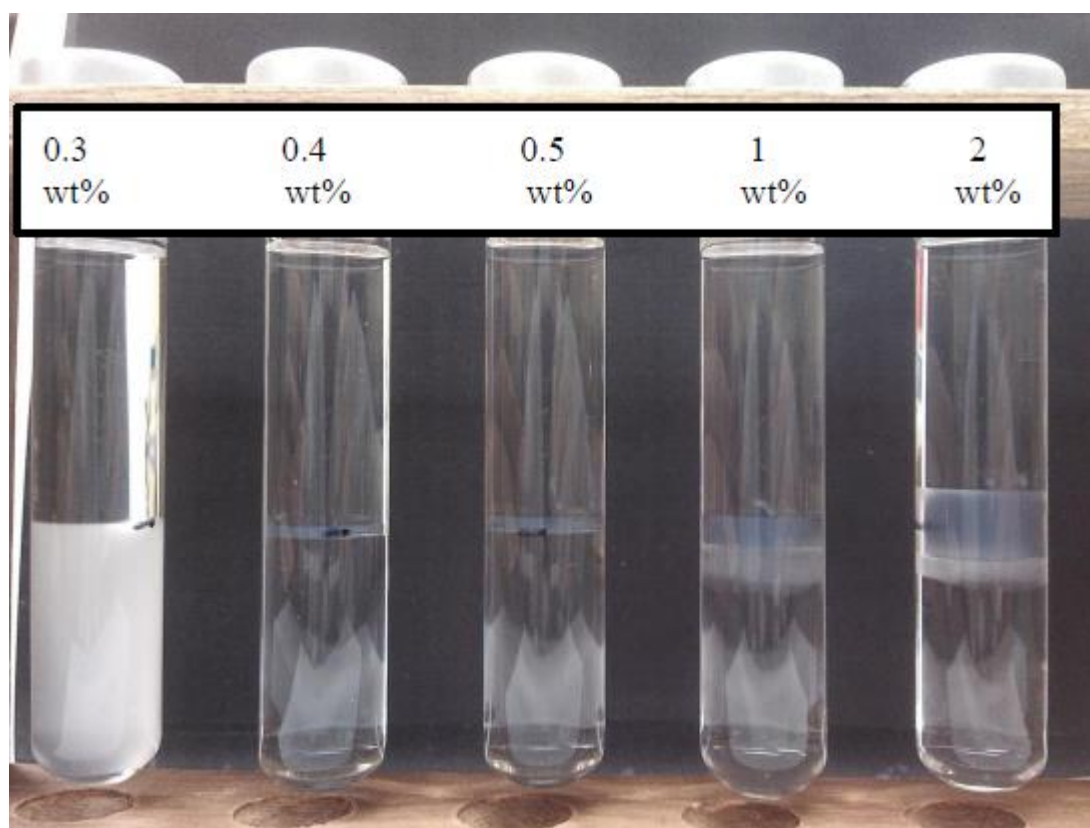


Fig.6.3—Effect of IOS 15-18 concentration on the phase behavior of the surfactant with dodecane at 90 °C.

6.3. Surfactant Formulation with Hexyl Glucoside

Hexyl glucoside (HG) was then investigated at difference concentration (0.05, 0.1, 0.15, 0.2, 0.25, 0.3 wt%) with 0.5 wt% IOS 15-18 to deveolp surfactant formulotion for the high salinity and high temperature formation (Figs. 6.4 and 6.5). The results showed that the surfactant formulation was cloudy prepared in high salinity brine at high temperature with 0.05- 0.15 wt% HG, even though several middle phase microemusions were formed.

However, as the HG concentration further increased from 0.2 to 0.3 wt%, the surfactant formulation was stable in the high salinity brine at high temperature, but the middle phase microemusions disappeared.

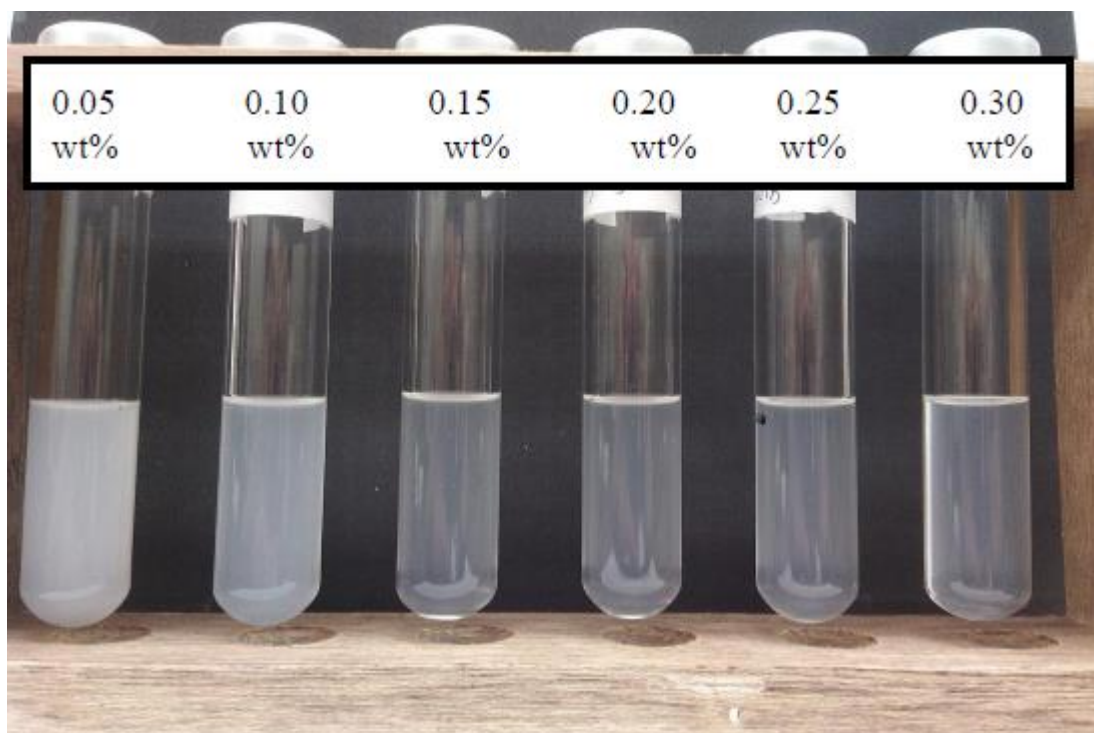


Fig.6.4—Effect of HG concentration on stability of 0.5 wt% IOS 15-18 at 90 °C.

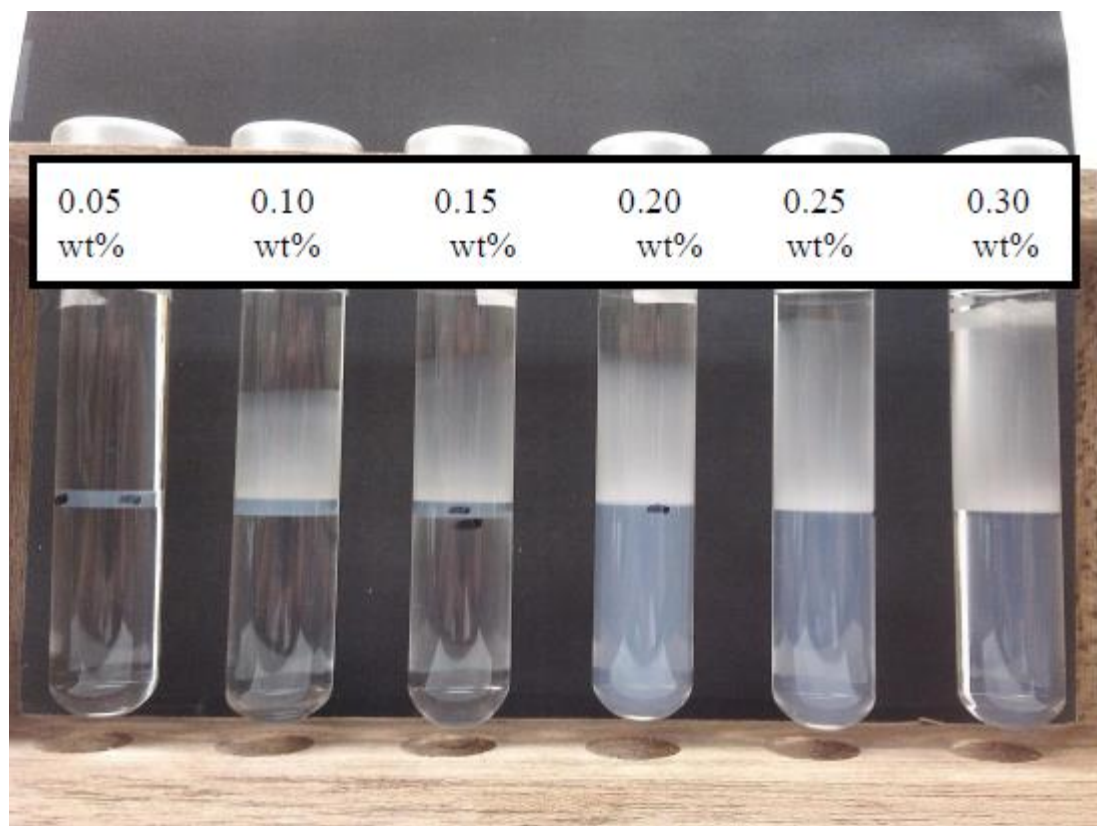


Fig.6.5—Effect of HG concentration on phase behavior of 0.5 wt% IOS 15-18 with dodecane at 90 °C.

6.4. Surfactant Formulation with Isopropanol

Isopropanol (IPA) was then investigated at difference concentration (0.5, 0.55, 0.6, 0.65, 0.7, 0.75 wt%) with 0.5 wt% IOS 15-18 to deveolp surfactant formualtion for the high salinity and high temperature reservoir (Figs. 6.6 and 6.7). The results showed that the surfactant formulation was cloudy, while phase separation occurred in the high salinity brine at high temperature with 0.5-0.6 wt% IPA. However, as the IPA concentration further increased from 0.65 to 0.75 wt%, the surfactant formulation was stable in the high salinity brine at high temperature. This is because IPA can help maintain the stability of surfactants under harsh conditons (Salager et al. 2005).

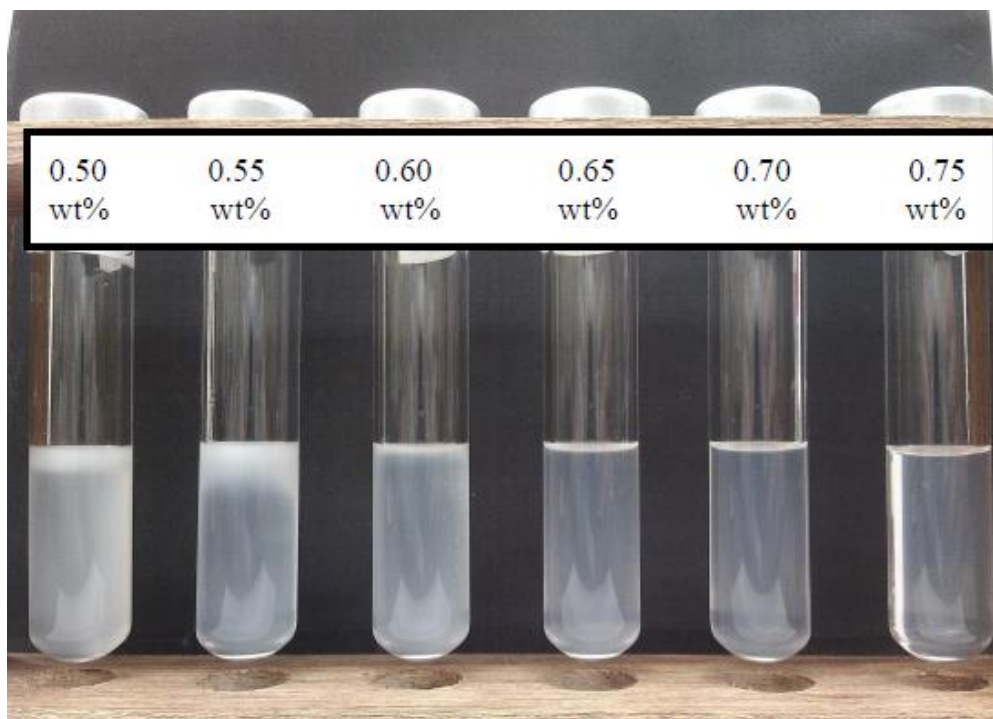


Fig.6.6—Effect of IPA concentration on stability of 0.5 wt% IOS 15-18 at 90 °C.

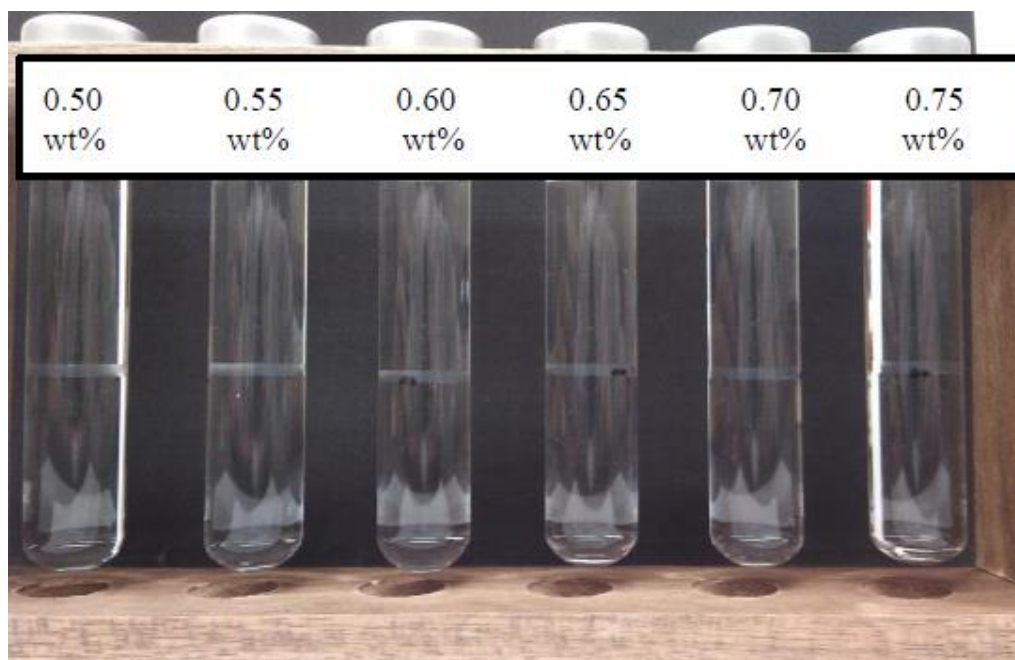


Fig.6.7—Effect of IPA concentration on phase behavior of 0.5 wt% IOS 15-18 with dodecane at 90 °C.

Middle phase microemulsions were formed in all the tests with IPA. As shown in Fig. 6.8, IFT of 0.5 wt% IOS 15-18 with dodecane increased slightly with increasing IPA concentration, but all resulting IFTs were below 0.01 mN/m.

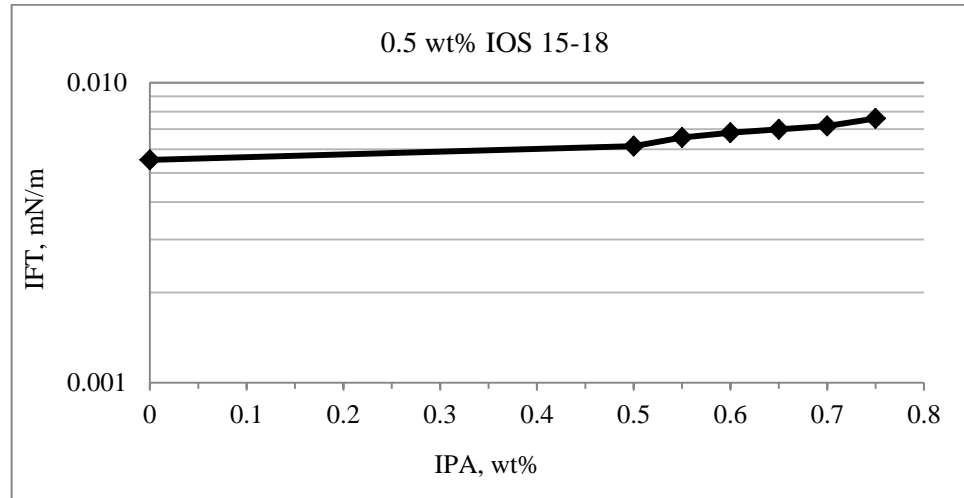


Fig.6.8—Effect of IPA concentration on IFT of 0.5 wt% IOS 15-18 formulation with dodecane at 90 °C.

6.5. Surfactant Formulation with sec-Butanol

The sec-Butanol (SB) was then investigated at difference concentration (0.25, 0.3, 0.35, 0.4, 0.45, 0.5 wt%) with 0.5 wt% IOS 15-18 to deveolp surfactant formualtion for the high salinity and high temperature reservoir (Figs. 6.9 and 6.10). The results showed that the surfactant formulation was cloudy in the high salinity brine at high temperature with 0.25- 0.35 wt% SB. However, as the SB concentration further increased from 0.4 to 0.5 wt%, the surfactant formulation was stable in the high salinity brine at high temperature. This is because SB can help maintain the stability of surfactants under harsh conditons (Salager et al. 2005). Middle phase microemulsions were formed in all the tests with SB. As shown in Fig. 6.11, IFT of 0.5 wt% IOS 15-18 with dodecane

increased slightly with increasing SB concentration, but all IFT values were below 0.01 mN/m.

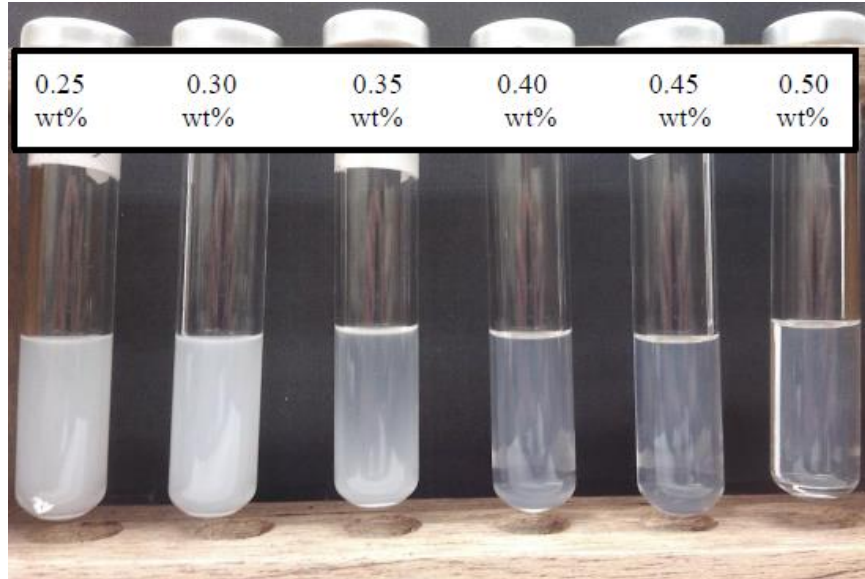


Fig.6.9—Effect of SB concentration on the stability of 0.5 wt% IOS 15-18 at 90 °C.

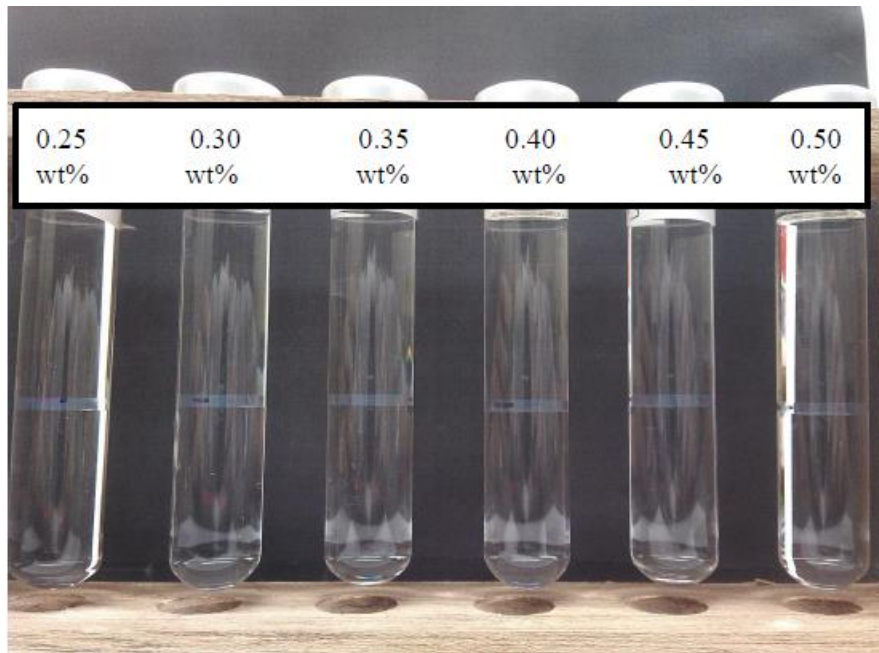


Fig.6.10—Effect of SB concentration on the phase behavior of 0.5 wt% IOS 15-18 with dodecane at 90 °C.

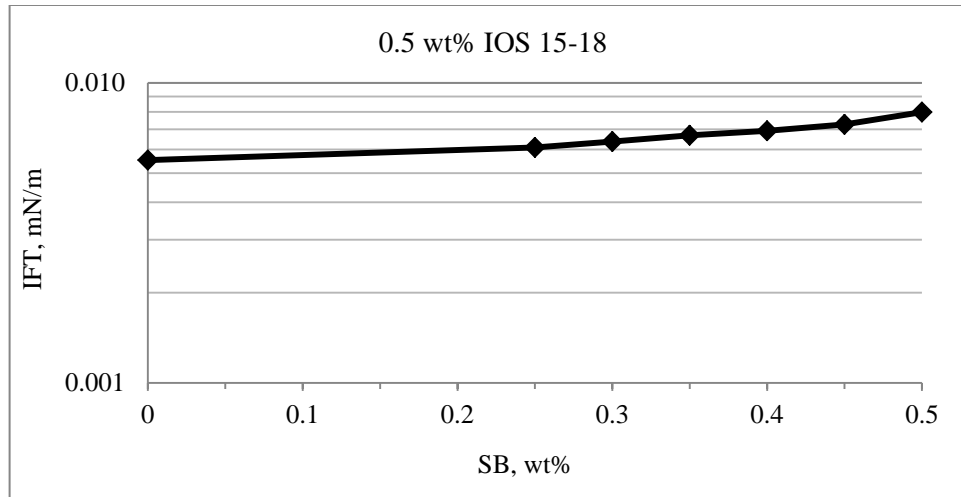


Fig.6.11—Effect of SB concentration on IFT of 0.5 wt% IOS 15-18 with dodecane at 90 °C.

6.6. Sand Packed Column Test

The surfactant formulation of 0.5 wt% IOS 15-18, 0.5 wt% SB was used for the 6 inch Ottawa sand (F-95) packed column test. 1 PV was 30 ml and porosity was 0.38. The Sor after water flood was 21% PV. The sand packed column test after injecting 1 PV surfactant slug exhibited 73% residual oil recovery after water flood (Fig. 6.12).

6.7. Core Flood Test

The injection strategy similar to the sand pack test described above was used for the core flood experiment. The dimension of the Berea core was three inch long and one inch of diameter with a permeability of 500 mD. 1 PV was 8.38 ml and porosity was 0.22. Sor after water flood was around 38% PV. A total of 50% residual oil after water flood was recovered in the core test by injecting 1 PV surfactant slug (Fig. 6.13). Pressure across the core was negligible and the core was not plugged during the core flood test.

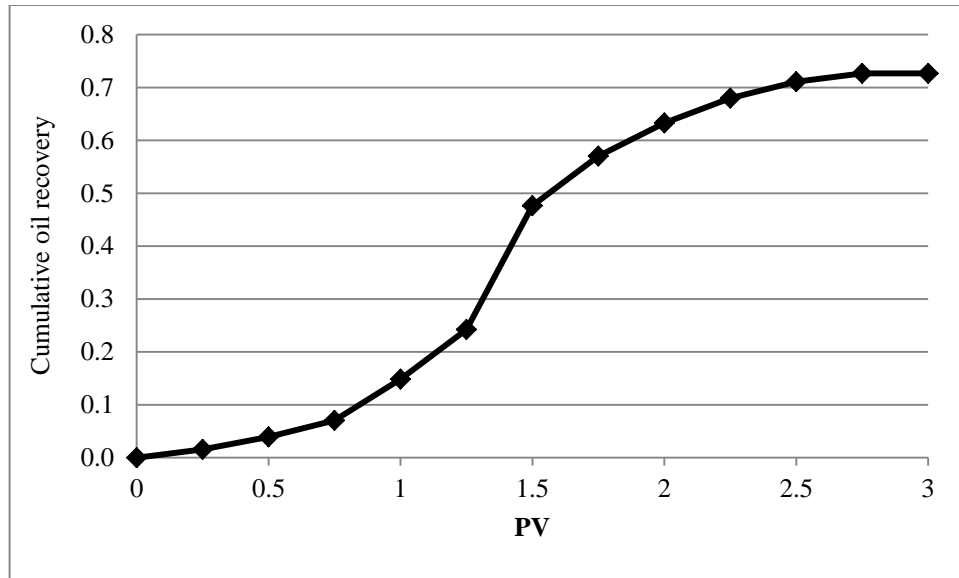


Fig.6.12—Cumulative oil recovery of sand packed column test using 1 PV surfactant slug.

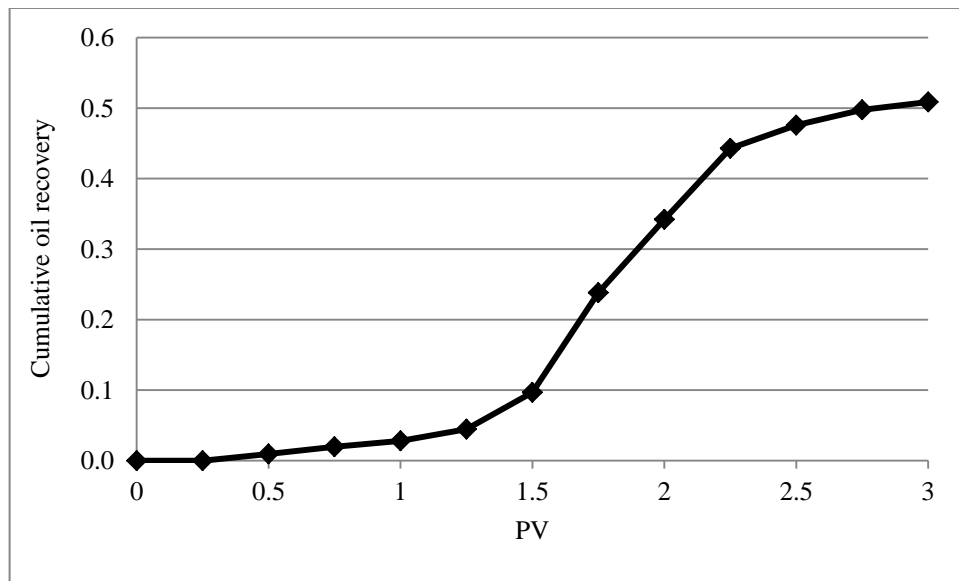


Fig.6.13—Cumulative oil recovery of core flood test using 1 PV surfactant slug.

6.8. Summary

This study successfully developed a surfactant formulation for a high salinity (15 wt% NaCl) and high temperature (90 °C) reservoir. Dodecane (EACN =12) was used as the oil. The results showed that 0.5 wt % internal olefin sulfonate IOS 15-18 could form middle phase microemulsions with dodecane, but the single surfactant was not stable in the high salinity brine at high temperature. Further study showed that the addition of 0.65- 0.75 wt% IPA could stabilize 0.5 wt% IOS 15-18 in the high salinity brine at high temperature and the surfactant formulation of 0.65- 0.75 wt% IPA with 0.5 wt% IOS 15-18 achieved ultralow IFT (0.007 mN/m) with dodecane. In addition, the addition of 0.4- 0.5 wt% SB could stabilize 0.5 wt% IOS 15-18 in the high salinity brine at high temperature and the surfactant formulation of 0.4- 0.5 wt% SB with 0.5 wt% IOS 15-18 achieved ultralow IFT (0.008 mN/m). The injection strategy with 1 PV 0.5 wt% IOS 15-18 and 0.5 wt% SB recovered 73% residual oil after water flood in the sand packed column test and recovered 50% residual oil after water flood in the core flood test.

Chapter 7. Conclusions and Recommendations

7.1. Conclusions

In this study, EACN of crude oil from field sites was determined by using salinity scan of the crude oil or mixed oil (a mixture of crude oil and decane) and an anionic surfactant to obtain the optimal salinity and then applying an empirical correlation. The EACN of crude oil determined by using salinity scan of crude oil and conventional surfactant (a mixture of 2.2 wt% AOT and 8 wt% isobutanol) (direct method) was very close to those determined by using the salinity scan of the mixed oil (a mixture of crude oil and decane) and the same conventional surfactant (indirect method). However, the direct method only needed to conduct one set of salinity scan, thus it is much simpler than the indirect method to determine EACN of crude oil. The EACN of crude oil determined by using the extended surfactant (2.5 wt% AF 8-41S) were very close to those determined by using conventional surfactant. However, the method of using extended surfactant to determine EACN of crude oil does not need co-solvent, thus it is simpler than conventional surfactant to determine EACN of crude oil. The EACN of crude oil determined was 6.0-11.3.

Phase behavior tests using extended surfactants were investigated. For a given single or binary surfactants, the middle phase microemulsion window became wider and wider with increasing butyl carbitol concentration, even though IFT slightly increased when increasing butyl carbitol concentration. Co-surfactant could also help the formation of middle phase microemulsions. Middle phase microemulsions formed at both room temperature and 46 °C for most extended surfactant and the optimal salinity decreased

with increasing the temperature. The presence of EO group, straight and shorter hydrocarbon chain could make the extended surfactants much more hydrophilic, thus more salt was needed to form middle phase microemulsion. The optimal salinity for the four extended surfactants investigated was much higher than that of AOT. $\ln S^*$ increased almost linearly with increasing ACN and there existed a very good linear relationship between $\ln S^*$ and ACN for the four extended surfactant studied.

This study successfully developed a surfactant/polymer formulation for three high salinity reservoirs. For Miller 29 site, the surfactant formulation of 0.18 wt% AOT, 0.12 wt% Steol CS-460 and 0.12 wt% Calfax DB 45 achieved ultralow IFT (0.006 mN/m) with crude oil. The addition of 3500 ppm SUPERPUSHER in the surfactant formulation gave ultralow IFT (0.008 mN/m) and high viscosity (7.7 cp at shear rate of 7.34 s^{-1}). The developed surfactant/polymer formulation was stable at reservoir conditions. The injection strategy with 1 PV of the surfactant/polymer slug recovered 45% residual oil after water flood in the sand packed column test and recovered 48 % residual oil after water flood in the core flood test. For Primexx site, the surfactant formulation of 0.1 wt% AOT, 0.22 wt% STEOL CS-460 and 0.02 wt% hexyl glucoside achieved ultralow IFT (0.002 mN/m) with crude oil. The addition of 1500 ppm xanthan gum in the surfactant formulation gave ultralow IFT (0.006 mN/m) and high viscosity (60.9 cp at shear rate of 7.34 s^{-1}). The developed surfactant/polymer formulation was stable at reservoir conditions. The injection strategy with 0.5 PV of the surfactant/polymer slug recovered 45% residual oil after water flood in the sand packed column test and recovered 50 % residual oil after water flood in the core flood test. For Litchfield site, the surfactant formulation of 0.125 wt% AF 123-8S and 0.2 wt% STEOL CS-460

achieved the ultralow IFT (0.006 mN/m) with crude oil. Wormlike micelles with 1 wt% STEOL CS-460 and 0.2 wt% hexyl glucoside gave the required viscosity (around 45 cp). The developed chemical formulation was stable at reservoir conditions. The injection strategy with 0.1 PV of wormlike micelles and 1.5 PV binary surfactant slug recovered 25% residual oil after water flood in the sand packed column test and recovered 30% residual oil after water flood in the core flood test.

This study also successfully developed a surfactant formulation for a high salinity (15 wt% NaCl) and high temperature (90 °C) reservoir. Dodecane (EACN =12) was used as the oil. The results showed that 0.5 wt % internal olefin sulfonate IOS 15-18 could form middle phase microemulsions with dodecane, but the single surfactant was not stable in the high salinity brine at high temperature. Further study showed that the addition of 0.65- 0.75 wt% IPA could stabilize 0.5 wt% IOS 15-18 in the high salinity brine at high temperature and the surfactant formulation of 0.65- 0.75 wt% IPA with 0.5 wt% IOS 15-18 achieved ultralow IFT (0.007 mN/m) with dodecane. In addition, the addition of 0.4- 0.5 wt% SB could stabilize 0.5 wt% IOS 15-18 in the high salinity brine at high temperature and the surfactant formulation of 0.4- 0.5 wt% SB with 0.5 wt% IOS 15-18 achieved ultralow IFT (0.008 mN/m). The injection strategy with 1 PV 0.5 wt% IOS 15-18 and 0.5 wt% SB recovered 73% residual oil after water flood in the sand packed column test and recovered 50% residual oil after water flood in the core flood test.

7.2. Recommendations

Surfactant loss due to adsorption onto mineral surface mainly occurs for anionic surfactants. pH dependent hydrolysis of surface species of the rock minerals can render

mineral surface with surface charge. The surface is positively charged under low pH conditions and negatively charged under high pH conditions. The pH at which the surface charge reverses is called the point of zero charge (PZC). The PZC for most reservoir rock is around pH=9, thus at neutral reservoir conditions, the mineral surface is positively charged. Thus the ionic attraction between positively charged mineral surface and the negatively charged surfactant anion results in the adsorption of anionic surfactants on mineral surface (Dang et al. 2011; Delamaide et al. 2014; Gao et al. 2010; Grigg and Mikhalin 2007).

In chemical flood, adsorption of anionic surfactant onto mineral surface can reduce the required surfactant concentration to achieve ultra-low IFT. Thus control of adsorption of anionic surfactant in chemical flood is of great importance to achieve a successful chemical flood project (Grigg et al. 2004; Morvan et al. 2009).

Traditionally, alkali such as sodium hydroxide, sodium carbonate and sodium orthosilicate has been used as sacrificial agent to reduce the adsorption of anionic surfactants on the rock mineral surface by increasing the pH of the reservoir fluid to make the mineral surface negatively charged. However, alkali cannot be used in formation with high hardness in the brine, because alkali can form precipitation with divalent ions (Solairaj et al. 2012; Zhou et al. 2005).

Sodium polyacrylate was reported recently as an effective sacrificial agent to reduce adsorption of anionic surfactants on carbonates, sandstones and clays even in the presence of anhydrite and the mechanism (Shamsijazeyi et al. 2013).

This study focused on the performance of surfactant formulation to recover oil after water flood without considering the adsorption of surfactants onto mineral surface in both the sand packed column tests and core flood tests. Quantification of surfactant adsorption in these tests can let us know how many surfactants are lost during the chemical flood, thus will help us design a much more cost effective chemical flood process in future.

Nomenclature

ACN = alkane carbon number, dimensionless

c = capillary

Cc = characteristic curvature of the surfactant, dimensionless

EACN = equivalent alkane carbon number, dimensionless

f(A) = a function of the alcohol type and concentration, dimensionless

HLD = hydrophilic-lipophilic deviation, dimensionless

K = a characteristic parameter of the anionic surfactant

k= permeability, L^2 , mD

M= mobility ratio, dimensionless

Nc =capillary number, dimensionless

p = pressure, m/Lt^2 , psi

r = radius, L, m

S = salinity, dimensionless, wt %

T = Temperature, T, °C

v = Darcy velocity, L/t

x = the mole fraction of surfactant, dimensionless

Greek Symbols

a = parameter for anionic surfactant, $1/T$, $1/^\circ\text{C}$

γ = IFT between the two fluids, m/t^2 , mN/m

Δ = difference

θ = contact angle, degree

λ = mobility

μ = viscosity, m/Lt , cp

ρ = density, m/L^3 , g/cc

ω = angular velocity, $1/t$, RMP

Subscripts

o = oil

w = water

i = surfactant i in the surfactant mixture

Superscripts

$*$ = optimal

SI Metric Conversion Factors

$$\text{cp} \times 1.0 \times 10^{-3} = \text{Pa}\cdot\text{s}$$

$$\text{darcy} \times 9.869233 \times 10^{-13} = \text{m}^2$$

$$\text{in.} \times 2.54 \times 10^0 = \text{cm}$$

$$\text{mL} \times 1.0 \times 10^0 = \text{cm}^3$$

$$\text{psi} \times 6.894\,757 \times 10^0 = \text{kPa}$$

References

Acosta, E.J. and Bhakta, A.S. 2009. The HLD-NAC Model for Mixtures of Ionic and Nonionic Surfactants. *Journal of Surfactants and Detergents* **12**(1): 7-19. <http://dx.doi.org/10.1007/s11743-008-1092-4>.

Acosta, E.J., Mai, P.D., Harwell, J.H., Sabatini., D.A. 2003. Linker-modified Microemulsions for A Variety of Oils and Surfactants. *Journal of Surfactants and Detergents* **6**(4): 353-363. <http://dx.doi.org/10.1007/s11743-003-0281-2>.

Acosta, E.J., Yuan, J.S., and Bhakta, A.S. 2008. The Characteristic Curvature of Ionic Surfactants. *Journal of Surfactants and Detergents* **11**(2): 145-158. <http://dx.doi.org/10.1007/s11743-008-1065-7>.

Albonico, P. and Lockhart, T.P. 1993. Divalent Ion-Resistant Polymer Gels for High-Temperature Applications: Syneresis Inhibiting Additives. Paper SPE 25220 presented at the SPE International Symposium on Oilfield Chemistry, New Orleans, Louisiana, 2-5 March. <http://dx.doi.org/10.2118/25220-MS>.

Anton, R.E., Garces, N., and Yajure, A. 1997. A Correlation for Three-Phase Behavior of Cationic Surfactant-Oil-Water Systems. *Journal of Dispersion Science and Technology* **18**(5): 539-555. <http://dx.doi.org/10.1080/01932699708943755>.

Aoudia, M., Wade, W.H., and Weerasooriya, V. 1995. Optimum Microemulsions Formulated with Propoxylated Tridecyl Alcohol Sodium Sulfates. *Journal of Dispersion Science and Technology* **16**(2): 115-135. <http://dx.doi.org/10.1080/01932699508943664>.

Aparna, R.S., Puerto, M. Yu, B., Miller, C.A., Hirasaki, G.J., Salehi, M., Thomas, C.P. Kwan, J.T. 2013. Laboratory Studies for Surfactant Flood in Low-Temperature, Low-Salinity Fractured Carbonate Reservoir. Paper SPE 164062 presented at the SPE International Symposium on Oilfield Chemistry held in the Woodlands, Texas, USA, 8-10 April. <http://dx.doi.org/10.2118/164062-MS>.

Arpornpong, N., Charoensaeng, A., Sabatini, D.A., Khaodhiar, S. 2010. Ethoxy Carboxylate Extended Surfactant: Micellar, Adsorption and Adsolubilization Properties. *Journal of Surfactants and Detergents* **13**(3):305-311. <http://dx.doi.org/10.1007/s11743-010-1179-6>.

Awang, M., Japper, A., and Iskandar Dzulkarnain, S. 2012. Wormlike Micelles for Mobility Control in EOR. Paper SPE 155059 presented at the SPE EOR Conference at Oil and Gas West Asia, Muscat, Oman, 16-18 April. <http://dx.doi.org/10.2118/155059-MS>.

Baran, J.R., Pope, G.A., Wade, W.H., Weerasooriya, V., and Yapa, A. 1994. Microemulsion Formation with Mixed Chlorinated-Hydrocarbon Liquids. *Journal of Colloid and Interface Science* **168**(1): 67-72. <http://dx.doi.org/10.1006/jcis.1994.1394>.

Barnes, J.R., Smit, J.P., Smit, J.R., Shpakoff, P.G., Raney, K.H., and Puerto, M.C. 2008a. Development of Surfactants for Chemical Flooding at Difficult Reservoir Conditions. Paper SPE 113313 presented at the SPE/DOE Symposium on Improved Oil Recovery, Tulsa, Oklahoma, 20-23 April. <http://dx.doi.org/10.2118/113313-MS>.

Barnes, J.R., Smit, J.P., Smit, J.R., Shpakoff, P.G., Raney, K.H., and Puerto, M.C. 2008b. Phase Behavior Methods for the Evaluation of Surfactants for Chemical Flooding at Higher Temperature Reservoir Conditions. Paper SPE 113314 presented at the SPE/DOE Symposium on Improved Oil Recovery, Tulsa, Oklahoma, 20-23 April. <http://dx.doi.org/10.2118/113314-MS>.

Bouton, F., Durand, M., Nardello-Rataj, V., Borosy, A.P., Quillet, C., and Aubry, J.M. 2010.A QSPR Model for the Prediction of the "Fish-Tail" Temperature of C₁E₄/water/polar Hydrocarbon Oil Systems. *Langmuir* **26**(11):7962-7970. <http://dx.doi.org/10.1021/la904836m>.

Boyd, D.T. 2008. Oklahoma: The Ultimate Oil Opportunity, <http://www.ogs.ou.edu/pdf/OKultoiloop.pdf>. (downloaded 25 May 2013).

Castellino, V., Cheng, Y.L., and Acosta, E. 2011. The Hydrophobicity of Silicone-Based Oils and Surfactants and Their Use in Reactive Microemulsions. *Journal of Colloid and Interface Science* **353**(1):196-205. <http://dx.doi.org/10.1016/j.jcis.2010.09.004>.

Cayias, J.L., Schechter, R.S., and Wade, W.H. 1976. Modeling Crude Oils for Low Interfacial-Tension. *SPE J.* **16**(6): 351-357. SPE-5813-PA. <http://dx.doi.org/10.2118/5813-PA>.

Charoensaeng, A., Sabatini, D.A., and Khaodhiar, S. 2008. Styrene Solubilization and Adsolubilization on an Aluminum Oxide Surface Using Linker Molecules and Extended

Surfactants. *Journal of Surfactants and Detergents* **11**(1):61-71.
<http://dx.doi.org/10.1007/s11743-007-1055-1>.

Charoensaeng, A., Sabatini, D.A., and Khaodhiar, S. 2009. Solubilization and Adsolubilization of Polar and Nonpolar Organic Solutes by Linker Molecules and Extended Surfactants. *Journal of Surfactants and Detergents* **12**(3):209-217.
<http://dx.doi.org/10.1007/s11743-009-1113-y>.

Dang, C. T. Q., Chen, Z. J., Nguyen, N. T. B., Bae, W., and Phung, T. H. 2011. Development of Isotherm Polymer/Surfactant Adsorption Models in Chemical Flooding. Paper SPE 147872 presented at the SPE Asia Pacific Oil and Gas Conference and Exhibition, Jakarta, Indonesia, 20-22 September. <http://dx.doi.org/10.2118/147872-MS>.

Delamaide, E., Rousseau, D., and Tabary, R. 2014. Chemical EOR in Low Permeability Reservoirs. Paper SPE 169673 presented at the SPE EOR Conference at Oil and Gas West Asia, Muscat, Oman, 31 March-2 April. <http://dx.doi.org/10.2118/169673-MS>.

Do, L.D. and Sabatini, D.A. 2010. Aqueous Extended-Surfactant Based Method for Vegetable Oil Extraction: Proof of Concept. *Journal of the American Oil Chemists' Society* **87**(10):1211-1220. <http://dx.doi.org/10.1007/s11746-010-1603-0>.

Do, L.D., Witthayapayanon, A., Harwell, J.H., and Sabatini, D.A. 2009. Environmentally Friendly Vegetable Oil Microemulsions Using Extended Surfactants and Linkers. *Journal of Surfactants and Detergents* **12**(2):91-99.
<http://dx.doi.org/10.1007/s11743-008-1096-0>.

Elraies, K.A., Tan, I.M., Awang, M., and Fathaddin M.T. 2010. A New Approach to Low-Cost, High Performance Chemical Flooding System. Paper SPE 133004 presented at the Production and Operations Conference and Exhibition, 2010, Tunis, Tunisia, 8-10 June. <http://dx.doi.org/10.2118/133004-MS>.

Falls, A.H., Thigpen, D.R., Nelson, R.C., Ciaston, J.W., Lawson, J.B., Good, P.A., Ueber, R.C., and Shahin, G.T. 1994. Field Test of Cosurfactant-Enhanced Alkaline Flooding. *SPE Res Eng* **9** (3): 217-223. SPE-24117-PA. <http://dx.doi.org/10.2118/24117-PA>.

Fernandez, A., Scorzza, C., Usubillaga, A., and Salager, J.L. 2005a. Synthesis of New Extended Surfactants Containing a Carboxylate or Sulfate Polar Group. *Journal of Surfactants and Detergents* **8**(2):187-191. <http://dx.doi.org/10.1007/s11743-005-346-2>.

Fernandez, A., Scorzza, C., Usubillaga, A., and Salager, J.L. 2005b. Synthesis of New Extended Surfactants Containing a Xylitol Polar Group. *Journal of Surfactants and Detergents* **8**(2):193-198. <http://dx.doi.org/10.1007/s11743-005-347-1>.

Flaaten, A.K., Nguyen, Q.P., Pope, G.A., and Zhang, J. 2009. A Systematic Laboratory Approach to Low-Cost, High-Performance Chemical Flooding. *SPE Res Eval & Eng* **12**(5): 713-723. SPE-113469-PA. <http://dx.doi.org/10.2118/113469-PA>.

Flaaten, A.K., Nguyen, Q.P., Zhang, J., Mohammadi, H., and Pope, G.A. 2010. Alkaline/Surfactant/Polymer Chemical Flooding Without the Need for Soft Water. *SPE J.* **15**(1): 184-196. SPE-116754-PA. <http://dx.doi.org/10.2118/116754-PA>.

Gao, P., Towler, B. F., Li, Y., and Zhang, X. 2010. Integrated evaluation of surfactant-polymer floods. Paper SPE 129590 presented at the SPE EOR Conference at Oil & Gas West Asia, Muscat, Oman, 11-13 April. <http://dx.doi.org/10.2118/129590-MS>.

Glover, C.J., Puerto, M.C., Maerker, J.M., and Sandvik, E.L. 1979. Surfactant Phase Behavior and Retention in Porous Media. SPE J. **19** (3): 183-193. SPE-7053-PA. <http://dx.doi.org/10.2118/7053-PA>.

Green D.W. and Willhite G. P. 1998. *Enhanced Oil Recovery*, Vol. 6, 1-100. Richardson, Texas: Textbook Series, SPE.

Grigg, R.B. and Mikhalin, A.A. 2007. Effects of Flow Conditions and Surfactant Availability on Adsorption. Paper SPE 106205 presented at the International Symposium on Oilfield Chemistry, Houston, Texas, 28 February-2 March. <http://dx.doi.org/10.2118/106205-MS>.

Grigg, R.B., Baojun, B., and Yi, L. 2004. Competitive Adsorption of a Hybrid Surfactant System onto Five Minerals Berea Sandstone and Limestone. In SPE Annual Technical Conference and Exhibition. Society of Petroleum Engineers. Paper SPE 90612 presented at the SPE Annual Technical Conference and Exhibition, Houston, Texas, 26-29 September. <http://dx.doi.org/10.2118/90612-MS>.

Hammond, C. and Acosta, E.J. 2010. Effect of Hydrocarbon Branching on the Packing of the Extended Surfactants at the Oil-Water Interfaces. Oral presentation given at the 101th AOCS Annual Meeting, Phoenix, Arizona, 16-19 May.

Han, C., Delshad, M., Pope, G.A., and Sepehrnoori, K. 2009. Coupling Equation-of-State Compositional and Surfactant Models in a Fully Implicit Parallel Reservoir Simulator Using the Equivalent-Alkane-Carbon-Number Concept. *SPE J.* **14**(2): 302-310. <http://dx.doi.org/10.2118/103194-PA>.

Hirasaki, G.J. and Pope, G.A. 1974. Analysis of Factors Influencing Mobility and Adsorption in the Flow of Polymer Solution through Porous Media. *SPE J.* **14**(4): 337-346. SPE-4026-PA. <http://dx.doi.org/10.2118/4026-PA>.

Hirasaki, G.J. and Zhang, D.L. 2004. Surface Chemistry of Oil Recovery From Fractured, Oil-Wet, Carbonate Formations. *SPE J.* **9** (2): 151-162. SPE-88365-PA. <http://dx.doi.org/10.2118/88365-PA>.

Hirasaki, G.J., Miller, C.A., and Puerto, M. 2011. Recent Advances in Surfactant EOR. *SPE J.* **16**(4): 889-907. SPE-115386-PA. <http://dx.doi.org/10.2118/115386-PA>.

Hsu, T., Lohateeraparp, P., Roberts, B.L., Wan, W., Lin, Z., Wang, X., Budhathoki, M., Shiau, B., and Harwell, J.H. 2012. Improved Oil Recovery by Chemical Flood from High Salinity Reservoirs-Single-Well Surfactant Injection Test. Paper SPE 154838 presented at the SPE EOR Conference at Oil and Gas West Asia, Muscat, Oman, 16-18 April. <http://dx.doi.org/10.2118/154838-MS>.

Huh, C. 1979. Interfacial Tensions and Solubilizing Ability of a Microemulsion Phase That Coexists with Oil And Brine. *Journal of Colloid and Interface Science* **71** (2): 408-426. [http://dx.doi.org/10.1016/0021-9797\(79\)90249-2](http://dx.doi.org/10.1016/0021-9797(79)90249-2).

Kayali, I., Qamhieh, K., and Olsson, U. 2010. Formulating Middle Phase Microemulsions Using Extended Anionic Surfactant Combined with Cationic Hydrotrope. *Journal of Dispersion Science and Technology* **32**(1): 41-46. <http://dx.doi.org/10.1080/01932690903543303>.

Kiran, S.K., Acosta, E.J., and Moran, K. 2009. Evaluating the Hydrophilic-Lipophilic Nature of Asphaltenic Oils and Naphthenic Amphiphiles Using Microemulsion Models. *Journal of Colloid and Interface Science* **336**(1):304-313. <http://dx.doi.org/10.1016/j.jcis.2009.03.053>.

Klaus, A., Tiddy, G.J.T., Touraud, D., Schramm, A., Stuhler, G., Drechsler, M., and Kunz, W. 2010a. Phase Behavior of an Extended Surfactant in Water and a Detailed Characterization of the Dilute and Semidilute Phases. *Langmuir* **26**(8): 5435-5443. <http://dx.doi.org/10.1021/la903899w>.

Klaus, A., Tiddy, G.J.T., Rachel, R., Trinh, A.P., Maurer, E., Touraud, D., and Kunz, W. 2011. Hydrotrope-Induced Inversion of Salt Effects on the Cloud Point of an Extended Surfactant. *Langmuir* **27**(8): 4403-4411. <http://dx.doi.org/10.1021/la104744e>.

Klaus, A., Tiddy, G.J.T., Touraud, D., Schramm, A., Stuhler, G., and Kunz, W. 2010b. Phase Behavior of an Extended Surfactant in Water and a Detailed Characterization of the Concentrated Phases. *Langmuir* **26**(22):16871-16883. <http://dx.doi.org/10.1021/la103037q>.

Levitt, D.B., Jackson, A.C., Heinson, C., Britton, L.N., Malik, T., Dwarakanath, V., and Pope, G.E. 2006. Identification and Evaluation of High-Performance EOR Surfactants.

Paper SPE 100089 presented at SPE/DOE Symposium on Improved Oil Recovery, Tulsa, Oklahoma, 22-26 April. <http://dx.doi.org/10.2118/100089-MS>.

Littmann, W., Kleinitz, W., Christensen, B.E., Stokke, B.T., and Haugvallstad, T. 1992. Late Results of a Polymer Pilot Test: Performance, Simulation Adsorption, and Xanthan Stability in the Reservoir. Paper SPE 24120 presented at the SPE/DOE Improved Oil Recovery Symposium, Tulsa, Oklahoma, 22-24 April. <http://dx.doi.org/10.2118/24120-MS>.

Morvan, M., Moreau, P., Degre, G., Leng, J., Masselon, C., Bouillot, J., and Zaitoun, A. 2009. New viscoelastic fluid for chemical EOR. Paper SPE 121675 presented at the SPE International Symposium on Oilfield Chemistry, The Woodlands, Texas, 20-22 April. <http://dx.doi.org/10.2118/121675-MS>.

Novosad, J. 1982. Surfactant Retention in Berea Sandstone- Effects of Phase Behavior and Temperature. SPE J. 22(6):962-970. SPE-10064-PA. <http://dx.doi.org/10.2118/10064-PA>.

Panswad, D., Sabatini, D.A., and Khaodhiar, S. 2011. Precipitation and Micellar Properties of Novel Mixed Anionic Extended Surfactants and a Cationic Surfactant. *Journal of Surfactants and Detergents* **14**(4):577-583. <http://dx.doi.org/10.1007/s11743-011-1282-3>.

Phan, T.T., Attaphong, C., and Sabatini, D.A. 2011. Effect of Extended Surfactant Structure on Interfacial Tension and Microemulsion Formation with Triglycerides.

Journal of the American Oil Chemists' Society **88**(8):1223-1228.
<http://dx.doi.org/10.1007/s11746-011-1784-1>.

Phan, T.T., Harwell, J.H., and Sabatini, D.A. 2010a. Effects of Triglyceride Molecular Structure on Optimum Formulation of Surfactant-Oil-Water Systems. *Journal of Surfactants and Detergents* **13**(2): 189-194. <http://dx.doi.org/10.1007/s11743-009-1155-1>.

Phan, T.T., Witthayapanyanon, A., Harwell, J.H., and Sabatini, D.A. 2010b. Microemulsion-Based Vegetable Oil Detergency Using an Extended Surfactant. *Journal of Surfactants and Detergents* **13**(3): 313-319. <http://dx.doi.org/10.1007/s11743-010-1184-9>.

Puerto, M., Hirasaki, G.J., Miller, C.A., and Barnes J.R. 2010. Surfactant Systems for EOR in High-Temperature, High-Salinity Environments. Paper SPE 129675 presented at the Symposium on Improved Oil Recovery, Tulsa, Oklahoma, 24-28 April. <http://dx.doi.org/10.2118/129675-MS>.

Raj A. 2013. Mobility Control Options for Chemical Flooding in Challenging Reservoir Conditions. MS thesis, University of Oklahoma, Norman, Oklahoma (May 2013).

Roshanfekar, M. and Johns, R.T. 2011. Prediction of Optimum Salinity and Solubilization Ratio for Microemulsion Phase Behavior with Live Crude at Reservoir Pressure. *Fluid Phase Equilibria* **304**(1): 52-60. <http://dx.doi.org/10.1016/j.fluid.2011.02.004>.

Salager, J.L., Antón, R.E., Sabatini, D.A., Harwell, J.H., Acosta, E.J., and Tolosa, L.I. 2005. Enhancing Solubilization in Microemulsions-State of The Art and Current Trends. *Journal of Surfactants and Detergents* **8**(1):3-21. <http://dx.doi.org/10.1007/s11743-005-0328-4>.

Salager, J.L., Forgiarini, A.M., Bullon, J. 2013a. How to Attain Ultralow Interfacial Tension and Three-Phase Behavior with Surfactant Formulation for Enhanced Oil Recovery: A Review. Part 1. Optimal Formulation for Simple Surfactant-Oil-Water Ternary Systems. *Journal of Surfactants and Detergents* **16**(4): 449-472. <http://dx.doi.org/10.1007/s11743-013-1470-4>.

Salager, J.L., Forgiarini, A.M., Marquez, L., Manchego, L., Bullon, J. 2013b. How to Attain an Ultralow Interfacial Tension and a Three-Phase Behavior with a Surfactant Formulation for Enhanced Oil Recovery: A Review. Part 2. Performance Improvement Trends from Winsor's Premise to Currently Proposed Inter- and Intra-Molecular Mixtures. *Journal of Surfactants and Detergents* **16**(5): 631-663. <http://dx.doi.org/10.1007/s11743-013-1485-x>.

Salager, J.L., Morgan, J.C., Schechter, R.S., Wade, W.H., and Vasquez, E. 1979. Optimum Formulation of Surfactant-Water-Oil Systems for Minimum Interfacial-Tension or Phase-Behavior. *SPE J.* **19**(2): 107-115. SPE-7054-PA. <http://dx.doi.org/10.2118/7054-PA>.

Sanz, C.A. and Pope, G.A. 1995. Alcohol-Free Chemical Flooding: From Surfactant Screening to Coreflood Design. Paper SPE 28956 presented at the SPE International

Symposium on Oilfield Chemistry, San Antonio, Texas, 14-17 February.
<http://dx.doi.org/10.2118/28956-MS>.

Seright, R.S., Fan T., Wavrik K., and Balaban, R.C. 2011. New Insights into Polymer Rheology in Porous Media. *SPE J.* **16**(1): 35-42. SPE-129200-PA.
<http://dx.doi.org/10.2118/129200-PA>.

Shamsijazeyi, H., Hirasaki, G., and Verduzco, R. 2013. Sacrificial Agent for Reducing Adsorption of Anionic Surfactants. Paper SPE 164061 presented at the SPE International Symposium on Oilfield Chemistry, The Woodlands, Texas, 8-10 April.
<http://dx.doi.org/10.2118/164061-MS>.

Sheng, J. 2010. *Modern Chemical Enhanced Oil Recovery: Theory and Practice*, 1st edition. Burlington, Massachusetts: Gulf Professional Publishing/Elsevier.

Shiau, B., Hsu, T., Lohateeraparp, P., Wan, W., Lin, Z., Roberts, B.L., and Harwell, J.H. 2012. Improved Oil Recovery by Chemical Flood from High Salinity Reservoirs. Paper SPE 154260 presented at the SPE Symposium on Improved Oil Recovery, Tulsa, Oklahoma, 14-18 April. <http://dx.doi.org/10.2118/154260-MS>.

Shiau, B.J., Harwell, J.H., Lohateeraparp, P., Dinh, A.V., Roberts, B.L., Hsu, T., Anwuri, O.I. 2010. Designing Alcohol-Free Surfactant Chemical Flood for Oil Recovery. Paper SPE 129254 presented at the SPE EOR Conference at Oil & Gas West Asia, Muscat, Oman, 11-13 April. <http://dx.doi.org/10.2118/129254-MS>.

Solairaj, S., Britton, C., Kim, D.H., Weerasooriya, U., Pope, G.A. 2012. Measurement and Analysis of Surfactant Retention. Paper SPE 154247 presented at SPE Symposium

on Improved Oil Recovery, Tulsa, Oklahoma, 14-18 April. <http://dx.doi.org/10.2118/154247-MS>.

Taber, J.J., Martin, F.D., and Seright, R.S. 1997a. EOR Screening Criteria Revisited-Part 1: Introduction to Screening Criteria and Enhanced Recovery Field Projects. *SPE Res Eng* **12**(3): 189-198. SPE-35385-P. <http://dx.doi.org/10.2118/35385-PA>.

Taber, J.J., Martin, F.D., and Seright, R.S. 1997b. EOR Screening Criteria Revisited-Part 2: Applications and Impact of Oil Prices. *SPE Res Eng* **12**(3):199-205. SPE-39234-PA. <http://dx.doi.org/10.2118/39234-PA>.

Thomas, S. 2008. Enhanced Oil Recovery -An Overview. *Oil & Gas Science and Technology* **63** (1):9-19. <http://dx.doi.org/10.2516/ogst:2007060>.

Veedu, F.K., Delshad, M., and Pope, G.A. 2010. Scaleup Methodology for Chemical Flooding. Paper SPE 135543 presented at the Annual Technical Conference and Exhibition, Florence, Italy, 19-22 September. <http://dx.doi.org/10.2118/135543-MS>.

Velasquez, J., Scorzza, C., Vejar, F., Forgiarini, A.M., Anton, R.E., and Salager, J.L. 2010. Effect of Temperature and Other Variables on the Optimum Formulation of Anionic Extended Surfactant-Alkane-Brine Systems. *Journal of Surfactants and Detergents* **13**(1):69-73. <http://dx.doi.org/10.1007/s11743-009-1142-6>.

Vermolen, E.C.M., van Haasterecht, M.J.T., Masalmeh, S.K., Faber, M.J., Boersma, D.M., and Gruenenfelder, M. 2011. Pushing the Envelope for Polymer Flooding Towards High-Temperature and High-Salinity Reservoirs with Polyacrylamide Based Ter-Polymers. Paper SPE 141497 presented at the SPE Middle East Oil and Gas Show

and Conference, Manama, Bahrain, 25-28 September.

<http://dx.doi.org/10.2118/141497-MS>.

Wade, W.H., Morgan, J.C., Jacobson, J.K., and Schechter, R.S. 1977. Low Interfacial-Tensions Involving Mixtures of Surfactants. *SPE J.* **17**(2): 122-128. SPE-6002-PA.

<http://dx.doi.org/10.2118/6002-PA>.

Watcharasing, S., Kongkowitz, W., and Chavadej, S. 2009. Motor Oil Removal from Water by Continuous Froth Flotation Using Extended Surfactant: Effects of Air Bubble Parameters and Surfactant Concentration. *Separation and Purification Technology* **70**(2): 179-189. <http://dx.doi.org/10.1016/j.seppur.2009.09.014>.

Wellington, S.L. and Richardson, E.A. 1997. Low Surfactant Concentration Enhanced Waterflooding. *SPE J.* **2**(4):389-405. SPE-30748-PA. <http://dx.doi.org/10.2118/30748-PA>.

Witthayapanyanon, A., Acosta, E.J., Harwell, J.H., and Sabatini, D.A. 2006. Formulation of Ultralow Interfacial Tension Systems using Extended Surfactants. *Journal of Surfactants and Detergents* **9**(4):331-339. <http://dx.doi.org/10.1007/s11743-006-5011-2>.

Witthayapanyanon, A., Harwell, J.H., and Sabatini, D.A. 2008. Hydrophilic-lipophilic Deviation (HLD) Method for Characterizing Conventional and Extended Surfactants. *Journal of Colloid and Interface Science* **325**(1):259-266. <http://dx.doi.org/10.1016/j.jcis.2008.05.061>.

Witthayapanyanon, A., Phan, T.T., Heitmann, T.C., Harwell, J.H., and Sabitini, D.A. 2010. Interfacial Properties of Extended-Surfactant-Based Microemulsions and Related Macroemulsions. *Journal of Surfactants and Detergents* **13**(2):127-134. <http://dx.doi.org/10.1007/s11743-009-1151-5>.

Wu, B., and Sabatini, D.A. 2000. Using Partitioning Alcohol Tracers to Estimate Hydrophobicity of High Molecular Weight LNAPLs. *Environmental Science & Technology* **34**(22): 4701-4707. <http://dx.doi.org/10.1021/es991336f>.

Wu, B., Shiau, B., Sabatini, D.A., Harwell, J.H., and Vu, D.Q. 2000. Formulating Microemulsion Systems for a Weathered Jet Fuel Waste Using Surfactant/Cosurfactant Mixtures. *Separation Science and Technology* **35** (12):1917 -1937. <http://dx.doi.org/10.1081/SS-100100627>.

Xia, H.F., Wang, D.M., Wang, G., Ma, W.G., Deng, H.W. and Liu, J. 2008. Mechanism of the Effect of Micro-Forces on Residual Oil in Chemical Flooding. Paper SPE 114335 presented at the SPE/DOE Symposium on Improved Oil Recovery, Tulsa, Oklahoma, 20-23 April. <http://dx.doi.org/10.2118/114335-MS>.

Yang, J. 2002. Viscoelastic wormlike micelles and their applications. *Current Opinion in Colloid & Interface Science* **7** (5): 276-281. [http://dx.doi.org/10.1016/S1359-0294\(02\)00071-7](http://dx.doi.org/10.1016/S1359-0294(02)00071-7).

Yu, M., Mahmoud, M.A., and Nasr-El-Din, H.A. 2009. Quantitative Analysis of an Amphoteric Surfactant in Acidizing Fluids and Coreflood Effluent. Paper SPE 121715

presented at the SPE International Symposium on Oilfield Chemistry, Woodlands, Texas, 20-22 April. <http://dx.doi.org/10.2118/121715-MS>.

Zhang, D.L., Liu, S., Yan, W., Puerto, M., Hirasaki, G.J., and Miller, C.A. 2006. Favorable Attributes of Alkali-Surfactant-Polymer Flooding. Paper SPE 99744 presented at the SPE/DOE Symposium on Improved Oil Recovery, Tulsa, Oklahoma, 22-26 April. <http://dx.doi.org/10.2118/99744-MS>.

Zhang, J., Nguyen, Q.P., Flaaten, A.K., and Pope, G.A. 2008. Mechanisms of Enhanced Natural Imbibition with Novel Chemicals. Paper SPE 113453 presented at the SPE/DOE Symposium on Improved Oil Recovery, Tulsa, Oklahoma, 20-23 April. <http://dx.doi.org/10.2118/113453-MS>.

Zhou, W., Dong, M., Liu, Q., and Xiao, H. 2005. Experimental Investigation of Surfactant Adsorption on Sand and Oil-Water Interface in Heavy Oil/Water/Sand Systems. Paper PETSOC-2005-192 presented at the Canadian International Petroleum Conference, Calgary, Alberta, 7-9 June. <http://dx.doi.org/10.2118/2005-192>.